CHARLES UNIVERSITY IN PRAGUE
FACULTY OF SCIENCE
INSTITUTE OF PETROLOGY AND STRUCTURAL GEOLOGY

HIGH-PRESSURE PARTIAL MELTING AND ITS RELATIONSHIP TO THE GRANULITE FACIES METAMORPHISM: IMPLICATIONS FOR THE ORIGIN OF FELSIC HIGH-*PT* GRANULITES IN THE BOHEMIAN MASSIF, CENTRAL EUROPE

PH.D. THESIS OF

RADMILA NAHODILOVÁ

2011

SUPERVISED BY:

PROF. ING. SHAH WALI FARYAD, CSC.
MGR. DAVID DOLEJŠ, PH.D.

I affirm that in the presented Ph.D. study I used only data acquired from my own research or from sources mentioned in the list of used literature.

I also affirm that I didn’t present this work, or even its significant part, to acquire another academic title or the same Ph.D. title at another university.

In Prague, ……..

Radmila Nahodilová

……

ACKNOWLEDGEMENT

The research of this thesis was financially supported by the research projects of Ministry of Education of the Czech Republic MSM 0021620855 and the Czech Geological Survey Internal Research Project 323500, the Charles University Grant Agency 258/2005/B-GEO/PrF (to Radmila Nahodilová), the Czech Science Foundation 205/06/0688 and 210/10/0249 (to Shah Wali Faryad) and 205/09/P135 (to David Dolejš).

Above all, I would like to thank my supervisors, Shah Wali Faryad and David Dolejš, without their enthusiasm and guidance this work could not have been accomplished.

Special thanks go to Jaroslava Pertoldová, Jiří Konopásek, Stanislav Vrána, Veronika Štědrá and others collegues at the Czech Geological Survey who supported my work and discussed with me.

Very special thanks go to my husband Otakar and to my sons Otakar and Dominik for their strong support during the long – sometimes good and sometimes bad – period of my Ph.D. work.

TABLE OF CONTENTS

INTRODUCTION

In most orogenic belts, granulite and migmatites of pelitic and granitic precursors were formed at medium- to low-pressure conditions. Information on high-pressure melting generally relate to mafic and ultramafic rocks. Recent studies in HP/UHP metamorphic rocks indicated that crustal rocks could be subducted to depth more than 100 km and during exhumation and heating converted to medium-pressure granulite or migmatite. However, there is not suficient information on phase relations, equilibrium conditions and mineral reaction during melt formation in felsic rocks at higher pressure conditions. The Bohemian Massif provides a unique opportunity for investigation of phase relations and HP-pressure partial melting in felsic granulites which associate with HT eclogites and garnet peridotites in the Moldanubian and Saxothuringian zones. One of the most characteristic feature of felsic granulite in the Bohemian Massif is weak foliation which is followed by the presence of almost parallel light stripes or bands within the light-grey host granulite. It is not always clear, if these light parallel stripes are pre-granulite facies layers or they were formed during mylonitization in ductile condition. However, in some cases, the light stripes are not conform with the foliation and form discrete veins which suggests partial melting. Both the host granulite and the light bands and occasionally also veins contain kyanite as stable phase with garnet that indicate relatively higher pressure conditions for their equilibrium. We focused on petrology of both light-colour stripes and host granulite and compare with the partial melting experiment on these rocks. We want to analyse pre-granulite facies HP metamorphism and its possible relation to subduction of continental crust material and also localize PT conditions for melt formation and related minerals.

PART I

1. paper

In the first paper we investigated the felsic granulites from the Kutná Hora complex in the Moldanubian zone. These granulites exhibit modal layering and discordant leucocratic veining, which is interpreted as evidence for partial melting along the exhumation path from the eclogite to granulite facies. The granulites consist of quartz, ternary feldspar, garnet, biotite, kyanite, and rutile. In the bulk rock garnet grains show relatively high Ca contents corresponding to 29-41 mol. % grossular end- member. They have remarkably flat compositional profiles in their cores but their rims exhibit an increase in pyrope and a decrease in grossular components ($Grs_{41\rightarrow29}$ $Prp_{08\rightarrow15}$ Alm_{47} Sps_{01} with X_{Fe} = 0.86→0.75). In

contrast, garnets from the leucocratic layers have relatively low Ca contents (15-26 mol. % grossular) that further decrease towards the rims. In addition to modelling of pressure-temperature pseudosections, compositions of garnet core composition, garnet rim-ternary feldspar-kyanite-quartz equilibrium, ternary feldspar composition, and the garnet-biotite equilibrium provide five constraints that were used to constrain the pressure-temperature path from eclogite through the granulite and amphibolite facies. In both layers, garnet cores grew during omphacite and phengite dehydration melting at 940 ^{o}C and 2.6 GPa. Subsequent decompression heating to 1020 ^{o}C and 2.1 GPa produced Ca- and Fe-poor garnet rims due to the formation of Ca-bearing ternary feldspar and partial melt. In both the mesocratic and leucocratic layer, the maximum melt productivity was 26 and 18 vol. %, respectively, at peak temperature constrained by the maximum whole-rock H_2O budget, ~1.05-0.75 wt. %, prior to the melting. The preservation of prograde garnet-rich assemblages required nearly complete melt loss (15-25 vol. %), interpreted to have occured at 1000-1020 ^{o}C and 2.2-2.4 GPa by garnet mode isopleths, followed by crystallization of small amounts of residual melt at 760 ^{o}C and 1.0 GPa. Phase formation and melt productivity were independently determined by experiments in the piston-cylinder apparatus at 850-1100 ^{o}C and 1.7-2.1 GPa. Both the thermodynamic calculations and phase equilibrium experiments suggest that the partial melt was produced by the dehydration melting: muscovite + quartz = melt + K-feldspar + kyanite. The presence of partial melt facilitated attainment of mineral equilibria at peak temperature thus eliminating any potential relics of early high-pressure phases such as phengite or omphacite (discuss below in the 2. paper). By contrast, adjacent mafic granulites and eclogites, which apparently share the same metamorphic path but have not undergone partial melting commonly preserve relics or inclusions of eclogite-facies mineral assemblages.

The presence of partially molten domains of felsic granulites in the Variscan orogenic continental root probably exerts major rheological control on the incorporation and immersion of lenses and boudins of mafic granulites, eclogites and garnet-bearing ultramafics and their common extrusion *via* an exhumation channel to the middle continental crust.

2. paper

The second paper describes our investigation of several mineral phases and their replacement products which occur as inclusions in garnets from felsic and mafic granulites of the Gföhl Unit in the Moldanubian Zone.

Garnets in felsic granulites of Kutná Hora complex contain inclusions of either fresh Ti-muscovite (Běstvina felsic granulite) or columnar-shaped inclusions of K-feldspar (Miškovice felsic granulite) which are always occur in the central and relatively Ca-rich parts of garnet.

In addition to K-feldspar, these inclusions contain kaolinite and Fe-oxide. The host garnet with the columnar-shaped inclusions is rich in Fe and Ca and has a relatively flat compositional profile in the core (Grs_{42-37}, Prp_{07-09}, Alm_{49-54}, Sps_{01}), but at the rims it shows an increase in Mg and a decrease in Ca (Grs_{29}, Prp_{22}, Alm_{48}, Sps_{01}). In the Blanský Les felsic granulite garnet contains columnar euhedral inclusions filled mostly by albite but K-feldspar and plagioclase (An_{14} and An_{43}) were also found. These inclusions occur in the Ca-rich internal parts of garnet and usually contain a mixture of Fe oxide + titanite with small holes. Calcic amphibole rimming apatite was also observed as inclusion in garnet. The mafic variety of granulite contains garnets with omphacite inclusions (Jd_{28}).

We suggest, that the Ti-rich muscovite preserves in garnet due to its high thermal stability (Spicer et al, 2004). The columnar pseudomorphs of K-feldspar with kaolinite and opaque phases in garnet from other granulite in the Kutná Hora Complex indicate their possible formation from muscovite by incipient melting: muscovite + quartz = K-feldspar + kyanite + melt. The lack of rutile or other titaniferous phase in the pseudomorphs suggests that this muscovite was Ti-poor and not stable at higher temperatures.

Based on their forms and composition, the columnar inclusions filled by albite, and partly also by Ca-rich plagioclase or K-feldspar, could have formed by transformation of jadeite, paragonite, glaucophane, or, in the case of plagioclase, from a mixture of paragonite and margarite. The presence of omphacite inclusion in garnet from mafic granulite suggests that these rocks passed through eclogite facies prior to their granulite facies overprint. The lack of clinopyroxene in felsic granulites could be due to inappropriate whole rock composition or could be a result of extensive granulite facies overprint in the following equilibrium: Ms + Qtz + Cpx = Grt + Ky + Kfs + Melt.

Most thermobarometric calculations for granulites are focused only on their exhumation and retrograde histories (see Kotková, 2007 and references therein). To trace the *PT* stability fields of the observed inclusion phases and to examine the possible prograde history from amphibolite/eclogite to granulite facies conditions, the pseudosection method (Perplex software by Conolly, 2005, in NCKFMASHT system) was applied to samples of Běstvina and Blanský Les felsic granulites. Considering that the muscovite in Běstvina granulite body was preserved due to its high Ti content and that the columnar inclusions of K-feldspar + kaolinite (after kyanite) in garnet are products of dehydration melting after phengite/muscovite, the Kutná Hora granulite should, based the pseudosection, have crossed the muscovite breakdown reaction at 2.2 GPa while at temperatures of 900–1000 ^{o}C (Vrána, 1989; O'Brien, 1999; Vrána et al., 2006; Kotková, 2007). *PT* conditions of 900 °C/2.1 GPa for partial melting of

granulite in the Kutná Hora Complex were obtained by combination of phase equilibrium modelling and experimental work (Nahodilová et al., 2008). These *PT* data fit well with the data from the adjacent kyanite-bearing eclogite lens of this locality, which contains garnet with prograde zoning and shows a maximum pressure of 3.4 GPa followed by decompression in granulite facies conditions at 900 ^{o}C (Faryad, 2009).

Pseudosection calculated for Blanský Les granulite contains a wide array of Na-Ca minerals (paragonite, jadeite, phengite, glaucophane, zoisite) that are suitable candidates for phases observed as inclusions in garnet. All of these phases are stable at temperatures exceeding 600 ^{o}C and pressures of up to 2.2 GPa. Phengite decomposes at 900 ^{o}C/2.2 GPa, and biotite is stable at higher temperatures. Preservation of a weak but prograde zoning in garnet in this sample suggests that its core composition was not completely modified by diffusion and may reflect PT conditions close to the metamorphic stage during which the phases were enclosed. This fits well with the garnet isopleths (X_{Fe} = 0.69-0.70 and X_{Ca} = 0.23-0.24) which are located in one of these fields with glaucophane, jadeite, and phengite at T = 620 ^{o}C and P = 2.2 GPa. The outer part of the garnet, with the highest pyrope content (X_{Ca} = 0.18 and X_{Fe} = 0.66), gives T = 820 ^{o}C and P = 1.6 GPa or T = 870 ^{o}C and P = 1.0 GPa and may record granulite facies conditions before modification of the marginal part of garnet during cooling.

So, there are consequent facts of this work:

1) Mineral inclusions in garnets from felsic granulites of the Gföhl Unit in the Kutná Hora Complex and in the Blanský Les Massif indicate a prograde PT path from eclogite facies conditions prior to granulite facies metamorphism.

2) Passage through the eclogite facies is further supported by the presence of omphacite inclusion or its pseudomorphs in garnet from mafic granulite that occur as discrete lenses in felsic granulites. The composition of Ti-rich muscovite inclusion in garnet from felsic granulite is comparable to that known from other UHT and UHP terranes, and its presentation is interpreted to be due to high Ti content.

3) Granulite has formed from a muscovite-bearing hence hydrous protolith as evidenced by the presence of mica inclusions and their pseudomorphs in garnet.

4) The relationship of granulite to LT/HP metamorphism, consistent with subduction geothermal regime, is supported by (1) the presence of UHP eclogite that has locally preserved garnet with prograde zoningt, and (2) the *PT* trajectory of granulite obtained using the pseudosection method with stability fields of mineral inclusions in garnet.

PART II.

3. paper

Except other, in this paper we analysed metamorphic evolution of Křišťanov granulite body and we try to estimate the *PT* conditions of fabric formation as a indicator of emplacement conditions of Knížecí Stolec durbachite pluton.

Granulite rarely preserves earlier steep S1 fabric whereas most of samples were collected from a domains with well-developed younger flat-lying S2 fabric. At the steep S1 foliation garnet forms subhedral grains, up to 300 μm in size, containing rare inclusions of kyanite, biotite and quartz and showing weak zoning from core to rim ($Grs_{10\rightarrow02}$ $Prp_{18\rightarrow20}$ $Alm_{66\rightarrow73}$ Sps_{02}). Kyanite (up to 500 μm in size) occurs either as relics in the matrix commonly overgrown by aggregates of prismatic sillimanite, or is enclosed in larger plagioclase grains (core→rim: $Ab_{75\rightarrow74}$ $An_{24\rightarrow25}$ Or_1). Feldspar grains, up to 1–2 mm in size, are rarely present in the matrix. Feldspars are typically mesoperthitic, except for cases where some parts of grains are replaced by fine-grained myrmekites.

The mineral assemblage in flat-lying S2 fabric replaces the minerals from older fabric. Biotite aggregates (X_{Mg} = 0.50–0.56) form the foliation bands or crystallize together with sillimanite around garnet in pressure shadows. The composition of garnet is approximately homogeneous (with no prominent zoning) and corresponds to Grs_{02} Prp_{20} Alm_{73} Sps_{02}. Feldspar aggregates (100–200 μm in size) indicate a higher degree of recrystallization and have compositions corresponding to orthoclase ($Ab_{11–17}$ $An_{00–01}$ $Or_{89–82}$) and plagioclase (Ab_{70} An_{29} Or_{01}).

The mineral succession suggests that the early metastable garnet-kyanite-biotite plagioclase-K-feldspar-quartz mineral assemblage (S1 fabric) has been replaced by the stable garnet-sillimanite-biotite-plagioclase-K-feldspar-quartz assemblage (S2 fabric). In order to semi-quantitatively characterize the *PT* conditions of formation of the flat-lying fabric in the granulite, the stable mineral assemblage was modelled thermodynamically in the Na_2O-CaO-K_2O-FeO-MgO-Al_2O_3-SiO_2-H_2O (NCKFMASH) system using the THERMOCALC software (Powell et al., 1998, recent upgrade) and the internally consistent thermodynamic dataset 5.5 (Holland and Powell, 1998, 2003 upgrade). The NCKFMASH chemical system uses the mineral and liquid/melt activity-composition models and the non-ideal interaction parameters of White et al. (2001). According to Ky-Grt-Melt (+Kfs+Pl+Qtz) stability field in pseudosection we estimated the max. *PT* conditions at about 1.0 – 1.5 GPa and 780 – 850 °C

which well fits to HP-HT stage at 1.3 GPa and 790 °C by Tajčmanová et al. (2006). Further *PT* evolution is characterized by the appearance of sillimanite as a result of overstepping the Ky = Sill curve due to decompression and the crystallization of biotite around the garnet suggests transition to the Bt-Sill-Grt-Melt (+Kfs+Pl+Qtz) stability field during cooling. The *PT* conditions of this late stable mineral assemblage were calculated by means of the ‘‘Average *PT*’’ method (Powell and Holland 1990) using the activities for particular end-member components of the garnet rim, matrix biotite, recrystallized feldspars and H_2O. The water activity ($aH_2O = 0.8$) in the melt phase was calculated from the melt-mixing model of White et al. (2001) using the ‘‘calc aH_2O’’ routine implemented in the THERMOCALC software set. Sillimanite and quartz were considered as pure end-member phases. The calculation of the *PT* conditions for the formation of the flat-lying foliation yielded a temperature of 765 ± 53 °C and pressure of 0.76 ± 0.15 GPa.

The ~340 Ma Knížecí Stolec durbachite pluton (located in southwestern part of the Moldanubian Unit) was emplaced into the centre of Křišťanov granulite body which was already juxtaposed against the mid-crustal metamorphic rocks of the Drosendorf Unit. The pluton evolved from a deep-seated cone-sheet-bearing complex followed by the nested intrusion of large magma pulses into the center of the outer sheeted complex. The older magmatic fabrics (margin-parallel geometry) may have recorded intrusive strain during its emplacement. After the emplacement but prior to final solidification, the pluton was overprinted by the regional orogenic flat-lying fabric operating during ~sub-vertical contraction of variscan orogenic root. So the *PT* conditions for the formation of the flat-lying foliation S2 in granulite (T = 765 ± 53 °C and P = 0.76 ± 0.15 GPa) may represent also the *PT* conditions of emplacement of Knížecí Stolec durbachite pluton.

References:

Connolly, J. A. D. (2005). Computation of phase equilibria by linear programming: a tool for geodynamic modeling and its application to subduction zone decarbonation. *Earth and Planetary Science Letters* **236**, 524-541.

Faryad, S.W. (2009). The Kutná Hora Complex (Moldanubian Zone, Bohemian Massif), a composite of crustal and mantle rocks subducted to HP/UHP conditions. *Lithos*, **109**, 193-208.

Holland, T. J. B. & Powell, R. (1998). An internally consistent thermodynamic data set for phases of petrological interest. *Jornal of Metamorphic Geology* **16**, 309–343.

Holland, T. & Powell, R. (2003). Activity–composition relationsfor phases in petrological calculations: an asymmetric multicomponent formulation. *Contributions to Mineralogy and Petrology* **145**, 492–501.

Kotková, J. (2007). High-pressure granulites of the Bohemian Massif: recent advances and open questions. *Journal of Geocsiences* **52**, 45-71.

Nahodilová, R., Faryad, S. W., Dolejs, D., Tropper & P., Konzett, J. (2008). High-to ultra-high pressure partial melting in orogenic belts: implications for the formation of felsic granulites

from the Bohemian Massif. *The 33rd International Geological Congress, Oslo, CD abstract guidelines*, URL: http://www.cprm.gov.br/33IGC/1315009.html.

O'Brien, P. J. (1999). Asymmetric zoning profiles in garnet from HP-HT granulite and implications for volume and grain-boundary diffusion. *Mineralogical Magazine* **63**, 227-238.

Powell, R. & Holland, T. J. B. (1990). Calculated mineral equilbria in the pelite system, KFMASH. *American Mineralogist* **75**, 367-380.

Powell, R., Holland, T. J. B. & Worley, B. (1998). Calculating phase diagrams involving solid solutions via non- linear equations, with examples using THERMOCALC. *Journal of Metamorphic Geology* **16** (4), 577-588.

Spicer, E.M., Stevens, G. & Buick, I. S. (2004). The low-pressure partial-melting behaviour of natural boron-bearing metapelites from the Mt. Stafford area, central Australia. *Contributions to Mineralogy and Petrology* **148**, 160-179.

Tajčmanová, L., Konopásek, J. & Schulmann, K. (2006). Thermal evolution of the orogenic lower crust during exhumation within a thickened Moldanubian root of the Variscan belt of Central Europe. *Journal of Metamorphic Geology* **24**, 119-134.

Tropper, P., Konzett, J. & Finger, F. (2005). Experimental constraints on the formation of high- P/high T granulites in the Southern Bohemian Massif. *Eur. J. Mineral,* **17,** 343-356.

Vrána, S. (1989). Perpotassic granulites from Southern Bohemia – A new rock-type derived from partial melting of crustal rocks under upper mantle conditions. *Contributions to Mineralogy and Petrology* **103**, 510-522.

Vrána, S., Štědrá, V. & Fišera, M. (2006). Petrology and geochemistry of the Běstvina granulite body metamorphosed at eclogite facies conditions, Bohemian Massif. *Journal of the Czech Geological Society* **50,** 81–94.

White, R W., Powell, R. & Holland, T. J. B. (2001). Calculation of partial melting equilibria in the system Na_2O–CaO–K_2O–FeO–MgO–Al_2O_3–SiO_2–H_2O (NCKFMASH). *Journal of Metamorphic Geology* **19**, 139–153.

PART I.

HIGH PRESSURE PARTIAL MELTING IN OROGENIC BELTS: IMPLICATIONS FOR THE ORIGIN OF FELSIC HIGH-*PT* GRANULITES IN THE BOHEMIAN MASSIF, CENTRAL EUROPE

In this study we document prograde mineral assemblages and exhumation paths of felsic granulites that, in addition, are extensively veined due to partial melting and melt migration at the transition from the eclogite to the granulite facies. The garnet core and ternary feldspar composition in parental rock (mesosome) was combined with pseudosection modelling and provide us the maximum pressure conditions at 2.6 GPa/940 ^{o}C, whereas the subsequent melting event at 2.1 GPa/1020 ^{o}C is the best recorded by mineral assemblages and composition in the melt-rich layers (leucosome). The reaction progress and melt productivity were simulated by dehydration melting experiments in a piston cylinder apparatus at 900-1100 ^{o}C and 1.7-2.1 GPa.

Results of this study indicated that banded structure in granulite was a result from partial melting contemporaneously with deformation that occurred after eclogite facies metamorphism of the felsic rocks. Their transition to granulite facies conditions with formation of partial melt occurred by decompression and heating from 2.6 GPa/940 ^{o}C to 2.1 GPa/1020 ^{o}C. The lack of hydrous phase coexisting with granulite facies assemblages at high-pressure conditions (while biotite represents a retrograde phase) suggests that the partial melting occurred with minimum fluid contents. Under equilibrium conditions in the absence of a H_2O-rich volatile phase, melting begins at multiphase grain junctions that include quartz and feldspar. The maximum melt productivity was 26 and 18 vol. %, respectively, at peak temperature constrained by the maximum whole-rock H_2O budget, ~1.05-0.75 wt. %, prior to the melting. The preservation of prograde garnet-rich assemblages required nearly complete melt loss (15-25 vol. %), interpreted to have occured at 1000-1020 ^{o}C and 2.2-2.4 GPa by garnet mode isopleths, followed by crystallization of small amounts of residual melt at 760 ^{o}C and 1.0 GPa. So the formation of foliation-parallel leucocratic bands and subsequent progressive coarsening of mineral grains as well as the increase of the modal amounts of quartz and feldspars indicate that syndeformational melting occurred contemporaneously with a decrease in pressure, i.e., during orogenic exhumation.

High-pressure partial melting and melt loss in felsic granulites in the Kutná Hora complex, Bohemian Massif (Czech Republic)

Radmila Nahodilová[1,2], S. Wali Faryad[1,*], David Dolejš[1,3], Peter Tropper[4], Jürgen Konzett[4]

[1] Institute of Petrology and Structural Geology, Charles University, 12843 Praha 2, Czech Republic

[2] Czech Geological Survey, 11821 Praha 1, Czech Republic

[3] Bayerisches Geoinstitut, University of Bayreuth, 95440 Bayreuth, Germany

[4] Institute of Mineralogy and Petrography, University of Innsbruck, 6020 Innsbruck, Austria

[*] Corresponding author. E-mail: faryad@natur.cuni.cz, fax: +420 221 951 533

ABSTRACT

Felsic granulites from the Kutná Hora complex in the Moldanubian zone of central Europe preserve mineral assemblage that record transition from early eclogite to granulite facies conditions, and exhibit discordant leucocratic veining, which is interpreted as evidence for melt loss during the decompression path. The granulites are layered and consist of variables proportions of quartz, ternary feldspar, garnet, biotite, kyanite, and rutile. In the mesocratic layers, garnet grains show relatively high Ca contents corresponding to 28-41 mol. % grossular end member. They have remarkably flat compositional profiles in their cores but their rims exhibit an increase in pyrope and a decrease in grossular and almandine components. In contrast, garnets from the leucocratic layers have relatively low Ca contents (15-26 mol. % grossular) that further decrease towards the rims. In addition to modelling of pressure-temperature pseudosections, compositions of garnet core composition, garnet rim-ternary feldspar-kyanite-quartz equilibrium, ternary feldspar composition, and the garnet-biotite equilibrium provide five constraints that were used to constrain the pressure-temperature path from eclogite through the granulite and amphibolite facies. In both layers, garnet cores grew during omphacite and phengite dehydration melting at 940 ^{o}C and 2.6 GPa. Subsequent decompression heating to 1020 ^{o}C and 2.1 GPa produced Ca- and Fe-poor garnet rims due to the formation of Ca-bearing ternary feldspar and partial melt. In both the mesocratic and leucocratic layer, the maximum melt productivity was 26 and 18 vol. %, respectively, at peak temperature constrained by the maximum whole-rock H_2O budget, ~1.05-0.75 wt. %, prior to the melting. The preservation of

prograde garnet-rich assemblages required nearly complete melt loss (15-25 vol. %), interpreted to have occured at 1000-1020 ^{o}C and 2.2-2.4 GPa by garnet mode isopleths, followed by crystallization of small amounts of residual melt at 760 ^{o}C and 1.0 GPa. Phase formation and melt productivity were independently determined by experiments in the piston-cylinder apparatus at 850-1100 ^{o}C and 1.7-2.1 GPa. Both the thermodynamic calculations and phase equilibrium experiments suggest that the partial melt was produced by the dehydration melting: muscovite + quartz = melt + K-feldspar + kyanite. The presence of partial melt facilitated attainment of mineral equilibria at peak temperature thus eliminating any potential relics of early high-pressure phases such as phengite or omphacite. By contrast, adjacent mafic granulites and eclogites, which apparently share the same metamorphic path but have not undergone partial melting commonly preserve relics or inclusions of eclogite-facies mineral assemblages.

Keywords: felsic granulite, high-pressure metamorphism, partial melting, Bohemian Massif, Variscan orogeny

1. INTRODUCTION

High-pressure (HP) metamorphic rocks, and eclogite-facies rocks in particular, are frequently considered as key evidence for fossil subduction zone settings (Newton and Anderson, 1986; Möller et al., 1995). However, later episodes of the orogenic cycle during continental collision and subsequent collapse may lead to transformation of eclogite-facies HP rocks into granulites (Carswell and O'Brien, 1993; Kryza et al., 1996; Faryad et al., 2010). Many orogenic belts assumed to have formed by subduction-to-collision convergence preserve no or only a small portion of pristine HP-metamorphic rocks that have escaped subsequent thermal equilibration and can thus be used to reconstruct the complete geodynamic scenario. Frequently, felsic granulites and migmatites from pelitic or quartzofeldspathic precursors have re-equilibrated at low pressures (Waters, 1988; Bhattacharya and Kar, 2002; Nair and Chacko, 2002; Brown, 2006). In constrast, several recent studies of ultra-high pressure (UHP) metamorphic rocks proposed that crustal rocks can be buried to depths exceeding 100 km (Massonne, 2001; Sobolev et al., 2003; Zhang et al., 2003; Liou et al., 2005) provided that mineral equilibria were sufficiently preserved through their exhumation and granulite facies overprint.

The Bohemian Massif provides a unique opportunity for the investigation of the petrological record of the early convergence history because felsic granulites are closely associated in space and time with high-temperature (HT) eclogites and garnet peridotites in the Moldanubian and Saxothuringian zones. The UHP conditions, above 3.5 GPa, of mafic and

ultramafic rocks were already documented by HP mineral inclusions and conventional thermobarometric calculations in the Saxothuringian zone (Schmädicke and Evans, 1997; Massonne and Bautsch, 2004) and in the Moldanubian zone (Kotková et al., 1997; Nakamura et al., 2004; Medaris et al., 2006). The presence of microdiamond in gneisses from the Saxothuringian zone (Massonne, 1999; Massonne and Nasdala, 2003) proved that crustal rocks were subducted to a depth exceeding 140 km. However, the associated felsic and intermediate granulites yield peak pressures of 2.3 GPa at 1000-1020 ^{o}C in the Saxothuringian zone (Rötzler et al., 2004) or 1.6-1.8 GPa at 850-1000 ^{o}C in the Moldanubian zone (Kotková and Harley, 1999, 2010; Cook and O´Brien, 2001; Štípská and Powell, 2005; Tajčmanová et al., 2006; O'Brien, 2006, 2008), respectively. The interpretation of granulite protoliths and their possible prograde history, if attempted, have remained controversial: they were interpreted to represent H_2O-poor magmas crystallized at the base of the orogenic root, up to 1170 ^{o}C and 2.3 GPa (Vrána and Jakeš 1982; Vrána, 1989; Kotková and Harley, 1999, 2010; Janoušek et al., 2004, Janoušek and Holub, 2007; Kotková, 2007) or products of prograde metamorphism of granitic, rhyolitic or sedimentary precursors (Fiala et al., 1987; Vrána et al., 2005) that have experienced fluid-absent melting to a limited extent only (Roberts and Finger, 1997; Tropper et al., 2005; Vrána et al., 2009). Thus, the prograde metamorphic path of central European granulites remains unresolved but its understanding is essential for the geodynamic reconstruction of the Variscan collisional convergence.

To better constrain the metamorphic conditions of the high-pressure granulites we have chosen sample of felsic granulite with leucocratic and mesocratic layering for a detailed petrological and experimental study. The modal and compositional variability allows us to apply a larger number of phase equilibria and compare their consistency. The pressure-temperature paths were reconstructed from the garnet zoning and several equilibria between inclusions, porphyroblast core and rims, and matrix phases. In addition, the reaction progress and melt productivity at peak conditions were simulated by dehydration melting experiments in a piston cylinder apparatus at 900-1100 ^{o}C and 1.7-2.1 GPa.

2. GEOLOGICAL SETTING

Numerous occurrences of garnet- and kyanite-bearing felsic granulites are associated with metasedimentary gneisses and migmatites in the Variscan orogen of Europe (e.g., Pin and Vielzeuf, 1983; O'Brien and Rötzler, 2003). In the Moldanubian zone, most granulites and migmatites are situated along its eastern border (the Gföhl unit), in its southern (South Bohemian

granulite massifs) and central parts (the Kutná Hora complex; Fig. 1). The granulites are commonly associated and intimately imbricated with high-temperature eclogites and garnet- or spinel-bearing peridotites. In the interpretation of Schulmann et al. (2005), the Gföhl unit has formed by extrusion of lower crustal rocks from the continental collision root, and has been sandwiched within and/or between the Monotonous series and Varied groups (*cf*. Matte, 1986; Franke, 1989; Finger and Steyer, 1995).

The Kutná Hora complex (KHC) forms a 50 km long NW-SE oriented belt in the northern part of the Moldanubian zone and predominantly consists of high-grade metasediments that were migmatized to a variable degree. Based on its lithology and high-grade metamorphism, the complex has been correlated with the Gföhl unit in the eastern part of the Moldanubian zone (Synek and Oliveriová, 1993). From top to bottom, the KHC is represented by felsic and intermediate granulites (Běstvina and Miškovice granulite body) and migmatites (Malín unit), the Kouřim nappe, and by two, inner and outer, Micaschist zones. The Kouřim nappe is built up of a sequence of fine-grained leucocratic migmatites and gneisses that were strongly mylonitized. The inner Micaschist zone consists of mica schists to migmatites with mafic and ultramafic rocks and skarns that were affected by amphibolization and serpentinization. The outer Micaschist zone is represented by mica schists with lenses of amphibolites; this unit is underlain by the Monotonous and Varied groups of the Moldanubian zone.

The structural record in the Kutná Hora metamorphic complex indicates three stages of deformation (Synek and Oliveriová, 1993): the oldest event (D_1) is contemporaneous with the eclogite-facies metamorphism of metabasic rocks, (re)crystallization of garnet lherzolites and metamorphic crystallization of HP/HT granulites (Brueckner et al., 1991) and it is documented by rare steeply dipping relic planar fabrics S_1 in granulites (Nahodilová et al., 2005). Subsequent deformation event (D_2) reworked the older planar S_1 fabrics into a flat S_2 foliation dipping to NW or NE, facilitated local amphibolite-facies retrogression of mafic rocks, and was accompanied by extensive partial melting and migmatization of quartzofeldspathic rocks that generated kyanite-bearing granitic leucosomes. A late reactivation (D_3) affected the previous structural pattern including migmatitic structures and resulted in a local near-subhorizontal foliation (S_3) associated with low-temperature mylonitization.

A granulite body with well preserved subhorizontal S_2 foliation and metamorphic mineral assemblages is located at the Miškovice village (Fig. 1). It forms a *ca*. 50 x 20 m large exposure along a creek beneath the Cretaceous sedimentary cover. The grey coloured felsic granulites contain lenses, approximately 3 by 1 m in size, of dark intermediate granulites, which show continuous gradations to the predominant felsic variety. The felsic granulites are characterized by

modal layering where light-coloured (leucocratic), 2-5 cm wide layers enriched in quartz and feldspar alternate with darker (mesocratic) layers characterized by higher modal abundance of garnet, locally retrogressed to biotite (Fig. 2). The leucocratic and mesocratic layers are mostly parallel to the weak S_2 foliation of granulites, dipping 20^o to NNW.

3. ANALYTICAL AND EXPERIMENTAL METHODS

We have selected complementary samples of the layered granulites from the Miškovice granulite body for a detailed study: KKF27-l represents an approx. 8 cm thick leucocratic layer and KKF27-p comes from the adjacent grey-coloured mesocratic layer. The latter granulite variety was also used as starting material in our experimental study. The natural samples and experimental run products were analyzed by: (1) CAMECA SX 100 electron microprobe at the Institute of Geological Sciences, Masaryk University in Brno (Czech Republic) using the following standards: pyrope, spinel, olivine (Mg), andradite (Ca, Fe), almandine (Fe), jadeite, albite (Na), sanidine (K, Si), andalusite (Al), rhodonite (Mn), amphibole, TiO_2 (Ti), chromite (Cr), apatite (P), zircon (Zr) and NaCl (Cl). The operating voltage was 15 kV and the beam current was set to 10-30 nA. The beam was focused to a diameter of 1–5 μm, (2) CAMECA SX 100 electron microprobe at the Institute of Mineralogy and Crystal Chemistry, University of Stuttgart (Germany) using the following standards: pyrope (Si, Al, Mg), andradite (Ca, Fe), jadeite (Na), spessartine (Mn), K-silicate glass (K), Ba-silicate glass (Ba), NaCl (Cl) as well as natural rutile (Ti) and topaz (F). The operating voltage was 15 kV and the beam current was set to 10-15 nA. The beam was focused to a diameter of 1–2 μm except for micas for which an 8–10 μm wide beam was used to prevent the loss of alkalis, and (3) backscattered electron (BSE) images were obtained with a scanning electron microscope CamScan at the Institute of Petrology and Structural Geology, Charles University in Prague (Czech Republic). The initial composition of exsolved ternary feldspars was calculated by reintegrating exsolution lamellae and host feldspar compositions using the image analysis system Lucia G, v. 4.82, Laboratory Imaging Ltd. in Prague (Czech Republic). The whole-rock composition, necessary for thermodynamic calculation of pressure-temperature equilibria, cannot be obtained by conventional bulk analysis due to centimeter-scale layering and was calculated by mass balance from mode, measured by grid counting in thin section, and electron microprobe compositions of all rock-forming and accessory minerals (Tab. 1).

High-pressure experiments were performed in an end-loaded piston-cylinder apparatus at the Institute of Mineralogy and Petrography, University of Innsbruck (UIB), Austria and at the

Bayerisches Geoinstitut in Bayreuth (BGI), Germany using the mesocratic granulite KKF27-p with 0.07 wt. % H_2O defined by the modal abundance of biotite in the charge. Small rock chips were crushed, finely ground and run in gold (UIB) and platinum capsules (BGI), respectively. Experiments were performed in ½-inch talc-pyrex assemblies with tapered graphite furnace in order to minimize the instrumental temperature gradients. Temperature was monitored by the Pt-PtRh thermocouples; the reported pressures were corrected for the effect of assembly friction.

4. RESULTS

Both granulite samples contain two feldspars, garnet, biotite, kyanite and quartz as well as accessory amounts of rutile, zircon, apatite and monazite. Garnet, kyanite and mesoperthite form porphyroblasts, up to 2 mm in size, which are irregularly disseminated in the fine-grained matrix of feldspars and quartz. Two ternary feldspars, perthitic K-feldspar and anthiperthitic plagioclase were found as inclusions in garnet in both samples. None of the medium- to low-pressure aluminosilicates (e.g., sillimanite, sapphirine, spinel and muscovite) observed elsewhere in the Moldanubian granulites (Vrána, 1989; Kotková, 1993; O´Brien, 1999; Tajčmanová, et al., 2006) are present at this locality. In addition, the late-stage hydration is limited to local and rare formation of biotite clusters at the expense of garnet. The centimeter-scale compositional layering is due to the modal variation of mafic phases (garnet ± biotite and kyanite).

4.1. Mesocratic granulite (KKF27-p)

The mesocratic granulite layers are fine- to medium-grained, and consist of quartz and two feldspars together with abundant garnet, kyanite and biotite (Fig. 3a). The perthitic and antiperthitic ternary feldspars have partially recrystallized into discrete fine grains of plagioclase and K-feldspar.

Garnet forms up to 1.5 mm large grains which contain inclusions of quartz, feldspars and kyanite that mostly concentrate in the garnet rims (Fig. 3a,b) whereas rutile inclusions are present in the garnet cores as well as in kyanite. Garnet is rich in Fe and Ca; core to rim variations are as follows: $Grs_{41\rightarrow29}$ $Prp_{08\rightarrow15}$ Alm_{47} Sps_{01} with x_{Fe} = 0.86→0.75 (Fig. 4a, 5a; Tab. 2) where x_{Fe} = molar Fe/(Fe + Mg) and mineral abbreviations follow Whitney and Evans (2010). Garnets exhibit a relatively flat compositional profile in the core but record an increase in Prp and decrease in Grs end-member and in x_{Fe} towards the rim. The Alm concentrations show an initial increase followed by a decrease in outward direction.

Plagioclase occurs in the granulite in several forms – porphyroclasts, coronitic overgrowths on kyanite, matrix grains, and inclusions in other phases. Large plagioclase crystals show

compositional zoning from Ca-rich core ($An_{35;}$ Tab. 3) to Ca-poor rim (An_{14}; Fig. 6). Matrix grains of antiperthitic plagioclase show a similar zoning pattern (core→rim: $An_{24→16}$). Plagioclase rims exsolved from perthitic K-feldspar inclusions in garnet have composition similar to recrystallized grains in matrix (An_{13} Ab_{87} Or_{01}). Plagioclase inclusions in the garnet cores and rims yield composition An_{33-16} Ab_{66-83} Or_{02}. Plagioclase lamellae in the perthites correspond to An_{15} Ab_{83}. An outward decrease of Ca ($An_{33→14}$ $Ab_{66→85}$ Or_{01}) was also observed in a plagioclase corona around kyanite. The original composition of ternary feldspar porphyroclasts was reintegrated from the host plagioclase and K-feldspar lamellae (Fig. 3f) and it varies within An_{17-19} Ab_{57-62} Or_{20-26} (Fig. 6).

K-feldspar without pethitic lamellae, which occurs in the matrix as well as in the form of inclusions in kyanite or garnet~~rim~~, is nearly pure orthoclase with no measurable Ca content (Ab_{06-08} Or_{94-92}; Tab. 3). K-feldspar lamellae occurring in the antiperthites show a composition of Ab_{04} Or_{96}. Perthitic K-feldspar enclosed near the garnet rim (Fig. 3b,e) has, in contrast, relatively high Na content (Ab_{26} Or_{74}; Tab. 3) but becomes a nearly pure potassium end-member at the inclusion margin (Ab_{05} Or_{95}) where it borders with exsolved plagioclase grain (Fig. 6a). The reintegrated composition of a ternary feldspar that was preserved as inclusion in garnet (Fig. 3e) shows a rather low Ca content (An_{03} Ab_{36} Or_{61}).

Biotite forms individual grains that are aligned parallel to the metamorphic foliation, or it forms replacement products of garnet. Tabular symplectitic intergrowths of biotite + plagioclase were also observed. The x_{Fe} and Ti concentration in biotite varies in dependence on its textural position and relation to other minerals. Most of biotites in the matrix near garnet have x_{Fe} ~ 0.37 and Ti ~ 0.09-0.21 apfu. The lowest x_{Fe} value (0.23) and low Ti content (0.08 apfu) were observed in biotite that overgrew antiperthitic plagioclase. By contrast, biotite with x_{Fe} = 0.57 and Ti = 0.24 apfu occurs in the vicinity of rutile (Tab. 4).

Some garnets from the Miškovice granulite contain parallel columnar inclusions of K-feldspar (Fig. 3c) accompanied by an Al-rich phase (now decomposed to a clay mineral). Kyanite forms up to 1 mm large grains in the matrix or it is partly enclosed in garnet, and it locally contains rutile inclusions (Fig 3b).

4.2. Leucocratic granulite (KKF27-l)

The leucocratic granulite layers are dominated by quartz and feldspars, accompanied by up to 4 vol. % biotite and 11 vol. % garnet and accessory kyanite, rutile, zircon, ilmenite and iron sulphide. Antiperthitic plagioclase has only rarely been preserved and it commonly recrystallized to homogeneous plagioclase grains (Fig. 3d).

Two varieties of garnet occur in the light-coloured layers: (i) relics of large atoll grains with composition similar to those that occur in the mesocratic layers (high Ca content in the core). Core to rim variations are: $Grs_{39\rightarrow28}\,Prp_{08\rightarrow21}\,Alm_{41\rightarrow44}\,Sps_{01}$, x_{Fe} = 0.83→0.68). Atoll garnets host inclusions of perthitic feldspar coexisting with plagioclase and quartz; (ii) small garnet crystals in the matrix (~ 0.2 mm in size) with low Ca contents that also show a decrease in Ca towards the rim ($Grs_{27\rightarrow15}\,Prp_{22}\,Alm_{41\rightarrow55}\,Sps_{01}$, x_{Fe} = 0.65→0.72; Fig. 4a, 5b; Tab. 2). Biotite has x_{Fe} ranging from 0.31 (inclusions in garnet) to 0.52 (matrix grains; Tab. 4). The latter exhibits elevated Ti contents (0.28 apfu).

The plagioclase composition depends on its textural position and local equilibrium with other adjacent phases. Its composition varies from An_{03} in inclusions in garnet through An_{16} (small grains in the matrix), $An_{13\text{-}15}$ (antiperthite host), $An_{18\text{-}22}$ (rims around perthite inclusion in garnet) and An_{31} (fine grained coronitic overgrowths on kyanite). The compositions of antiperthitic plagioclase and K-feldspar lamellae were reintegrated to obtain the estimate for the original ternary feldspar $An_{10}\,Ab_{62}\,Or_{28}$ (Fig. 6). Plagioclase that forms tabular symplectitic intergrowths with biotite has composition of An_{25}.

K-feldspar forms individual grains in the matrix, inclusions in garnet, perthitic grains and lamellae in antiperthitic plagioclase. All K-feldspar grains exhibit low albite contents, $Ab_{04\text{-}10}$ (Tab. 3; Fig. 6b).

5. PRESSURE-TEMPERATURE EVOLUTION

We interpret the metamorphic history of the leucocratic and mesocratic granulite varieties by constructing the pressure-temperature (*P-T*) pseudosections, using changes in modal abundance and utilizing univariant equilibria and isopleths defined by mineral compositions. The *P-T* pseudosections were calculated in the system SiO_2-TiO_2-Al_2O_3-FeO-MgO-CaO-Na_2O-K_2O-H_2O (KNCFMASHT) system by Gibbs energy minimization (Connolly, 2005) using an internally consistent thermodynamic dataset for mineral end members and aqueous fluids (Holland and Powell, 1998), upgraded in 2003. We used the following non-ideal solution models: garnet (White et al., 2001), orthopyroxene (Powell and Holland, 1999), clinopyroxene (Green et al., 2007), ternary feldspar (Holland and Powell, 2003, modified in Section 7.1), biotite (White et al., 2007), muscovite (Coggon and Holland, 2002), and hydrous silicate melt (White et al., 2001, 2007). The effect of ferric iron was explored by adding oxygen as additional component to the system. Addition of up to 0.1 wt. % O leads to the stability of magnetite but has no significant effects on omphacite, garnet or biotite equilibria. Therefore, excess oxygen was not introduced in

our calcuations. MnO was not included in our system due to the lack of thermodynamic data for numerous Mn-bearing end-members and their solutions but their effect is deemed negligible due to the very small whole-rock MnO concentrations. The nine-component KNCFMASHT system is, therefore, taken as representative of the observed sample and mineral variation.

The *P*-*T* pseudosections for the mesocratic and leucocratic granulite layers, respectively, are shown in Fig. 7. Both phase diagrams show wide stability fields of quartz + K-feldspar + phengitic muscovite + kyanite + garnet + omphacite + rutile that are located above P = 1.3 GPa at T = 500 °C and P = 2.3 GPa at T = 1000 °C. The location of the low-pressure boundary of this assemblage depends on H_2O activity and it slightly shifts to higher pressures at lower H_2O activities. At medium pressures, the mineral assemblages are quartz + K-feldspar + plagioclase + garnet ± biotite + phengitic muscovite + rutile; the latter two phases would become replaced by sillimanite and ilmenite, respectively, at very low pressures. In the high-pressure granulite facies, both samples are predicted to become partially molten but they remain multiply saturated by quartz, two feldspars, kyanite, garnet and rutile, owing to the predicted small amount of the granitic melt formed.

Assuming no significant modification of composition of the garnet cores during decompression due to slow diffusivity of calcium (Chakraborty and Ganguly, 1992; Faryad and Chakraborty, 2005), we interpret the flat compositional profiles (Fig. 5) as a result of high-temperature reequilibration of original prograde metamorphic zoning. Similar Ca-rich, cores were also found in garnet from eclogite lenses in felsic granulites at Běstvina, located in the same metamorphic complex (Faryad, 2009). The measured Ca contents in the garnet cores of both samples are well reproduced in the pseudosections, at 980-990 ^{o}C and 2.4-2.5 GPa (Fig. 8). This is a narrow divariant representation of garnet formation by omphacite breakdown, as follows:

$$NaAlSi_2O_6\ (omph) + SiO_2\ (qtz) = NaAlSi_3O_8\ (fsp) \quad (1)$$

$$3\ Ca(Mg,Fe)Si_2O_6\ (omph) + 4\ Al_2SiO_5\ (ky) = (Mg,Fe)_3Al_2Si_3O_{12}\ (grt) + 3\ CaAl_2Si_2O_8\ (fsp) + SiO_2\ (qtz) \quad (2)$$

In both pseudosections, the modal amount of garnet increases by 4-5 vol. % in the mesocratic and leucocratic layer, respectively (Fig. 7). The enrichment in Mg and depletion in Ca observed in garnet rims (Fig. 5) is a record of increasing temperature and decreasing pressure due to the following equilibria – breakdown of grossular component and formation of Ca-bearing feldspar

$Ca_3Al_2Si_3O_{12}$ (grt) = $CaAl_2Si_2O_8$ (fsp) + Al_2SiO_5 (ky) + SiO_2 (qz) (3)

and Mg-Fe exchange between partial melt and garnet. The pressure conditions of the garnet rim formation can be further constrained by the garnet-feldspar-kyanite-quartz univariant (Eq. (3)). Using the thermodynamic dataset of Holland and Powell (1998), updated in 2004, and non-ideal solution models of Diener et al. (2008) and Holland and Powell (2003) as revised in Section 7.1, the Ca contents in the garnet rim and reintegrated ternary feldspar composition for the assemblage in the mesocratic layer yeild P = 2.1 GPa and T = 1020 ^{o}C.

Thermometric constraints on the peak temperatures are provided by the ternary feldspar solvus. The reintegrated feldspar compositions in the mesocratic layer (An_{17-19} Ab_{57-62} Or_{20-26}), lie on the solvus along a curve with steep dP/dT slope, located at 1000-1020 ^{o}C for an expected pressure range of 1.8-2.2 GPa (Fig. 8a). Its intersection with Eq. (2) reveals the minimum peak temperature. In the leucocratic layer, an analogous procedure has been adopted, that is, formation of a single ternary feldspar from K-feldspar and plagioclase. This univariant equilibrium is located at 1010 ^{o}C for a pressure range of 1.7-2.1 GPa, thus defining a minimum peak temperature for the formation of ternary feldspar (Fig. 8b).

In the granulite facies, mineral assemblages of both samples correspond to a large stability field of quartz, K-feldspar, plagioclase, garnet, rutile and partial melt (Fig. 7), in agreement with petrographic observations. The amount of partial melt, predicted to be consistent with the garnet-biotite assemblage, is very low, less than 3 vol. % (Fig. 7). Phase compositions do not change appreciably because the entire assemblage is low-variant and there is only a limited number of chemical components (elements) that are shared between and thus can be exchanged by several phases. In detail, garnet is the by far predominant host of the MgO and FeO whole-rock budget and exchange of these components with a small amount of leucogranitic melt does not have a detectable effect on its composition and zonation. Ternary feldspar would have undergone unmixing with decreasing temperature at 1.9-2.2 GPa but this process is obscured by low-temperature diffusional re-equilibration affecting feldspar grains, especially in the rock matrix.

During cooling, at the granulite-amphibolite facies boundary, biotite becomes stable as a product of incongruent melt crystallization accompanied by garnet breakdown, as follows:

Grt + melt = Bt + Kfsp + Pl + Qtz (4)

The reaction proceeds until the melt is completely consumed, therefore, its amount determines the resulting ratio of garnet and biotite at subsolidus conditions. The temperature of biotite crystallization was independently estimated by the Mg-Fe exchange thermometry between biotite and garnet:

$Fe_3Al_2Si_3O_{12}$ (grt) + $KMg_3AlSi_3O_{12}(OH)_2$ (bi) = $Mg_3Al_2Si_3O_{12}$ (grt) + $KFe_3AlSi_3O_{12}(OH)_2$ (bi) (5)

2 $Fe_3Al_2Si_3O_{12}$ (grt) + 3 $KMg_2FeAlSi_3O_{12}(OH)_2$ (bi) =
2 $Mg_3Al_2Si_3O_{12}$ (grt) + 3 $KFe_3AlSi_3O_{12}(OH)_2$ (bi) (6)

These two equilibria were solved simultaneously using the thermodynamic data set of Holland and Powell (1998), updated in 2004, and non-ideal solution models of Diener et al. (2008) and White et al. (2007) and yield equilibrium temperatures of 720-810 ^oC at a pressure range of 1.0-1.3 GPa that are consistent with its crystallization at the dehydration solidus (Figs. 7 and 8). To summarize, the *P-T* pseudosections, modal abundance and several univariant equilibria utilizing phase compositions allow us to reconstruct the metamorphic path of the well preserved granulites at the Miškovice locality. The reconstructed paths from the mesocratic and leucocratic layer are mutually consistent (Fig. 8), and the amount of partial melt predicted to be retained at the solidus was similar in both rock types, 1-2 vol. %.

6. EXPERIMENTAL RESULTS

We have performed four experiments using the mesocratic variety of the felsic granulite in the piston-cylinder apparatus in order to document the garnet and ternary feldspar composition and melt productivity at *P-T* conditions inferred from pseudosections for phengite dehydration melting (Tab. 5). The choice of experimental pressure and temperature was guided by pseudosection modelling and chosen to correspond to the coexistence of garnet + kyanite + silicate melt in addition to quartz, K-feldspar and plagioclase. Three experiments were conducted at 850 ^oC and 1.7 GPa, and 900 ^oC and 2.1 GPa, respectively, whereas the fourth run was pre-conditioned at 1100 ^oC and equilibrated at 900 ^oC and 2.1 GPa. All experiments produced new high-*PT* mineral assemblage and silicate melt, in addition to relics of original rock-forming minerals (Fig. 9). The relict phases were quartz, antiperthitic plagioclase, K-feldspar, garnet, kyanite, biotite with accessory amounts of rutile, apatite and iron sulphide. Several grains of clinopyroxene have also formed due to local equilibrium effects (Fig. 9f).

6.1. Feldspars

The formation of feldspar and attainment of its equilibrium composition was facilitated by the presence of partial melt (Tab. 6, Fig. 10). Plagioclase is depleted in potassic end-member ($An_{15\text{-}21}$ $Ab_{71\text{-}80}$ $Or_{05\text{-}12}$) but a substantial increase in orthoclase component was recorded in run #4 ($An_{16\text{-}09}$ $Ab_{71\text{-}52}$ $Or_{13\text{-}39}$) that was pre-conditioned at 1100 ^{o}C. This observation is a consequence of feldspar solvus closure with increasing temperature. Alkali feldspar grains have composition similar in all experiments and span the range of $An_{02\text{-}03}$ $Ab_{32\text{-}38}$ $Or_{59\text{-}65}$. We note that composition of feldspars in runs #3 and #4 corresponds closely to that of reintegrated antiperthite (An_{19} Ab_{62} Or_{20}) and perthite (An_{03} Ab_{36} Or_{61}) in natural sample (Fig. 3e, f).

6.2. Mafic minerals

Garnet composition provides a sensitive record of local equilibrium with surrounding phases. As equilibrium was approched in experiments, some garnet grains may have preserved compositional zoning. Generally, new garnet grains (Fig. 9) are characterized by elevated Mg and lowered Ca contents that are in agreement with those found in natural samples. In run #1, the Mg contents decrease and those of Ca increase from the core to the rim ($Grs_{09\rightarrow16}$ $Prp_{51\rightarrow44}$ $Alm_{38\rightarrow39}$; x_{Fe} = 0.43→0.47; Tab. 7; Fig. 11). In run #4 performed with a down-temperature step the newly formed garnet is enriched in Ca and Fe ($Grs_{23\text{–}33}$ $Prp_{18\text{–}12}$ $Alm_{48\text{–}40}$ x_{Fe} = 0.73–0.77; Tab. 7) in good agreement with composition of small garnet grains in the leucocratic variety as well as garnet rims in the mesocratic variety (Fig. 7). Breakdown of original Ca-rich garnet has locally led to the (metastable) formation of clinopyroxene and amphibole in run products. Subcalcic clinopyroxene shows a moderate enrichment in jadeite component (Jd_{36} Di_{41} Hd_{11} En_{10} Fs_{03}) whereas amphibole corresponds to pargasite (^{VI}Al = 1.6 apfu, ^{M4}Na = 0.44 apfu). Among accessory phases, monazite formed by replacement of allanite.

New biotite, which formed by local recrystallization of pre-existing biotite flakes, is poor in Fe (x_{Fe} = 0.19) and shows elevated Ti contents (0.26 apfu). Kyanite has formed in runs #2 through 4 in the form of needles that are preferentially concentrated in melt pools (Fig. 9b, c, e).

6.3. Silicate melt

Partial melt formed a network or individual melt pools between recrystallized feldspars, quartz and mafic phases (Fig. 9a, b). It has peraluminous granitic composition with 68.5–72.1 wt. % SiO_2, 14.7-15.5 wt. % Al_2O_3, 0.71-1.30 wt. % CaO and 2.16-4.13 wt. % K_2O (Fig. 12a). The abundance of ferromagnesian components is very low, 0.32-0.71 wt. % $MgO+FeO^{TOT}$ (Fig. 12b).

In comparison to results obtained on a bulk composition corresponding to granulites in the Southern Bohemian Massif and at similar temperatures and pressures (Tropper et al., 2005), melt composition in our study is more SiO_2-rich (68.5–72.1 *vs*. 65.4–68.4 wt. %) and more leucocratic (0.32–0.71 *vs*. 0.88–1.65 wt. % MgO + FeO^{TOT}). These observations suggest that the MgO and FeO^{TOT} abundances were controlled by local availability of garnet and biotite in our starting material and do not represent maximum solubilities in the melt buffered by solid phases in excess (*cf*. Grochau and Johannes, 1997).

7. DISCUSSION

7.1. Ternary feldspar equilibria at high temperatures and pressures

Phase equilibria of feldspars and their solvus in the or-ab-an ternary represent one of the most important thermometers for granulites (Štípská and Powell, 2005; O'Brien, 2008). The existing ternary solution models (Fuhrman and Linsdley, 1988; Lindsley and Nekvasil, 1989; Elkins and Grove, 1990; Holland and Powell, 2003; Benisek et al., 2010) tend to diverge at progressively increasing temperatures, and predict locations of ternary solvi that differ by as much as 10 mol. % at 900 ^oC, which causes the estimates of equilibrium temperature based on ternary feldspar composition to differ by up to 120 ^oC. At temperatures of 900-1100 ^oC and pressures above 2 GPa, the locations of ternary feldspar solvi are inconsistent up to 50 mol. %, probably due to poorly constrained excess volumes of mixing.

Recently, Benisek et al. (2010) proposed a new thermodynamic solution model that re-evaluates all caloric and volumetric non-ideal contributions and advocates its application to feldspars in granulites facies rocks. At 900 ^oC and 0.1-1.0 GPa, this model substantially differs from all existing thermodynamic calibrations, and it predicts a significant shift of the ternary solvus from the albite end-member towards the centre of the composition space (Benisek et al., 2010; their Figs. 1 and 2). As a consequence, the feldspar equilibrium temperatures are by ~100 ^oC lower than from other calibrations (Fuhrman and Lindsley, 1988; Elkins and Grove, 1990; Holland and Powell, 2003) and this discrepancy has been attributed by Benisek et al. (2010) to incomplete equilibrium in previous experimental work.

In addition to experimental runs reported in Table 5, we have carried out 5 new experiments with synthetic glass An_{20} Ab_{46} Or_{35} seeded with 3 wt. % K-feldspar and 3 wt. % plagioclase, and with 0.9-2.4 wt. % H_2O added at 900, 1000 and 1100 ^oC, and 2 GPa. The presence of small amount of H_2O leads to the formation of partial melt, which facilitates attainment of equilibrium. All runs produced a three-phase assemblage of K-feldspar, plagioclase and partial melt, and experimental results are summarized in Fig. 13a. The location of

experimental isotherms at 900, 1000 and 1100 ^{o}C is satisfactorily reproduced by the asymmetric van Laar model rather than by the asymmetric Margules formalism with ternary terms. The termodynamic model of Holland and Powell (2003) was, therefore, recalibrated using the new experimental data. The location of the solvus isotherms in the ternary space strongly depends on the interaction term between $KAlSi_3O_8$ and $CaAl_2Si_2O_8$ and its temperature dependence, whereas other binary interactions have much smaller influence. The interaction parameter $W_{\text{or-an}}$ was fitted as follows:

$$W_{\text{or–an}} = 75450 - 32.75T \quad (7)$$

where T is temperature in Kelvin, based on current experimental data, high-temperature calorimetry (Benisek et al., 2003) and liquidus equilibria of the K-feldspar-anorthite binary (Nekvasil and Carroll, 1993). The existence of positive excess entropy of mixing is also characteristic for the $KAlSi_3O_8$-$NaAlSi_3O_8$ binary (Haselton et al., 1983; Hovis et al., 1991; Holland and Powell, 2003; Benisek et al., 2004), and it most likely originates from progressive disordering on tetrahedal sites at high temperature, which is not included in configurational entropy for simple molecular mixing with short-range order.

In Fig. 13b, we plot solvus isotherms at 800-1000 ^{o}C and 2 GPa for several solution models together with our experimental results. The revised solvus isotherms are in better agreement with those of Elkins and Grove (1990), also based experimentally, and differ from the model of Benisek et al. (2010), supported by calorimetry and X-ray diffraction at 1 atm. Importantly, the re-integrated ternary feldspar compositions obtained in this study are located very close to our experimental results at 1000 ^{o}C and 2.0 GPa using natural and additional synthetic materials. The effect of the revised model of Holland and Powell (2003) and Benisek et al. (2010) on the *P-T* estimates for the mesocratic granulite in this study is illustrated in Fig. 14. When the latter thermodynamic formulation is used, the pressure estimates decrease marginally (by 0.1-0.2 GPa) but peak temperatures decrease from 1020 to 900 ^{o}C.

7.2. Whole-rock H_2O content and melt loss during the granulite evolution

The whole-rock H_2O concentrations commonly used in phase equilibrium calculations are those determined on the exhumed rocks. In our study, the estimated H_2O contents are defined by the amount of biotite that formed along the cooling path, when a small amount of partial melt preserved in the granulite solidified. By contrast, the initial whole-rock H_2O budget determines the melt productivity during dehydration melting reactions (Vielzeuf and Holloway, 1988; Holtz

and Johannes, 1991, 1994; Thompson, 1996; Holtz, et al., 2001). At low whole-rock H_2O concentrations, generally < 1 wt. %, the melt productivity at peak temperature is below ~30 vol. %, and the rock remains multiply saturated by quartz, K-feldspar, plagioclase, garnet, kyanite and rutile (not shown). A high amount of saturating phases, that is, low variance causes such asemblages to be insensitive to the amount of the melt. Therefore, the actual melt fraction and the related whole-rock H_2O budget during peak conditions cannot be estimated from petrological observations and mineral compositions.

Felsic granulites in the Kutná Hora complex originated either from siliciclastic sediments (Vrána et al., 2005) or represent SiO_2-rich calc-alkaline metaigneous rocks (Janoušek et al., 2004). We have calculated the maximum H_2O concentrations in the pressure-temperature space defined by fluid saturation (Fig. 15). For the reconstructed *P-T* path, the granulite precursor contains 0.75-1.10 wt. % H_2O, as maximum values, stored in phengite prior to the high-pressure dehydration melting. The former existence of phengite has been documented by its preservation as inclusions in garnet grains with prograde chemical zoning in felsic granulites elsewhere in the Kutná Hora complex (Faryad et al., 2010). We have used these results to constrain the maximum melt productivity in the granulite facies. The amount of partial melt formed along the reconstructed P-T path increases to 18-26 vol. % as the peak temperature (1020 ^{o}C) was approached (Fig. 15). The predicted melt fraction is in good agreement with estimates based on geochemical mass balance from other granulite occurrences in the Bohemian Massif (Kotková and Harley, 2010).

If the melt were preserved in the granulite, its amount would have decreased to 8-12 vol. %, when biotite has crystallized during decompression and cooling. As a consequence, melting could be observed texturally and H_2O released upon melt crystallization *in situ* would convert the original mineral assemblage into a biotite-bearing gneiss (White et al., 2001). Instead, our samples preserve the granulite-facies mineral assemblage (garnet with minor amounts of biotite only) and this indicates inavailability of H_2O to complete this reaction because the hydrous melt was lost.

In order to constrain the extent and conditions of the melt migration, we have calculated a composition section along our reconstructed metamorphic path (Fig. 16). The composition scale ranges from an anhydrous, melt-free mesocratic granulite to a mixture of 80 % granulite and 20 % calculated partial melt (by mass), which contains 2 wt. % H_2O in the bulk; the melt composition was that calculated to be in equilibrium with the mineral assemblage at peak temperature.

The preserved granulite assemblage with abundant garnet and minor biotite corresponds to ~1-3 vol. % melt existing at the solidus at 740-770 ^{o}C and 1.0-1.2 GPa. If the granulite precursor had contained a maximum of 1.05 wt. % H_2O in the eclogite facies prior to the phengite dehydration melting, about 15-25 vol. % melt must have been lost during decompression path. The conditions of the melt loss can be constrained by considering that mineral phases with preserved prograde chemical zoning did not dissolve along the *P-T* path, that is, the melt loss could have only occurred under conditions, which intersect progressively higher isopleths of their mode. The melt loss path in Fig. 16 must have a more gentle slope than that of garnet mode isopleths. This implies that the melt loss occurred early in the granulite facies, from 1000 ^{o}C and 2.2 GPa to 1020 ^{o}C and 2.0 GPa, simultaneously with progressive heating and melt formation (*cf*. Fig. 15).

Although physical aspects of the melt segregation still remain controversial (Watson and Brenan, 1987; Holness, 1993; Laporte et al., 1997; Watson, 1999), it has been proposed that sites of initial melting situated along appropriately oriented multiphase grain boundaries weaken as melting progresses (Rabinowicz and Vigneresse, 2004). Shear instabilities may develop at these sites and/or intrinsic anisotropy of permeability facilitate nucleation and lateral growth of melt pores after some critical volume of the melt was achieved. These selective sites of strain accommodation grow to form melt-rich layers and hence melt is concentrated in these layers driven by the difference in normal stress, further enhancing their ability to accommodate strain. Despite that deformation substantially reduces the melt fraction in the source region, it is probable that at the end of a dehydration melting event, some liquid (at least a few tenths of vol. %) remains trapped in the source rock (Vielzeuf and Schmidt, 2001). In addition to be responsible for the formation of foliation-parallel modal variations, the presence of the partial melt in the both types of layers probably facilitates the attainment of equilibrium during granulite facies overprint, as already proposed for phengite and clinopyroxene breakdown in ultra-high pressure pelites of the Greenland Caledonides (Lang and Gilotti, 2007). Such melt-mediated mechanism may provide explanation for the absence of relics of eclogite-facies mineral assemblages (e.g., phengite, omphacite) in the felsic granulites and their presence (e.g., diopside replacing omphacite) in the adjacent mafic varieties and eclogites that have not undergone partial melting. In addition to parallel modal layering, granulites at our locality contain discordant veins of coarse-grained quartzofeldspathic material that cross cut the granulite foliation thus indicating local pathways of melt migration and escape.

The formation of foliation-parallel leucocratic bands and subsequent progressive coarsening of mineral grains as well as the increase of the modal amounts of quartz and feldspars indicate

that syndeformational melting occurred contemporaneously with a decrease in pressure, i.e., during orogenic exhumation. These observations on intimate relationships between the presence of melt, localization of deformation and melt migration further strengthen the feedback relations between melting and deformation (see Brown and Rushmer, 1997; Brown and Solar, 1998).

7.3. Natural observations *vs*. experimental results

Our thermodynamic modeling of phase equilibria indicates that phengite dehydration melting commenced along a prograde path from eclogite to granulite facies at $T \sim 940$ °C and $P = 2.6$ GPa. Our samples contain rare garnet-plagioclase symplectites, retrogressed to biotite-plagioclase intergrowths, which are interpreted to result from phengite breakdown (Groppo et al., 2007; Faryad et al., 2009). Importantly, the felsic granulites from the Kutná Hora complex contain phengite inclusions in garnet grains that were enclosed at this stage as evidenced by preserved prograde chemical zoning. Our experiments performed along the dehydration melting ($T = 900$ °C and $P = 1.7$-2.1 GPa, runs #2-4 in Tab. 5) show formation of granitic partial melt and new kyanite. These results are consistent with the equilibrium:

muscovite + quartz = melt + K-feldspar + kyanite (8)

which was independently proposed by Tropper et al. (2005) for the formation of felsic granulites in the Moldanubian zone.

The natural granulite samples contain recrystallized feldspars: K-feldspar (Ab_{08} Or_{92}) and plagioclase ($An_{16\text{-}13}$ $Ab_{84\text{-}87}$ Or_{01}; Fig. 3a, 6a, b; Tab. 3) whose composition was reintegrated to obtain the original ternary feldspar composition: An_{03} Ab_{36} Or_{61} and $An_{10\text{-}19}$ $Ab_{57\text{-}62}$ $Or_{20\text{-}28}$ from perthitic K-feldspar and antiperthitic plagioclase, respectively (Fig. 3e,f). The reintegrated composition of ternary feldspar is very close to that obtained experimentally at 900 °C and 2.1 GPa (run #3 and 4; Tab. 6; Fig. 10) despite possible uncertainties resulting from modification during decompression and subsequent recrystallization.

Ca-rich garnets, which formed along the HP prograde path during the phengite dehydration melting, were found in the mesocratic layers or as rare unstable relics with atoll shapes in the leucocratic layers. By contrast, small garnet grains that formed newly in the leucocratic portions and also in the melt-bearing experimental runs lack the Ca enrichment but have elevated Mg and Fe concentrations, consistent with *P*-*T* conditions of the dehydration melting. Small garnet grains formed in the quartz + ternary feldspar + melt pools in our experimental runs #3 and 4 also show composition similar to that found in the leucocratic layers (Fig. 11). Therefore, the lack of Ca-

rich cores indicates nucleation and growth of garnets in natural samples in the presence of partial melt, as indicated by pseudosection modelling.

7.4. Geodynamic implications for Variscan collision and exhumation in the Bohemian Massif

The metamorphic history and preservation of peak mineral assemblages of granulites in the Bohemian Massif have been subject of long-lasting discussions (see Kotková, 2007 and O'Brien, 2008, for reviews). The *P-T* conditions of 1.2 GPa and 800 ^{o}C were routinely recorded as minimum estimates for the central European granulites whereas peak pressures and temperatures as high as ~2.3 GPa and 1100-1200 ^{o}C were reported, for instance, from the occurrences in the Saxothuringian zone (Rötzler et al., 2004). The high-pressure felsic granulites of the Moldanubian zone in the Bohemian Massif are intimately associated with their mafic counterparts, eclogites and garnet-bearing pyroxenites and peridotites (e.g., Nakamura et al., 2004; Medaris et al., 2005; Štípská et al., 2006; Ackerman et al., 2009; Faryad et al., 2009). Phase assemblages of eclogite lenses enclosed in felsic granulites in the Kutná Hora complex record a prograde metamorphic history through ultra-high pressures, 3.3 to 4.0 GPa (Nakamura et al., 2004; Faryad, 2009), and spatially associated mafic granulites contain diopside, which represents relics after omphacite breakdown during decompression (Faryad et al., 2010).

Our reconstructed clockwise metamorphic path from 2.5 GPa for felsic granulites is consistent with those of mafic granulites and eclogites in the Kutná Hora complex and it points out to a shared exhumation history of these units (Carswell and O´Brien, 1993; Cooke and O´Brien, 2001; O´Brien and Rötzler, 2003; Schulmann et al., 2005). This present-day spatial association of metasedimentary, calc-alkaline metaigneous, oceanic-crust and upper mantle fragments is a result of tectonic amalgamation in the continental root during the Variscan convergence at 351–338 Ma (Kröner et al., 1988; Brueckner et al., 1991; Kotková et al., 1996; Kröner et al., 2000; Schulmann et al., 2005, 2009). According to our interpretations and previous studies by Roberts and Finger (1997), Tropper et al. (2005), Janoušek et al. (2006) the tectonic assembly and subsequent exhumation of high-pressure units to mid-crustal levels took place in the presence of a partial melt in felsic granulites. The presence of partial melt in felsic granulites may have exerted primary rheological control on rheological weakening during incorporation of the lenses and boudins of mafic and ultramafic metamorphics in felsic granulite units. This case study provides an example of subducted crustal fragments, which were amalgamated with oceanic and mantle-derived UHP rocks in a subduction channel, detached and exhumed from a

collisional orogenic root (Štípská et al., 2004, 2008; Schulmann et al., 2005, 2008; Franěk et al., 2006; Racek et al., 2006; O'Brien, 2008; Schulmann et al., 2009; Faryad, 2011).

8. ACKNOWLEDGEMENTS

This study was financially supported by the research projects of the Ministry of Education of the Czech Republic MSM 0021620855 and the Czech Geological Survey Internal Research Project 323500, the Charles University Grant Agency 258/2005/B-GEO/PrF (to R. N.), the Czech Science Foundation 205/06/0688 and 210/10/0249 (to S. W. F.) and 205/09/P135 (to D.D.). We theank Alexander Proyer, Erling Kravna, Hans-Joachim Massonne and an anonymous reviewer for their thoughtful reviews.

9. REFERENCES

Ackerman, L., Jelínek, E., Medaris, G. Jr., Ježek, J., Siebel, W., Strnad, L., 2009. Geochemistry of Fe-rich peridotites and associated pyroxenites from Horni Bory, Bohemian Massif: Insights into subduction-related melt-rock reactions. Chemical Geology 259, 152-167.

Benisek, A., Kroll, H., Cemič, L., Kohl, V., Breit, U., Heying, B., 2003. Enthalpies in (Na, Ca)- and (K, Ca)-feldspar binaries: a high temperature solution calorimetric study. Contributions to Mineralogy and Petrology 145, 119-129.

Benisek, A., Kroll, H., Cemič, L., 2004. New developments in two-feldspar thermometry. American Mineralogist 89, 1496-1504.

Benisek, A., Dachs, E., Kroll, H., 2010. A ternary feldspar-mixing model based on calorimetric data: development and application. Contributions to Mineralogy and Petrology 160, 327-337.

Bhattacharya, S., Kar, R., 2002. High-temperature dehydration melting and decompressive P-T path in a granulite complex from the Eastern Ghats, India. Contributions to Mineralogy and Petrology 143, 175-191.

Brown, M., 2006. Duality of thermal regimes is the distinctive characteristic of plate tectonics since the Neoarchean. Geology 34, 961-964.

Brown, M., Rushmer, T., 1997. The role of deformation in the movement of granite melt: views from the laboratory and the field, in: Holness, M.B. (ed.), Deformation-Enhanced Fluid Transport in the Earth's Crust and Mantle. The Mineralogical Society Series 8, London: Chapman and Hall, pp. 111-144.

Brown, M., Solar, G.S., 1998. Granite ascent and emplacement during contractional deformation in convergent orogens. Journal of Structural Geology 20, 1365-1393.

Brueckner, H.K., Medaris, L.G., Bakun Czubarow, N., 1991. Nd and Sr age and isotope patterns from Variscan eclogites of the eastern Bohemian Massif. Neues Jahrbuch für Mineralogie, Abhandlungen 163, 169-196.

Carswell, D.A., O´Brien, P.J., 1993. Thermobarometry and geotectonic significance of high-pressure granulites: examples from the Moldanubian Zone of the Bohemian Massif in Lower Austria. Journal of Petrology 34, 427-459.

Chakraborty, S., Ganguly, J., 1992. Cation diffusion in aluminosilicate garnets – experimental-determination in spessartine-almandine diffusion couples, evaluation of effective binary diffusion-coefficients, and applications. Contributions to Mineralogy and Petrology 111, 74-86.

Coggon, R., Holland, T.J.B., 2002. Mixing properties of phengitic micas and revised garnet-phengite thermobarometers. Journal of Metamorphic Geology 20, 683-696.

Connolly, J.A.D., 2005. Computation of phase equilibria by linear programming: a tool for geodynamic modeling and its application to subduction zone decarbonation. Earth and Planetary Science Letters 236, 524-541.

Cooke, R. A., O'Brien, P. J., 2001. Resolving the relationship between high P-T rocks and gneisses in collisional terranes: an example from the Gföhl gneiss-granulite association in the Moldanubian Zone, Austria. Lithos 58, 33-54.

Diener, J. F. A., White, R. W., Powell, R., 2008. Granulite facies metamorphism and subsolidus fluid-absent reworking, Strangways Range, Arunta Block, central Australia. Journal of Metamorphic Geology, 26, 603-622.

Elkins, L.T., Grove, T.L., 1990. Ternary feldspar experiments and thermodynamic models. American Mineralogist, 75, 544-559.

Faryad, S.W., 2009. The Kutná Hora Complex (Moldanubian zone, Bohemian Massif), a composite of crustal and mantle rocks subducted to HP/UHP conditions. Lithos 109, 193-208.

Faryad, S.W., 2011. Distribution and geological position of high-/ultrahigh-pressure units within the European Variscan Belt: a review, in: Dobrzhinetskaya, L., Faryad, S.W., Wallis, S., Cuthbert, S. (Eds.), Ultrahigh Pressure Metamorphism: 25 Years After the Discovery of Coesite and Diamond, Elsevier, pp. 361-397.

Faryad, S.W., Chakraborty, S., 2005. Duration of Eo-Alpine metamorphic events obtained from multicomponent diffusion modeling of garnet: a case study from the Eastern Alps. Contributions to Mineralogy and Petrology 150, 306-318.

Faryad, S.W., Dolejš, D., Machek M., 2009. Garnet exsolution in pyroxene from clinopyroxenites in the Moldanubian zone: constraining the early pre-convergence history of ultramafic rocks in the Variscan orogen. Journal of Metamorphic Geology, 27, 655-671.

Faryad, S.W, Nahodilová, R., Dolejš, D., 2010. Incipient eclogite facies metamorphism in the Moldanubian granulite recorded by inclusion patterns in garnet. Lithos 114, 54-69.

Fiala, J., Matějovská, O., Vaňková, V., 1987. Moldanubian granulites – source material and petrogenetic considerations. Neues Jahrbuch für Mineralogie, Abhandlungen 157, 133-165.

Finger, F., Steyer, H.P., 1995. A tectonic model for the eastern Variscides: indications from a chemical study of amphibolites in the south-eastern Bohemian Massif, Austria. Geologica Carpathica 46, 1-14.

Franěk, J., Schulmann, K., Lexa, O., 2006. Kinematic and rheological model of exhumation of high pressure granulites in the Variscan orogenic root: example of the Blanský les granulite, Bohemian Massif, Czech Republic. Mineralogy and Petrology 86, 253-276.

Franke, W., 1989. Variscan plate-tectonics in central Europe – current ideas and open questions. Tectonophysics 169, 221-228.

Franke, W., 2000. The mid-European segment of the Variscides: tectonometamorphic units, terrane boundaries and plate tectonic evolution, in: Franke, W. (Eds.), Orogenic Processes: Quantification and Modelling in the Variscan Belt. Geological Society of London: Special Publications 179, pp. 35-61.

Fuhrman, M.L., Lindsley, D.H., 1988. Ternary feldspar modeling and thermometry. Americal Mineralogist 73, 201-215.

Green, E.C.R., Holland T.J.B., Powell, R., 2007. An order-disorder model for omphacitic pyroxenes in the system jadeite-diopside-hedenbergite-acmite, with applications to eclogite rocks. American Mineralogist 92, 1181-1189.

Grochau, B., Johannes, W., 1997. Stability of phlogopite in granitic melts, an experimental investigation. Contributions to Mineralogy and Petrology 126, 315-330.

Groppo, C., Lombardo, B., Rolfo, F., Pertusati, P., 2007. Clockwise exhumation path of granulitized eclogites from the Ama Drime range (Eastern Himalayas). Journal of Metamorphic Geology 25, 51-75.

Haselton, H.T., Hovis, G.L., Hemingway, B.S., Robie, R.A., 1983. Calorimetric investigation of the excess entropy of mixing in analbite-sanidine solutions: Implications for Na,K short range order and two-feldspar thermometry. American Mineralogist 68, 398-413.

Holland, T.J.B., Powell, R., 1998. An internally consistent thermodynamic data set for phases of petrological interest. Jornal of Metamorphic Geology 16, 309–343.

Holland, T.J.B., Powell, R., 2003. Activity-composition relations for phases in petrological calculations: an asymmetric multicomponent formulation. Contributions to Mineralogy and Petrology 145, 492-501.

Holness, M.B., 1993. Temperature and pressure-dependence of quartz aqueous fluid dihedral angles – the control of adsorbed H_2O on the permeability of quartzites. Earth and Planetary Science Letters 117, 527-544.

Holtz, F., Johannes, W., 1991. Genesis of peraluminous granites. I. Experimental investigation of melt compositions at 3 and 5 kb and various H_2O activities. Journal of Petrology 32, 935-958.

Holtz, F., Johannes, W., 1994. Maximum and minimum water contents of granitic melts – implications for chemical and physical properties of ascending magmas. Lithos 32, 149-159.

Holtz, F., Johannes, W., Tamic, N., Behrens H., 2001. Maximum and minimum water contents of granitic melts generated in the crust: a reevaluation and implications. Lithos 56, 1-14.

Hovis, G.L., Delbove, F., Bose, M.R., 1991. Gibbs energies and entropies of K-Na mixing for alkali feldspars from phase equilibrium data: Implications for feldspar solvi and short-range order. American Mineralogist 76. 913-927.

Hrouda, F., Faryad, S.W., Chlupáčová, M., Jeřábek, P., Kratinová, Z., 2009. Determination of field-independent and field-dependent components of anisotropy of susceptibility through standard AMS measurement in variable low fields II: An example from the ultramafic body and host granulitic rocks at Bory in the Moldanubian Zone of Western Moravia, Czech Republic. Tectonophysics 466, 123-134.

Janoušek, V., Holub, F.V., 2007. The causal link between HP-HT metamorphism and ultrapotassic magmatism in collisional orogens: case study from the Moldanubian Zone of the Bohemian Massif. Proceedings of the Geologists Association 118, 75-86.

Janoušek, V., Finger, F., Roberts, M., Frýda J., Pin, C., Dolejš, D., 2004. Deciphering the petrogenesis of deeply buried granites: whole-rock geochemical constraints on the origin of largely undepleted felsic granulites from the Moldanubian Zone of the Bohemian Massif. Transactions of the Royal Society of Edinburgh: Earth Sciences 95, 141-159.

Janoušek, V., Gerdes, A., Vrána, S., Finger, F., Erban, V., Friedl, G., Braithwaite, C.J.R., 2006. Low-pressure granulites of the Lišov Massif, Southern Bohemia: Visean metamorphism of Late Devonian plutonic arc rocks. Journal of Petrology 47, 705-744.

Kotková, J., 1993. Tectonometamorphic history of lower crust in the Bohemian Massif – example of north Bohemian granulites. Czech Geological Survey Special Papers 2, 56.

Kotková, J., 2007. High-pressure granulites of the Bohemian Massif: recent advances and open questions. Journal of Geocsiences 52, 45-71.

Kotková, J., Harley, S.L., 1999. Formation and evolution of high-pressure leucogranulites: Experimental constraints and unresolved issues. Physics and Chemistry of the Earth, A 24, 299-304.

Kotková, J., Harley, S.L., 2010. Anatexis during high-pressure crustal metamorphism: evidence from garnet-whole rock REE relationships and zircon-rutile Ti-Zr thermometry in leucogranulites from the Bohemian Massif. Journal of Petrology 51, 1967-2001.

Kotková, J., Kröner, A., Todt, W., Fiala, J., 1996. Zircon dating of north Bohemian granulites, Czech Republic: Further evidence for the lower carboniferous high-pressure event in the Bohemian Massif. Geologische Rundschau 85, 154-161.

Kotková, J., Harley, S.L., Fišera, M., 1997. A vestige of very high-pressure (ca. 28 kbar) metamorphism in the Variscan Bohemian Massif, Czech Republic. European Journal of Mineralogy 9, 1017-1033.

Kröner, A., Wendt, I., Liew, T.C., Compston, W., Todt, W., Fiala, J., Vaňková, V., Vaněk, J., 1988. U-Pb zircon and Sm-Nd model ages of high-grade Moldanubian metasediments, Bohemian Massif, Czechoslovakia. Contributions to Mineralogy and Petrology 99, 257-266.

Kröner, A., O'Brien, P.J., Nemchin, A.A., Pidgeon, R.T., 2000. Zircon ages for high pressure granulites from South Bohemia, Czech Republic, and their connection to Carboniferous high temperature processes. Contributions to Mineralogy and Petrology 138, 127-142.

Kryza, R., Pin, C., Vielzeuf, D., 1996. High-pressure granulites from Sudetes (south-west Poland): Evidence of crustal subduction and collisional thickening in the Variscan Belt. Journal of Metamorphic Geology 14, 531-546.

Lang, H.M., Gilotti, J.A., 2007. Partial melting of metapelites at ultrahigh-pressure conditions, Greenland Caledonides. Journal of Metamorphic Geology 25, 129-147.

Laporte, D., Rapaille, C., Provost, A., 1997. Wetting angles, equilibrium melt geometry, and the permeability threshold of partially molten crustal protoliths, in: Bouchez, J.-L., Hutton,

D.H., Stephens, W.E. (Eds.), Granite: From Segregation of Melt to Emplacement Fabrics. Kluwer Academic Publishers, Norwell, pp. 31–54.

Lindsley, D.H., Nekvasil, H., 1989. A ternary feldspar model for all reasons. American Geophysical Union EOS 70, 506.

Liou, J.G., Tsujimori, T., Zhang, R.Y., Katayama, I., Maruyama, S., 2005. UHP Metamorphism and Continent Subduction/Collision, in: Thomas, H. (Eds.), Metamorphism and Crustal Evolution. Atlantic Publishers and Distributors, New Delhi, India, pp. 285-313.

Matte, P., 1986. Tectonics and plate-tectonics model for the Variscan belt of Europe. Tectonophysics 126, 329-374.

Massonne, H.-J., 1999. Experimental aspects of UHP metamorphism in pelitic systems. International Geology Review 41, 623-638.

Massonne, H.-J., 2001. First find of coesite in the ultrahigh-pressure metamorphic area of the central Erzgebirge, Germany. European Journal of Mineralogy 13, 565-570.

Massonne, H.-J., Nasdala, L, 2003. Characterization of an early metamorphic stage through inclusions in zircon of a diamon-diferous quartzofeldspathic rock from the Erzgebirge, Germany American Mineralogist 88, 883-889.

Massonne, H.-J., Bautsch, H.J., 2004. Ultrahigh and high pressure rocks of Saxony. 32nd International Geological Congress, Florence, Italy, Field Trip Guide Books 2, 36.

Medaris, G., Wang, H., Jelínek, E., Mihaljevič, M., Jakeš, P., 2005. Characteristics and origins of diverse Variscan peridotites in the Gföhl Nappe, Bohemian Massif, Czech Republic. Lithos 82, 1-23.

Medaris, L.G., Ghent, E.D., Wang, H.F., Fournelle, J.H., Jelínek, E., 2006. The Spacice eclogite: constraints on the P-T-t history of the Gföhl granulite terrane, Moldanubian Zone, Bohemian Massif. Mineralogy and Petrology 86, 203-220.

Möller, A., Appel, P., Mezger, K., Schenk, V., 1995. Evidence for a 2 Ga subduction zone: Eclogites in the Usagaran Belt of Tanzania. Geology 23, 1067-1070.

Nahodilová, R., Faryad, S.W., Pertoldová, J., Konopásek, J., Štědrá, V., 2005. HP melting and its relationship to the granulite facies metamorphism – an example of the „Gföhl nappe“ in the Kutná Hora crystalline komplex. Geolines 19, 86-87.

Nair, R., Chacko, T., 2002. Fluid-absent melting of high-grade semi-pelites: P-T constraints on orthopyroxene formation and implications for granulite genesis. Journal of Petrology 43, 2121-2141.

Nakamura, D., Svojtka, M., Naemura, K., 2004. Very high-pressure (>4 GPa) eclogite associated with the Moldanubian Zone garnet peridotite (Nové Dvory, Czech Republic). Journal of Metamorphic Geology 22, 593–603.

Nekvasil, H., Carroll, W.J., 1993. Experimental constraints on the high-temperature termination of the anhydrous 2 feldspar + L curve in the feldspar system at 11.3 kbar. American Mineralogist 78, 601-606.

Newton, R.C., Anderson, A.T., 1986. The Dharwar Craton of South India – an Archean Protocontinent – editors preface. Journal of Petrology 94, 127-128.

O'Brien, P.J., 2006. Type-locality granulites: high pressure rocks formed at eclogite-facies conditions. Mineralogy and Petrology 86, 167-175.

O'Brien, P.J., 2008. Challenges in high-pressure granulite metamorphism in the era of pseudosections: reaction textures, compositional zoning and tectonic interpretation with examples from the Bohemian Massif. Journal of Metamorphic Geology 26, 235-251.

O'Brien, P.J., Rötzler, J., 2003. High-pressure granulites: formation, recovery of peak conditions and implications for tectonics. Journal of Metamorphic Geology 21, 3-20.

Pin, C., Vielzeuf, D., 1983. Granulites and related rocks in Variscan Median Europe – A dualistic interpretation. Tectonophysics 93, 47-74.

Powell, R., Holland, T.J.B., 1999. Relating formulations of the thermodynamics of mineral solid solutions; activity modeling of pyroxenes, amphiboles and micas. American Mineralogist 84, 1–14.

Rabinowicz, M., Vigneresse, J.-L., 2004. Melt segregation under compaction and shear channeling: Application to granitic magma segregation in a continental crust. Journal of Geophysical Research 109, B04407, 1-20.

Racek, M., Štípská, P., Pitra, P., 2006. Metamorphic record of burial and exhumation of orogenic lower and middle crust: a new tectonothermal model for the Drosendorf window (Bohemian Massif, Austria). Mineralogy and Petrology 86, 221-251.

Roberts, M.P., Finger, F., 1997. Do U-Pb zircon ages from granulites reflect peak metamorphic conditions? Geology 25, 319-322.

Rötzler, J., Romer, R.L., Budzinski, H., Oberhänsli, R., 2004. Ultrahigh-temperature high-pressure granulites from Tirschheim, Saxon Granulite Massif, Germany: P-T-t path and geotectonic implications. European Journal of Mineralogy 16, 917–937.

Schmädicke, E., Evans, B.W., 1997. Garnet-bearing ultramafic rocks from the Erzgebirge, and their relation to other settings in the Bohemian Massif. Contributions to Mineralogy and Petrology 127, 57-74.

Schulmann, K., Kröner, A., Hegner, E., Wendt, I., Konopásek, J., Lexa, O., Štípská, P., 2005. Chronological constraints on the pre-orogenic history, burial and exhumation of deep-seated rocks along the eastern margin of the Variscan orogen, Bohemian Massif, Czech Republic. American Journal of Science 305, 407-448.

Schulmann, K., Lexa, O., Štípská, P., Racek, M., Tajčmanová, L., Konopásek, J., Edel, J.B., Peschler, A., Lehmann, J., 2008. Vertical extrusion and horizontal channel flow of orogenic lower crust: key exhumation mechanisms in large hot orogens? Journal of Metamorphic Geology 26, 273-297.

Schulmann, K., Konopásek, J., Janoušek, V., Lexa O., Lardeaux, J.-M., Edel, J.-B., Štípská, P., Ulrich S., 2009. An Andean type Palaeozoic convergence in the Bohemian Massif. Comptes Rendus Geosciences 341, 266-286.

Sobolev, N.V., Shatsky, N.V., Liou, J.G., Zhang, R.Y., Hwang, S.L., Shen, P., Chu, H.T., Yui, T.F., Zayachkovsky, A.A., Kasymov, M.A., 2003. US-Russian Civilian Research and Development Fund Project: An Origin of Microdiamonds in Metamorphic Rocks of the Kokchetav Massif, Northern Kazakhstan. Episodes 26, 290-294.

Štípská, P., Powell, R., 2005. Does ternary feldspar constrain the metamorphic conditions of high-grade meta-igneous rocks? Evidence from orthopyroxene granulites, Bohemian Massif. Journal of Metamorphic Geology 23, 627-647.

Štípská, P., Schulmann, K., Kröner, A., 2004. Vertical extrusion and middle crustal spreading of omphacite granulite: a model of syn-convergent exhumation (Bohemian Massif, Czech Republic). Journal of Metamorphic Geology 22, 179-198.

Štípská, P., Pitra, P., Powell, R., 2006. Separate or shared metamorphic histories of eclogites and surrounding rocks? An example from the Bohemian Massif. Journal of Metamorphic Geology 24, 219-240.

Štípská, P., Schulamnn, K., Powell, R., 2008. Contrasting metamorphic histories of lenses of high-pressure rocks and host migmatites with a flat orogenic fabric (Bohemian Massif, Czech Republic): a result of tectonic mixing within horizontal crustal flow? Journal of Metamorphic Geology 26, 623-646.

Synek, J., Oliveriová, D., 1993. Terrane character of the north-east margin of the Moldanubian zone: the Kutná Hora Crystalline Complex, Bohemian Massif. Geologische Rundschau 82, 566-582.

Tajčmanová, L., Konopásek, J., Schulmann, K., 2006. Thermal evolution of the orogenic lower crust during exhumation within a thickened Moldanubian root of the Variscan belt of Central Europe. Journal of Metamorphic Geology 24, 119-134.

Thompson, A.B., 1996. Fertility of crustal rocks during anatexis. Transactions of the Royal Society Edinburgh: Earth Sciences 87, 1-10.

Tropper, P., Konzett, J., Finger, F., 2005. Experimental constraints on the formation of high-P/high T granulites in the Southern Bohemian Massif. European Journal of Mineralogy 17, 343-356.

Vielzeuf, D., Holloway, J.R., 1988. Experimental determination of the fluid-absent melting relations in the pelitic system. Consequences for crustal differentiation. Contributions to Mineralogy and Petrology 98, 257-276.

Vielzeuf, D., Schmidt, M.W., 2001. Melting relations in hydrous systems revisited: application to metapelites, metagreywackes and metabasalts. Contributions to Mineralogy and Petrology 141, 251-267.

Vrána, S., 1989. Perpotassic granulites from Southern Bohemia – A new rock-type derived from partial melting of crustal rocks under upper mantle conditions. Contributions to Mineralogy and Petrology 103, 510-522.

Vrána, S., Jakeš, P., 1982. Orthopyroxene and two-pyroxene granulites from a segment of charnockitic crust in southern Bohemia. Bulletin of the Geological Survey, Prague 57, 129-143.

Vrána, S., Štědrá, V., Fišera, M., 2005. Petrology and geochemistry of the Běstvina granulite body metamorphosed at eclogite facies conditions, Bohemian Massif. Journal of the Czech Geological Society 50, 81-94.

Vrána, S., Štědrá, V., Nahodilová, R., 2009. Geochemistry and petrology of high-pressure kyanite-garnet-albite-K-feldspar felsic gneisses and granulites from the Kutná Hora Complex, Bohemian Massif. Journal of Geosciences 54, 159-179.

Waters, D.J., 1988. Partial melting and the formation of granulite facies assemblages in Namaqualand, South Africa. Journal of Metamorphic Geology 6, 387-404.

Watson, E.B., 1999. Lithologic partitioning of fluids and melts. American Mineralogist 84, 1693-1710.

Watson, E.B., Brenan, J.M., 1987. Fluids in the lithosphere. 1. experimentally-determined wetting characteristics of CO_2–H_2O fluids and their implications for fluid transport, host rock physical-properties, and fluid inclusion formation. Earth and Planetary Science Letters 85, 497-515.

White, RW., Powell, R., Holland, T.J.B., 2001. Calculation of partial melting equilibria in the system Na_2O–CaO–K_2O–FeO–MgO–Al_2O_3–SiO_2–H_2O (NCKFMASH). Journal of Metamorphic Geology 19, 139–153.

White, R.W., Powell, R., Holland T.J.B., 2007. Progress relating to calculation of partial melting equilibria for metapelites. Journal of Metamorphic Geology 25, 511-527.

Whitney, D.L. and Evans, B.W. (2010). Abbreviations for names of rock-forming minerals. American Mineralogist 95, 185-187.

Zhang, R.Y., Liou, J.G., Zhang, Y.F., Fu, B., 2003. Transition of UHP eclogites to gneissic rocks of low-grade amphibolite facies during exhumation: Evidence from the Dabie terrane, central China. Lithos 70, 269-291.

Tables

Table 1. Modal and chemical composition of the mesocratic and leucocratic granulite layers

	Mesocratic layer KKF27-p	Leucocratic layer KKF27-l
Modal composition (vol. %)		
Qtz	26	30
Pl	35	30
Kfs	11	24
Grt	22	11
Bt	2	3
Ky	3	1
Accessories	1	1
Chemical composition (wt. %)		
SiO_2	65.56	70.85
TiO_2	0.62	0.69
Al_2O_3	17.04	14.60
FeO	5.89	3.23
MnO	0.12	0.05
MgO	0.76	0.93
CaO	4.68	2.27
Na_2O	3.25	2.99
K_2O	1.86	4.13
P_2O_5	0.12	0.14
H_2O	0.07	0.12

Table 2. Garnet composition from natural granulite samples

	mesocratic type			leucocratic type	
	core	rim	rim*	core	rim
SiO_2 (*wt. %*)	38.22	38.22	37.92	38.23	37.68
TiO_2	0.27	0.12	0.13	0.13	0.02
Al_2O_3	21.49	21.82	21.51	21.78	21.42
Fe_2O_3	0.51	1.23	1.81	2.18	1.81
FeO	22.07	21.95	22.96	20.46	26.76
MnO	0.45	0.40	0.49	0.26	0.48
MgO	2.06	5.46	4.24	6.27	5.87
CaO	14.92	10.71	10.93	10.71	5.73
Total	99.98	99.91	99.98	100.02	99.77
Si (*per 12 O*)	2.989	2.961	2.958	2.944	2.955
Ti	0.016	0.007	0.008	0.007	0.001
Al	1.981	1.993	1.978	1.977	1.980
Fe^{3+}	0.030	0.071	0.106	0.126	0.107
Fe^{2+}	1.443	1.422	1.498	1.318	1.755
Mn	0.030	0.026	0.032	0.017	0.032
Mg	0.240	0.630	0.492	0.719	0.686
Ca	1.250	0.889	0.913	0.884	0.481
prp (*mol. fr.*)	0.078	0.202	0.154	0.223	0.216
alm	0.469	0.455	0.470	0.408	0.553
grs	0.406	0.285	0.286	0.274	0.151
sps	0.010	0.008	0.010	0.005	0.010
Fe/(Fe+Mg)	0.857	0.693	0.753	0.647	0.719

* indicates analysis of a rim affected by diffusion

Table 3. Feldspar composition from natural granulite samples

	mesocratic type					leucocratic type			
Mineral	plagioclase			K-feldspar		plagioclase		K-feldspar	
Location	matrix (relic)	matrix (recryst.)	grt core (incl.)	matrix (recryst.)	grt rim	matrix (recryst.)	grt (incl.)	matrix (recryst.)	grt (incl.)
SiO_2 (*wt. %*)	59.73	66.02	59.90	65.30	65.64	64.88	66.02	64.86	64.74
Al_2O_3	25.88	21.67	25.16	18.71	18.87	22.01	21.40	18.78	18.44
Fe_2O_3	0.13	0.00	0.40	0.00	0.00	0.00	0.00	0.31	0.28
FeO	0.00	0.02	0.00	0.04	0.16	0.04	0.57	0.02	0.84
CaO	7.32	2.65	6.85	0.00	0.06	3.13	0.57	0.08	0.08
Na_2O	7.51	10.27	7.64	0.88	2.85	9.38	10.39	0.88	0.39
K_2O	0.09	0.13	0.26	15.29	12.41	0.11	1.26	15.26	15.15
Total	100.68	100.76	100.21	100.22	99.99	99.55	100.20	100.18	99.92
Si (*per 8 O*)	2.646	2.883	2.666	3.007	2.999	2.883	2.894	2.996	3.016
Al	1.351	1.115	1.320	1.015	1.016	1.153	1.106	1.022	1.012
Fe^{3+}	0.004	0.000	0.013	0.000	0.000	0.000	0.021	0.000	0.000
Fe^{2+}	0.000	0.001	0.000	0.002	0.006	0.001	0.000	0.001	0.033
Ca	0.347	0.124	0.326	0.000	0.003	0.149	0.027	0.004	0.004
Na	0.645	0.869	0.659	0.079	0.252	0.808	0.883	0.078	0.035
K	0.005	0.007	0.015	0.898	0.723	0.006	0.071	0.899	0.900
an (*mol. fr.*)	0.348	0.124	0.326	0.000	0.003	0.155	0.027	0.004	0.004
ab	0.647	0.869	0.659	0.080	0.258	0.839	0.901	0.080	0.037
or	0.005	0.007	0.015	0.920	0.739	0.006	0.072	0.916	0.958

Table 4. Biotite composition from natural granulite samples

	mesocratic type				leucocratic type	
Location	matrix	grt rim (with ky, rt)	grt (rim)	pl (incl.)	matrix	grt (incl.)
SiO_2 (*wt. %*)	38.09	35.01	36.58	39.76	35.94	36.43
TiO_2	3.68	3.95	1.52	1.46	4.84	1.73
Cr_2O_3	0.05	0.00	0.03	0.34	0.05	0.00
Al_2O_3	16.42	17.61	18.87	16.56	16.83	20.18
FeO	13.98	20.22	14.80	9.45	18.29	11.93
MnO	0.00	0.05	0.03	0.03	0.03	0.00
MgO	13.29	8.52	14.09	17.35	9.50	15.23
CaO	0.00	0.00	0.07	0.02	0.02	0.00
Na_2O	0.07	0.09	0.14	0.10	0.09	0.00
K_2O	10.10	9.42	9.30	9.76	9.59	9.94
H_2O*	3.93	3.76	3.96	4.01	3.95	4.09
Total	99.61	98.64	99.39	98.84	99.13	99.53
Si (*per 11 O*)	2.909	2.785	2.771	2.970	2.731	2.669
Ti	0.211	0.236	0.087	0.082	0.276	0.095
Cr	0.003	0.000	0.002	0.020	0.003	0.000
Al	1.478	1.651	1.685	1.458	1.507	1.742
Fe^{2+}	0.893	1.345	0.938	0.590	1.162	0.731
Mn	0.000	0.003	0.002	0.002	0.002	0.000
Mg	1.513	1.010	1.591	1.932	1.076	1.664
Ca	0.000	0.000	0.006	0.002	0.001	0.000
Na	0.010	0.013	0.021	0.014	0.014	0.000
K	0.984	0.956	0.899	0.930	0.930	0.929
Fe/(Fe+Mg)	0.371	0.571	0.371	0.234	0.520	0.310

* calculated by stoichiometry

Table 5. Experimental conditions and results

Run	Laboratory*	*P* (GPa)	*T* initial (°C)	*T* final (°C)	Duration (hours)	Relic phases	New phases
1	UIB	1.7	850	850	504	kfs, pl, grt, bt, qtz	grt, pl, kfs
2	UIB	2.1	900	900	434	kfs, pl, grt, bt, ky, qtz	grt, ky, cpx, pl, kfs, glass
3	BGI	2.1	900	900	505.4	grt, qtz	grt, ky, cpx, pl, kfs, glass
4	BGI	2.1	1100	900	316.1+	grt, ky, qtz	grt, ky, cpx, pl, kfs, glass

* UIB – University of Innsbruck, BGI – Bayerisches Geoinstitut

+ experiment was held at 1100 °C for 50.3 hr, cooled to 900 °C at 10 °C/hr and equilibrated at 900 °C for additional 245.8 hr.

Table 6. Feldspar composition from experimental run products

Run	1		2		3		4		
Phase	pl	kfs	pl	kfs	pl	kfs	pl	pl	kfs
SiO_2 (*wt. %*)	62.67	64.56	64.26	64.88	65.29	65.64	64.47	64.71	65.11
Al_2O_3	22.72	19.06	21.34	18.73	21.78	19.63	21.76	20.33	18.8
FeO	0.00	0.00	0.00	0.02	0.16	0.13	0.14	0.21	0.1
CaO	4.38	0.33	3.21	0.47	3.21	0.68	3.33	1.85	0.63
Na_2O	8.19	4.04	9.33	3.55	7.44	4.28	8.06	5.72	3.51
K_2O	1.25	10.97	0.79	10.82	1.91	10.06	2.23	6.59	11.11
Total	99.21	98.96	98.93	98.46	99.79	100.41	99.99	99.41	99.26
Si *(per 8 O)*	2.807	2.956	2.869	2.998	2.930	2.963	2.871	2.931	2.985
Al	1.200	1.029	1.123	1.020	1.152	1.044	1.142	1.086	1.016
Fe^{2+}	0.000	0.000	0.000	0.001	0.006	0.005	0.005	0.008	0.004
Ca	0.210	0.016	0.154	0.023	0.155	0.033	0.159	0.090	0.031
Na	0.711	0.359	0.807	0.318	0.648	0.375	0.696	0.502	0.312
K	0.071	0.641	0.045	0.638	0.109	0.579	0.126	0.381	0.650
an (*mol. fr.*)	0.212	0.016	0.153	0.024	0.170	0.033	0.162	0.092	0.031
ab	0.716	0.353	0.803	0.325	0.711	0.380	0.709	0.516	0.315
or	0.072	0.631	0.045	0.652	0.120	0.587	0.129	0.391	0.654

Table 7. Garnet composition from experimental run products

Run	1		2		3	4	
Location	core	rim	core	rim	core	core	core
SiO_2 (*wt. %*)	40.38	39.70	38.76	39.82	37.68	37.64	38.82
TiO_2	0.00	0.00	1.12	0.80	0.10	0.17	0.60
Al_2O_3	22.38	22.49	20.84	21.78	22.47	21.60	21.08
Fe_2O_3	0.00	0.52	0.98	0.00	2.82	3.28	0.00
FeO	18.81	18.67	22.06	19.06	26.68	20.68	24.26
MnO	0.00	0.00	0.14	0.06	0.12	0.38	0.51
MgO	13.99	11.95	8.49	10.95	8.41	3.48	4.98
CaO	3.47	5.87	7.06	6.78	2.56	13.12	9.00
Total	99.04	99.20	99.45	99.26	100.84	100.35	99.24
Si *(per 12 O)*	3.018	2.988	2.979	3.005	2.895	2.923	3.040
Ti	0.000	0.000	0.065	0.045	0.006	0.010	0.035
Al	1.971	1.995	1.887	1.937	2.035	1.977	1.946
Fe^{3+}	0.000	0.030	0.057	0.000	0.163	0.191	0.000
Fe^{2+}	1.176	1.174	1.418	1.203	1.714	1.343	1.588
Mn	0.000	0.000	0.009	0.004	0.008	0.025	0.034
Mg	1.558	1.340	0.972	1.232	0.963	0.402	0.581
Ca	0.278	0.473	0.581	0.548	0.211	1.091	0.755
prp (*mol. fr.*)	0.507	0.440	0.299	0.390	0.293	0.120	0.177
alm	0.383	0.386	0.436	0.381	0.521	0.399	0.483
grs	0.090	0.155	0.179	0.174	0.064	0.325	0.230
sps	0.000	0.000	0.003	0.001	0.002	0.007	0.010
Fe/(Fe+Mg)	0.430	0.467	0.593	0.494	0.640	0.769	0.732

Figure captions

Fig. 1. Main geological units of the Bohemian Massif in the European Variscan belt: (a) schematic view of the Variscan orogenic zones in western and central Europe; (b) tectonic sketch map of the Bohemian Massif (modified after Franke, 2000); (c) geological map of the Kutná Hora complex (simplified after Synek and Oliveriová, 1993). The label Miškovice KK27F indicates the location of the granulite body beneath the Cretaceous sedimentary cover.

Fig. 2. (a) Field photograph of felsic granulites with prominant light and dark layering due to the variations in garnet ± kyanite and biotite contents. Layering is parallel to the subhorizontal S_2 foliation; (b) detailed view of the layered felsic granulite.

Fig. 3. Photomicrographs in backscattered electron mode of the mineral assemblages and textural relations in the felsic granulite. (a) shows antiperthitic plagioclase in the matrix and relics of garnet that partly enclose kyanite and rutile (KK27F-p), (b) garnet grain that partly encloses perthitic K-feldspar and kyanite with an inclusion of rutile (KK27F-p), (c) garnet porphyroblast with inclusions of columnar lamellae of K-feldspar an an Al-rich phase (clay mineral; possible replacement product after phengite?; KK27F-p). (d) shows partly recrystallized antiperthitic plagioclase with kyanite inclusions (KK27F-l). (e) and (f) show perthitic K-feldspar and antipertitic plagioclase enclosed in garnet and in the matrix, respectively (KK27F-p). The compositions of the ternary feldspars were calculated by reintegration of the proportions and compositions of the host and the lamellae.

Fig. 4. Composition of garnet of the granulite (a) from the mesocratic layer (KK27F-p - solid circles) and leucocratic layer (KK27F-l - open circles for small Ca-poor grains). The arrow indicates the compositional trend from garnet core to rim. The ellipsoidal field indicates composition of garnet rims affected by diffusion. Note that composition of the garnet in the leucocratic layer is close to that from the rim of large porphyroblasts in the mesocratic layer, and compositions of the diffusional rims in both garnets are similar. (b) shows core to rim composition in a single grain from a well preserved garnet in granulites of the Kutná Hora complex and from Horní Bory in the Gföhl unit (Hrouda et al., 2009).

Fig. 5. Representative compositional profiles through garnet grains from the (a) mesocratic (KK27F-p) and (b) leucocratic layer (KK27F-l).

Fig. 6. Composition of feldspars from the (a) mesocratic and (b) leucocratic layer. Symbols: white diamonds - K-feldspars in the matrix and lamellae in antiperthitic plagioclase; gray diamonds – perthite host inclusions enclosed in garnet; white circles - plagioclase grains in the matrix: Ca-rich compositions are from the core of a plagioclase porphyroblast and from plagioclase in contact with kyanite; black circles – plagioclase inclusions in garnet core; gray circles – antiperthitic plagioclase; stars – reintegrated ternary feldspars.

Fig. 7. Pressure-temperature pseudosections calculated for the (a) mesocratic and (b) leucocratic granulite layers in the NCKFMASHT system. Bulk compositions are given in Table 1. Phase assemblages in (a) are: (1) 1fsp grt ilm liq, (2) 1fsp grt ilm liq di, (3) 1fsp grt ilm liq, (4) 1fsp grt ilm liq di opx, (5) 1fsp grt ilm liq opx, (6) 1fsp ilm liq opx, (7) 1fsp ilm liq, (8) 2fsp grt ilm liq di opx, (9) 2fsp grt bt ilm di opx, (10) 2fsp grt bt ilm liq di, (11) 2fsp grt bt ilm liq, (12) 2fsp grt bt rt liq; phase assemblages in (b) are: (1) 2fsp grt bt rt liq di, (2) 2fsp grt bt ilm rt liq, (3) 2fsp grt bt ilm liq, (4) 2fsp grt ilm liq, (5) 2fsp grt ilm liq di, (6) 1fsp grt ilm liq opx, (7) 1fsp grt ilm rt liq opx, (8) 1fsp ilm rt liq opx, (9) 1fsp ilm liq opx.

Fig. 8. Reconstructed pressure-temperature paths for the (a) mesocratic and (b) leucocratic granulite layers. Garnet composition isopleths for x_{Ca} = molar Ca/(Ca+Mg+Fe) and x_{Fe} = molar Fe/(Fe+Mg) are shown by dashed curves. Univariant equilibria described in the text are shown by solid lines and highlighted by gray shades.

Fig. 9. Photomicrographs of experimental run products: (a) formation of partial melt and new mineral grains (garnet, ternary feldspar) in run #3; (b) melt pools located at grain boundaries of recrystallizing quartz, feldspars and garnet in run #2; (c) detailed view of melt-assisted formation of garnet and kyanite, and recrystallization of feldspars to ternary composition in run #4; (d) detailed view of new garnet grains and overgrowths in the matrix of quartz, plagioclase and K-feldspar in run #1; (e) formation of acicular kyanite in the presence of partial melt in run #4; (f) clinopyroxene overgrowth at the contact between garnet and quartz in run #3.

Fig. 10. Feldspar composition in experimental run products. Solvus isotherms at P = 2 GPa were calculated using the revised model of Holland and Powell (2003). Results of previous experiments by Tropper *et al.* (2005) are shown for comparison.

Fig. 11. Composition of garnet from experimental run products. Garnet composition from the mesocratic and leucocratic varieties of granulite is also shown for comparison.

Fig. 12. Composition of partial melts in experimental run products: (a) SiO_2 vs. Al_2O_3 diagram, and (b) SiO_2 vs. FeO_{tot} +MgO diagram. Gray fields outline the melt compositions in experiments by Tropper *et al.* (2005) at 850-1000 ^oC and 1.2-1.6 GPa.

Fig. 13. Ternary feldspar diagrams: (a) experimental results at 900, 1000 and 1100 ^oC and 2 GPa, with solvus isotherms calculated with the revised model of Holland and Powell (2003), Eq. (7) (b) the re-integrated feldspar compositions, obtained in this study (gray asterisks), with solvus isotherms at 800, 900, 1000 ^oC and 2 GPa: dotted curves – Elkins and Grove (1990), dashed curves – Benisek et al. (2010), solid curves – Holland and Powell (2003) as revised in this study.

Fig.14. Reconstructed pressure-temperature path for the mesocratic granulite using the thermodynamic model for feldspars by Benisek et al. (2010), shown in dark gray solid curve. The *P-T* path, derived in Fig. 8 with the modified thermodynamic model of Holland and Powell (2003), is illustrated by gray dashed curve for comparison.

Fig. 15. Pressure-temperature phase diagrams for the mesocratic granulite (a) and for the mesocratic granulite composition with 20 vol. % melt added (b) to illustrate the maximum whole-rock H_2O concentrations during prograde metamorphism (thin dashed curves) and the melt productivity by dehydration melting (thick dashed curves). See text for discussion.

Fig. 16. Pressure (temperature)-composition pseudosection for the mesocratic granulite. The composition ranges from anhydrous, melt-free granulite to the partial melt composition (20 wt. % melt + 80 wt. % granulite), and is labeled by the weight proportion of H_2O in the system. Temperature varies according to the P-T path reconstructed in Fig. 8a. The evolutionary path including the melt loss consistent with increasing modal amount of garnet is shown by black arrows. Numbered stability fields contain the following phase

assemblages: (1) grt ky rt ms omp, (2) grt ky rt ms omp zo, (3) 1fsp grt rt liq, (4) 2fsp grt bt rt, (5) 2fsp grt bt ms rt, (6) 2fsp grt bt ms rt ilm, (7) 2fsp grt bt ms ilm, (8) 2fsp grt bt ms ilm ttn, (9) 2fsp grt bt ms ttn, (10) 2fsp grt bt ms zo ttn, (11) 2fsp bt ms zo ttn, (12) 1fsp bt ms zo ttn, (13) 1fsp bt ms zo ttn H_2O.

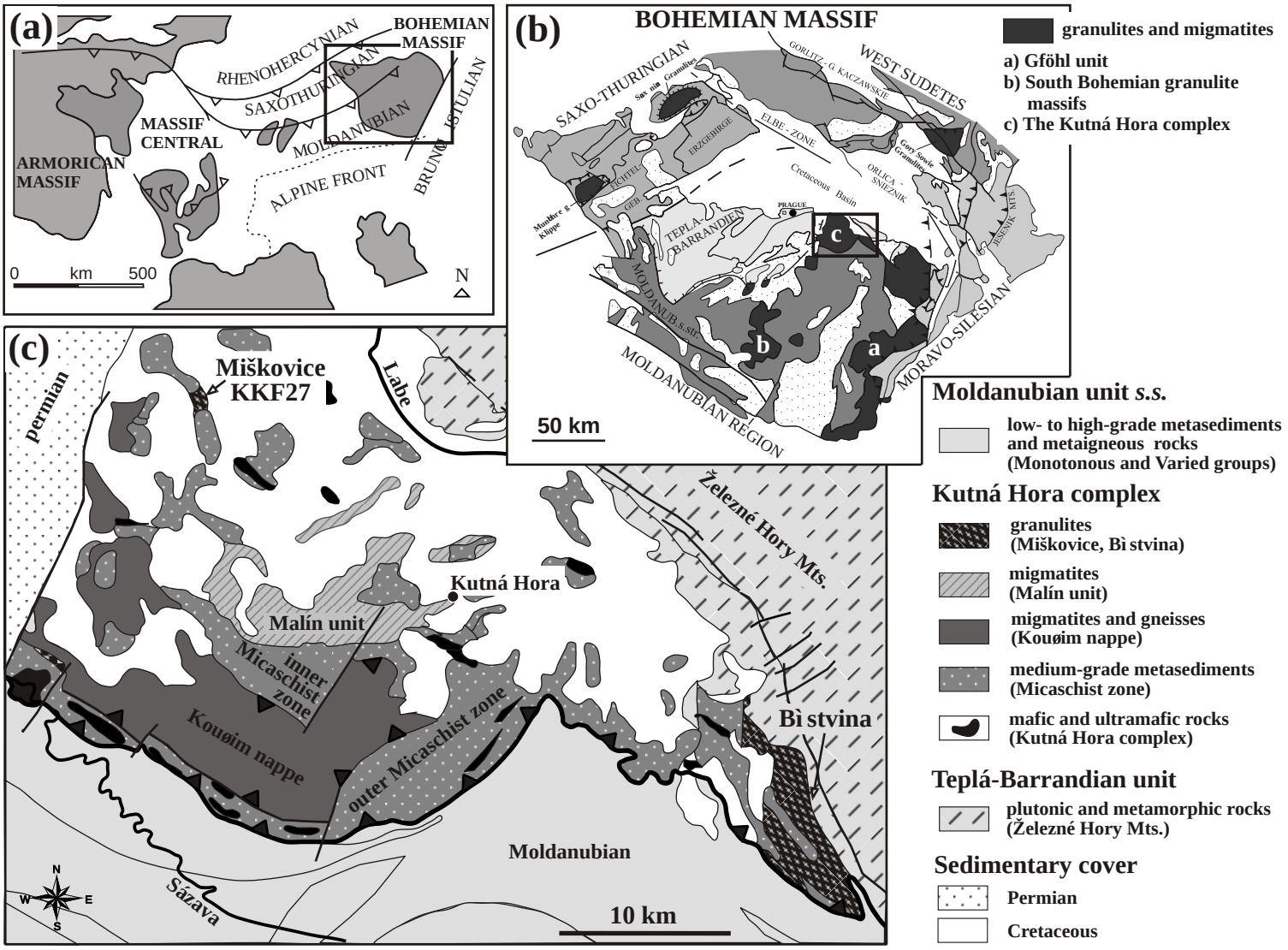
(a)
BOHEMIAN MASSIF
RHENOHERCYNIAN
SAXOTHURINGIAN
MOLDANUBIAN
BRUNOVISTULIAN
MASSIF CENTRAL
ARMORICAN MASSIF
ALPINE FRONT
0 km 500
N
(b)
BOHEMIAN MASSIF
SAXO-THURINGIAN
WEST SUDETES
ELBE - ZONE
ERZGEBIRGE
Cretaceous Basin
TEPLÁ-BARRANDIEN
MOLDANUB. s.str.
MORAVO-SILESIAN
MOLDANUBIAN REGION
PRAGUE
50 km
granulites and migmatites
a) Gföhl unit
b) South Bohemian granulite massifs
c) The Kutná Hora complex
(c)
Miškovice
KKF27
Labe
permian
Železné Hory Mts.
Kutná Hora
Malín unit
inner Micaschist zone
Kouøim nappe
outer Micaschist zone
Bì stvina
Moldanubian
Sázava
10 km
Moldanubian unit s.s.
low- to high-grade metasediments and metaigneous rocks (Monotonous and Varied groups)
Kutná Hora complex
granulites (Miškovice, Bì stvina)
migmatites (Malín unit)
migmatites and gneisses (Kouøim nappe)
medium-grade metasediments (Micaschist zone)
mafic and ultramafic rocks (Kutná Hora complex)
Teplá-Barrandian unit
plutonic and metamorphic rocks (Železné Hory Mts.)
Sedimentary cover
Permian
Cretaceous

Fig. 1

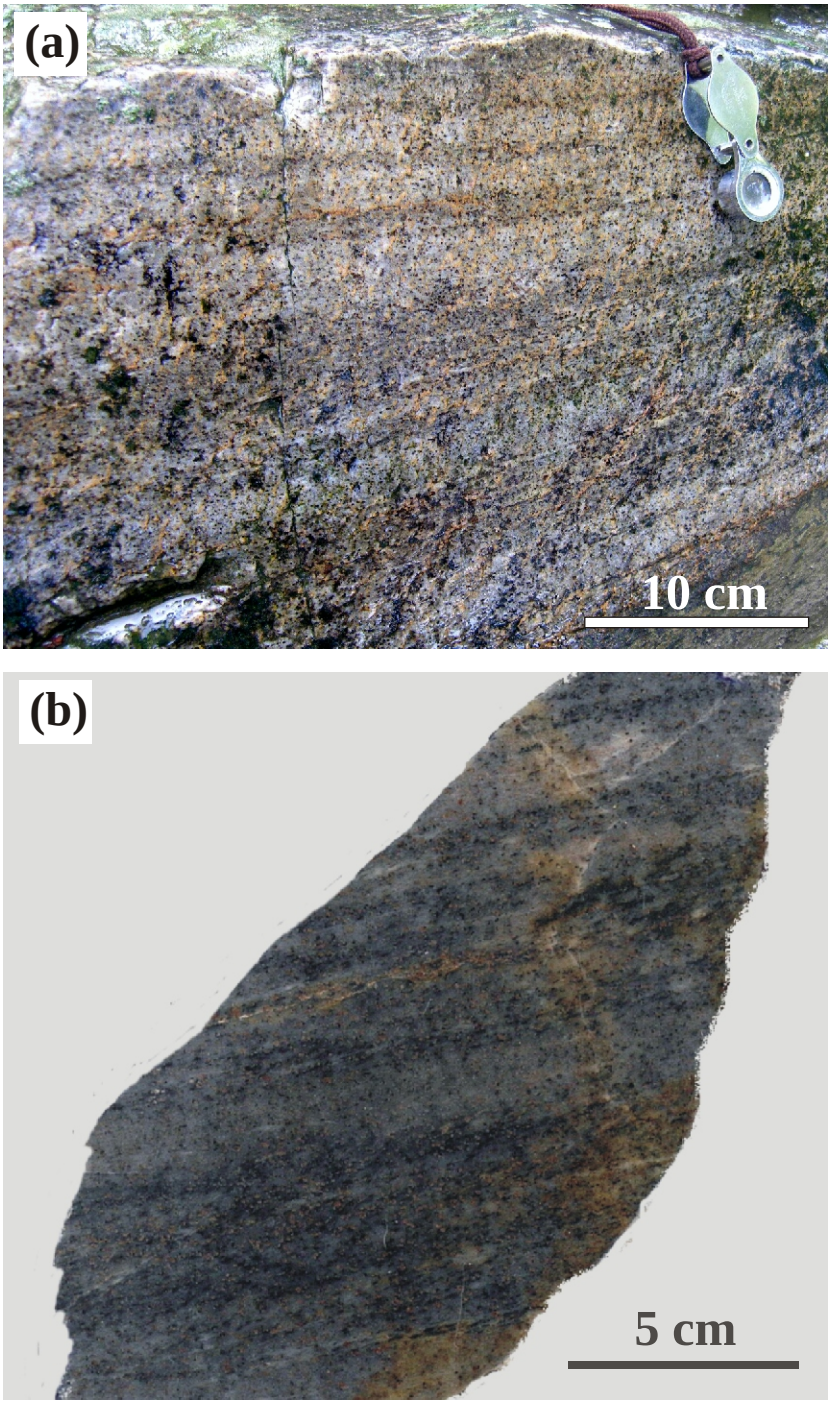

Fig. 2

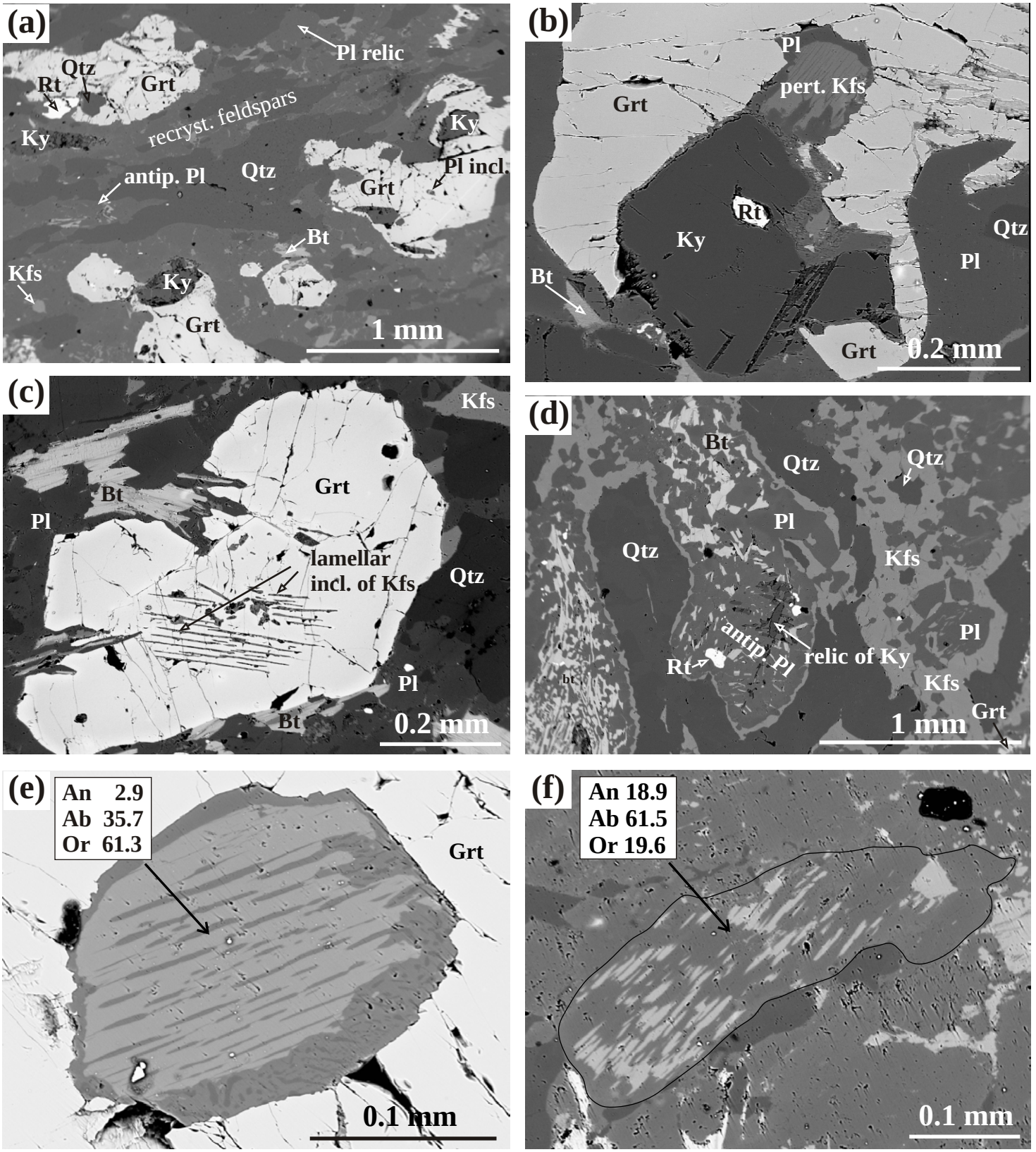
(a)
Pl relic
Qtz
Rt
Grt
recryst. feldspars
Ky
Ky
antip. Pl
Qtz
Pl incl.
Grt
Bt
Kfs
Ky
Grt
1 mm
(b)
Pl
pert. Kfs
Grt
Rt
Ky
Qtz
Pl
Bt
Grt
0.2 mm
(c)
Kfs
Grt
Bt
Pl
lamellar
incl. of Kfs
Qtz
Pl
Bt
0.2 mm
(d)
Bt
Qtz
Qtz
Pl
Qtz
Kfs
Pl
antip. Pl
relic of Ky
Rt
Kfs
Grt
1 mm
(e)
An 2.9
Ab 35.7
Or 61.3
Grt
0.1 mm
(f)
An 18.9
Ab 61.5
Or 19.6
0.1 mm

Fig. 3

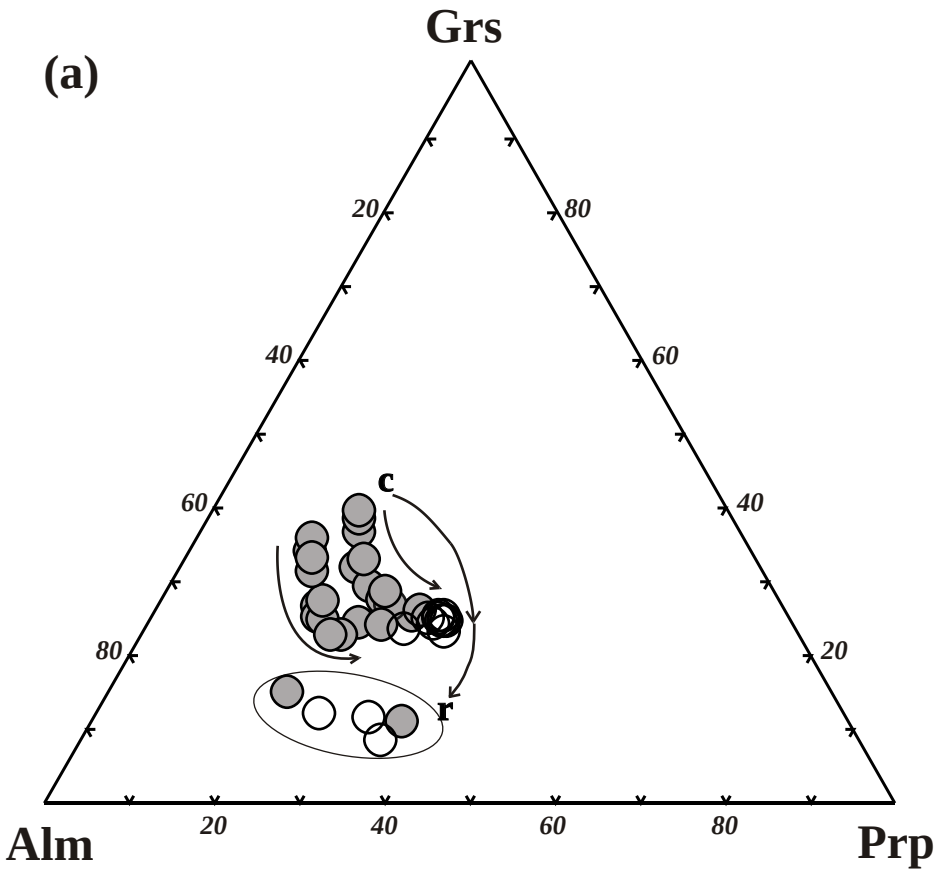
(a)
Grs
20
80
40
60
60
40
80
20
c
r
Alm
20
40
60
80
Prp

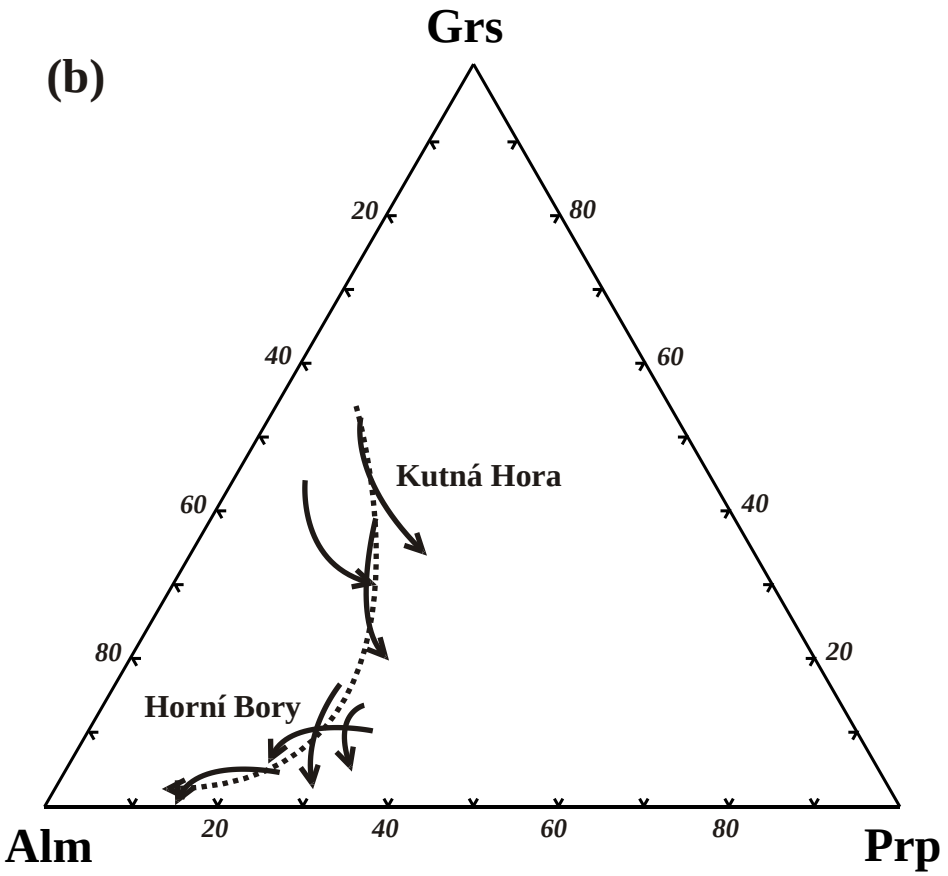
(b)
Grs
20
80
40
60
60
40
80
20
Kutná Hora
Horní Bory
Alm
20
40
60
80
Prp

Fig. 4

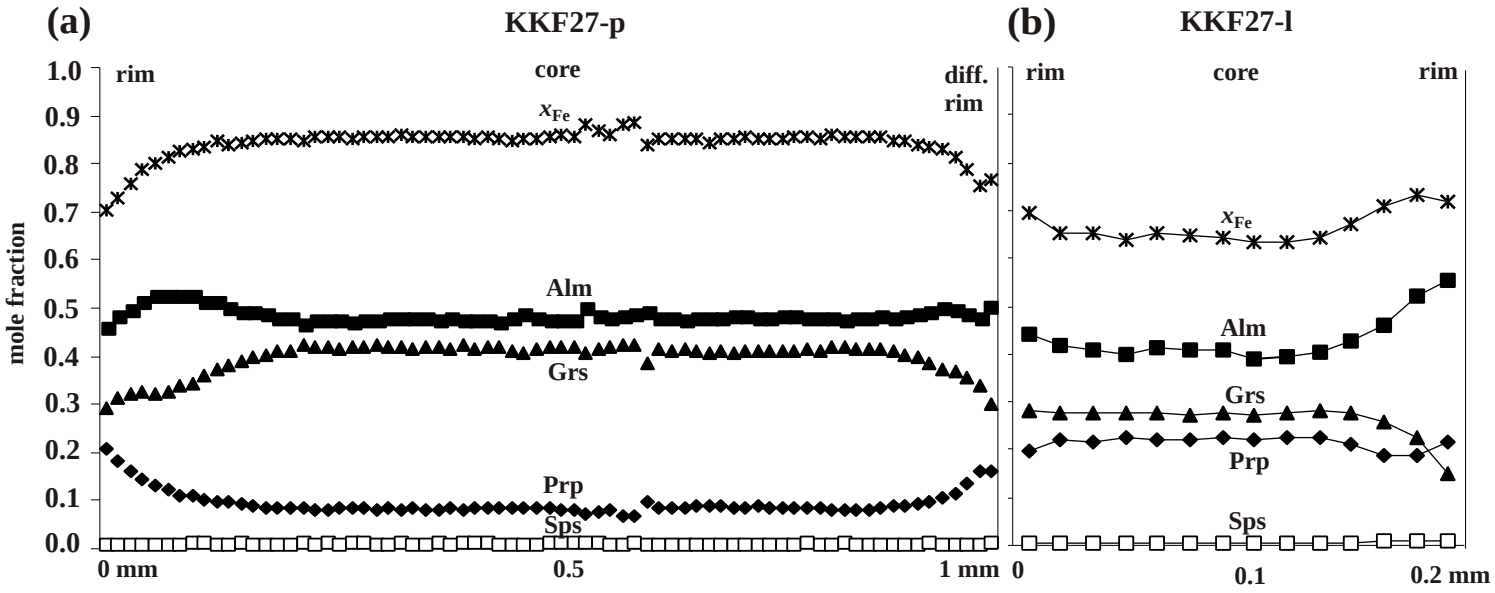
(a)
KKF27-p
(b)
KKF27-l
rim
core
diff. rim
rim
core
rim
mole fraction
1.0
0.9
0.8
0.7
0.6
0.5
0.4
0.3
0.2
0.1
0.0
x_{Fe}
Alm
Grs
Prp
Sps
0 mm
0.5
1 mm
0
0.1
0.2 mm

Fig. 5

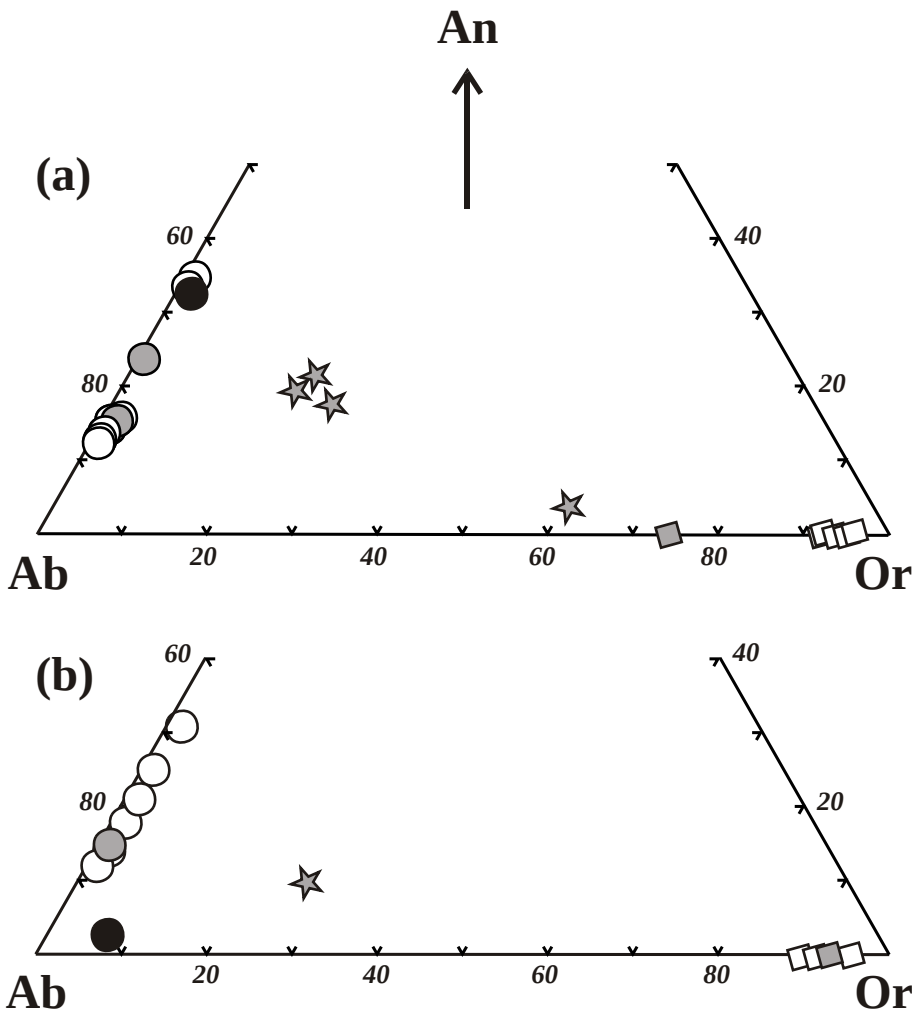

Fig. 6

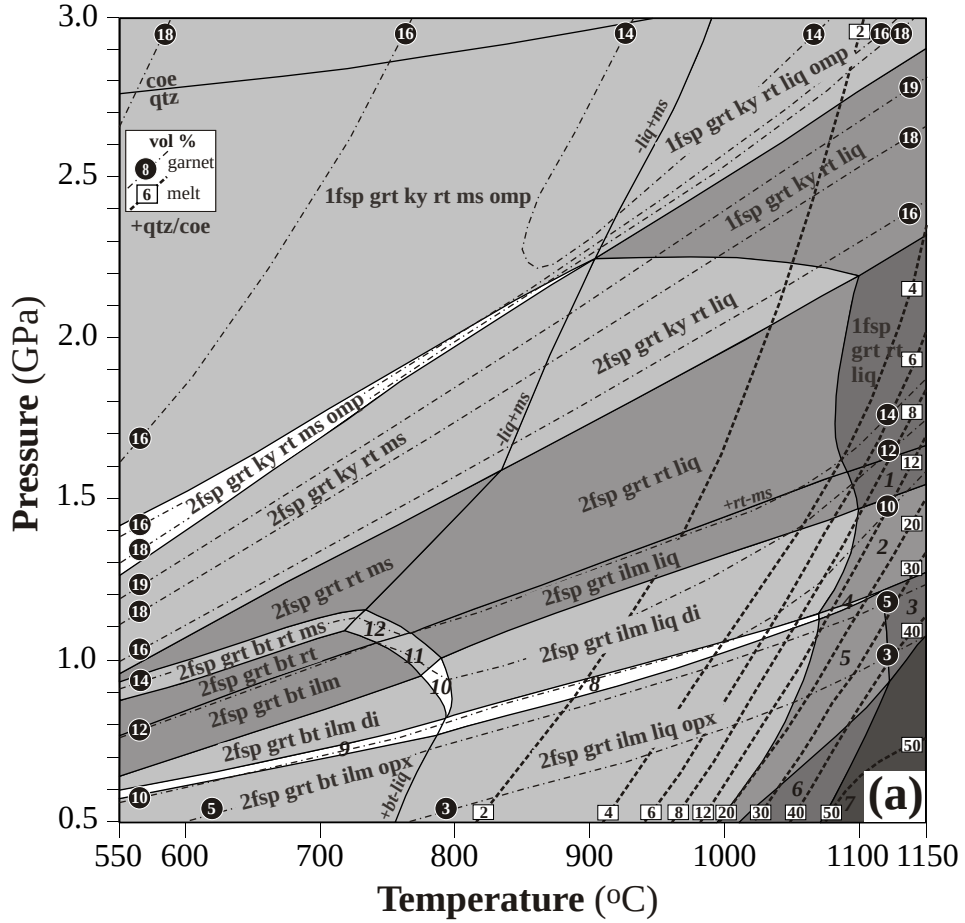
Pressure (GPa)
Temperature (°C)
vol %
garnet
melt
coe
qtz
+qtz/coe
1fsp grt ky rt ms omp
1fsp grt ky rt liq omp
1fsp grt ky rt liq
2fsp grt ky rt ms omp
2fsp grt ky rt ms
2fsp grt ky rt liq
2fsp grt rt ms
2fsp grt rt liq
2fsp grt bt rt ms
2fsp grt bt rt
2fsp grt bt ilm
2fsp grt ilm liq
2fsp grt ilm liq di
2fsp grt bt ilm di
2fsp grt ilm liq opx
2fsp grt bt ilm opx
1fsp grt rt liq
-liq+ms
+rt-ms
+bt-liq
(a)

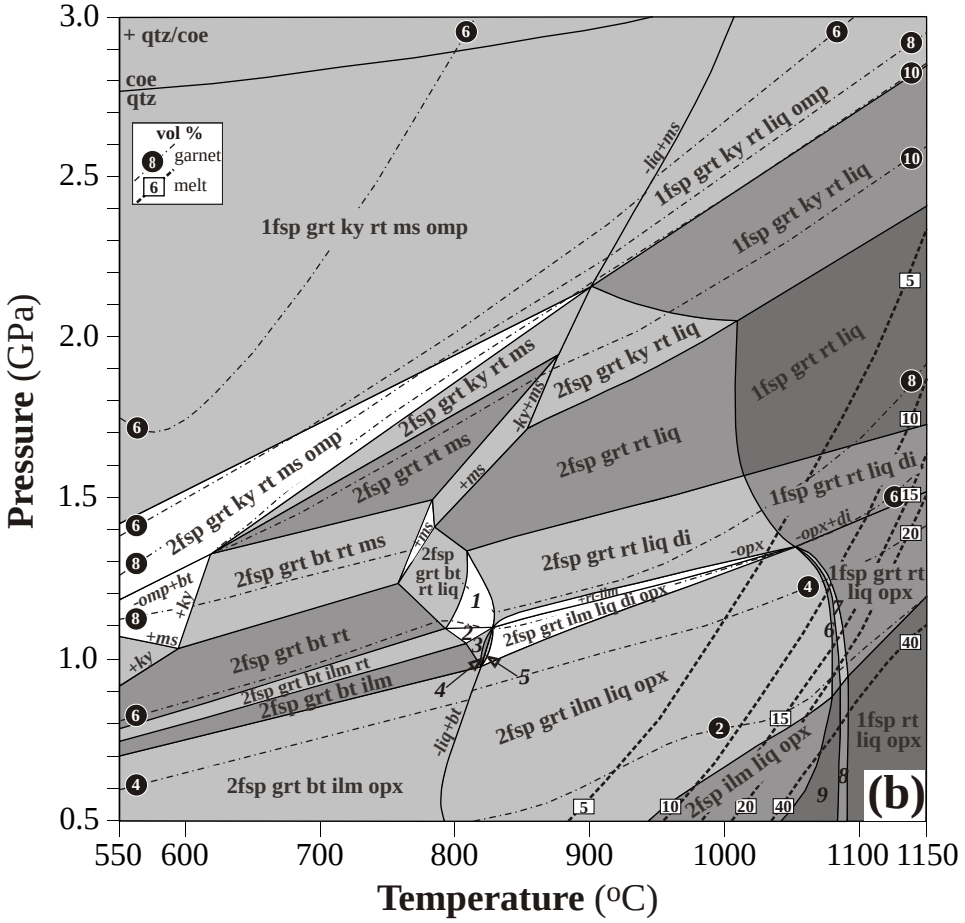
Pressure (GPa)
Temperature (°C)
+ qtz/coe
coe
qtz
vol %
garnet
melt
1fsp grt ky rt ms omp
1fsp grt ky rt liq omp
1fsp grt ky rt liq
2fsp grt ky rt ms omp
2fsp grt ky rt ms
2fsp grt ky rt liq
2fsp grt rt ms
2fsp grt rt liq
1fsp grt rt liq
1fsp grt rt liq di
2fsp grt bt rt ms
2fsp grt bt rt
2fsp grt bt ilm rt
2fsp grt bt ilm
2fsp grt rt liq di
2fsp grt ilm liq di opx
2fsp grt ilm liq opx
1fsp grt rt liq opx
2fsp grt bt ilm opx
2fsp ilm liq opx
-liq+ms
-ky+ms
-omp+bt
+ky
+ms
-liq+bt
-opx
-opx+di
+rt-ilm
(b)

Fig. 7

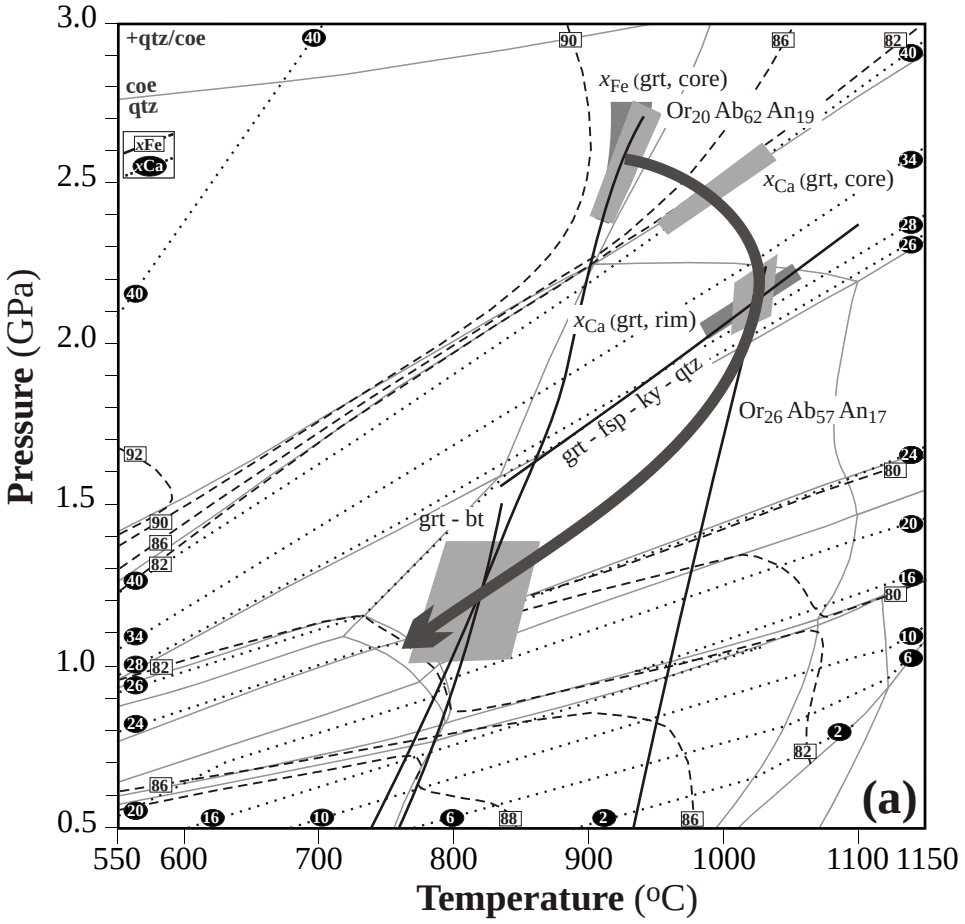
+qtz/coe
coe
qtz
xFe
xCa
x_{Fe} (grt, core)
Or_{20} Ab_{62} An_{19}
x_{Ca} (grt, core)
x_{Ca} (grt, rim)
grt - fsp - ky - qtz
Or_{26} Ab_{57} An_{17}
grt - bt
(a)
Pressure (GPa)
Temperature (°C)
3.0
2.5
2.0
1.5
1.0
0.5
550
600
700
800
900
1000
1100
1150

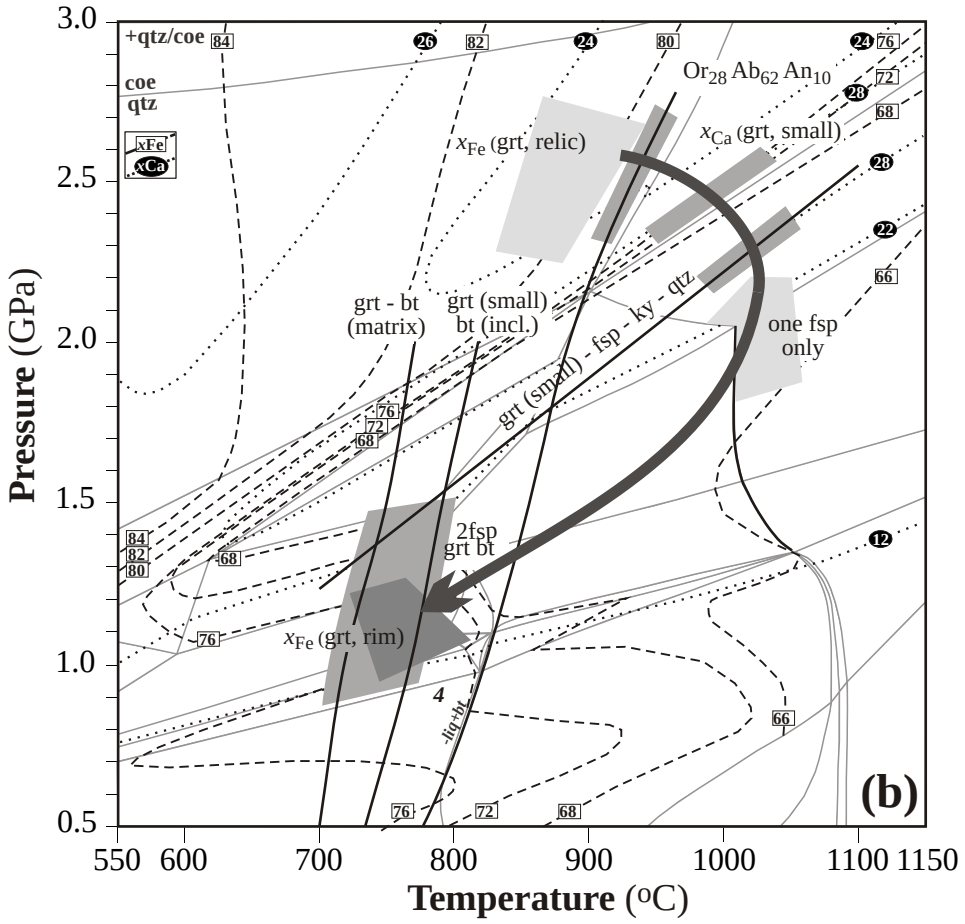
+qtz/coe
coe
qtz
xFe
xCa
Or_{28} Ab_{62} An_{10}
x_{Fe} (grt, relic)
x_{Ca} (grt, small)
grt - bt
(matrix)
grt (small)
bt (incl.)
grt (small) - fsp - ky - qtz
one fsp
only
2fsp
grt bt
x_{Fe} (grt, rim)
4
-liq+bt
(b)
Pressure (GPa)
Temperature (°C)
3.0
2.5
2.0
1.5
1.0
0.5
550
600
700
800
900
1000
1100
1150

Fig. 8

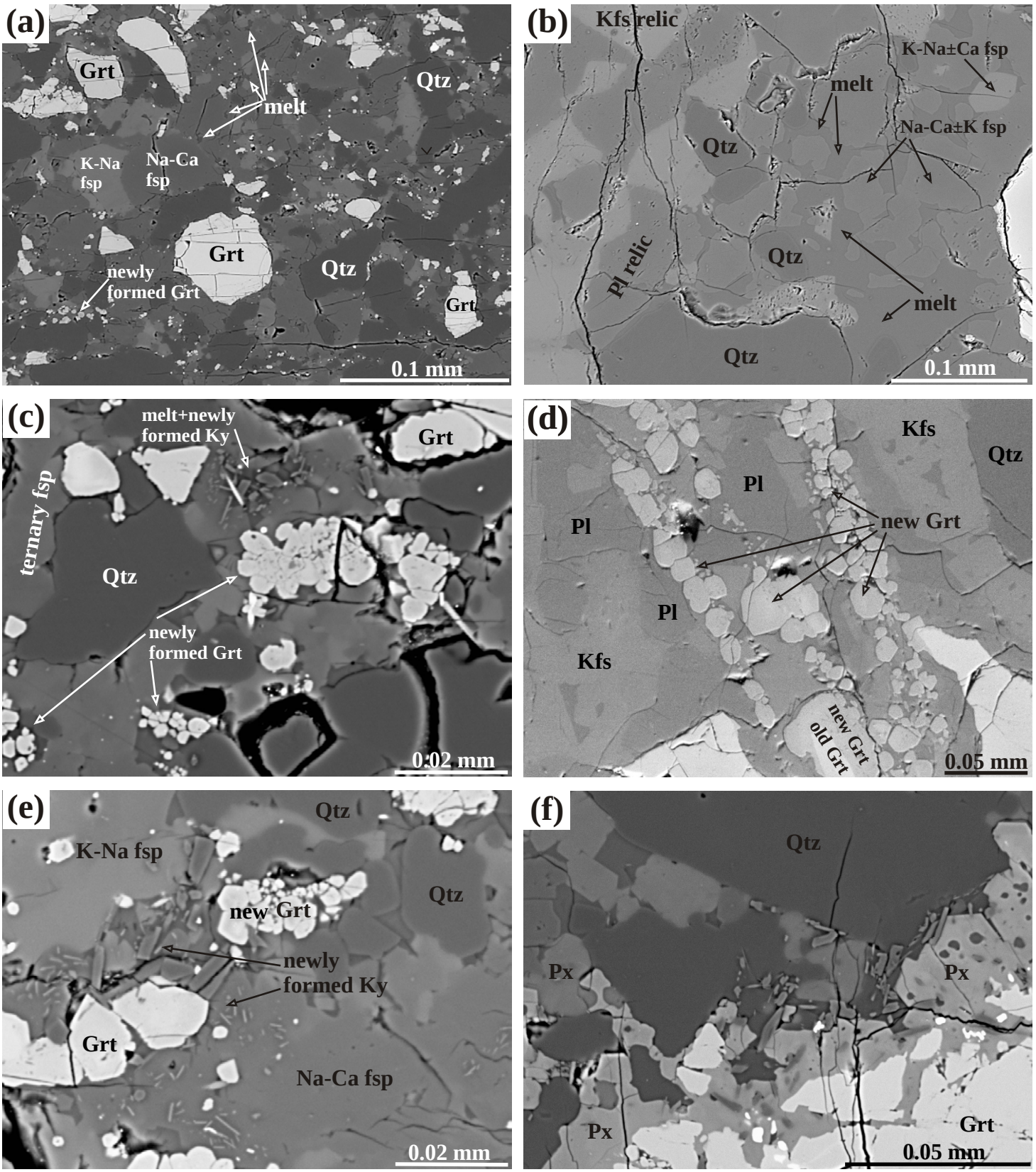
(a)
Grt
melt
Qtz
K-Na fsp
Na-Ca fsp
Grt
Qtz
newly formed Grt
Grt
0.1 mm
(b)
Kfs relic
K-Na±Ca fsp
melt
Na-Ca±K fsp
Qtz
Pl relic
Qtz
melt
Qtz
0.1 mm
(c)
melt+newly formed Ky
Grt
ternary fsp
Qtz
newly formed Grt
0.02 mm
(d)
Kfs
Qtz
Pl
Pl
new Grt
Pl
Kfs
new Grt
old Grt
0.05 mm
(e)
Qtz
K-Na fsp
Qtz
new Grt
newly formed Ky
Grt
Na-Ca fsp
0.02 mm
(f)
Qtz
Px
Px
Px
Grt
0.05 mm

Fig. 9

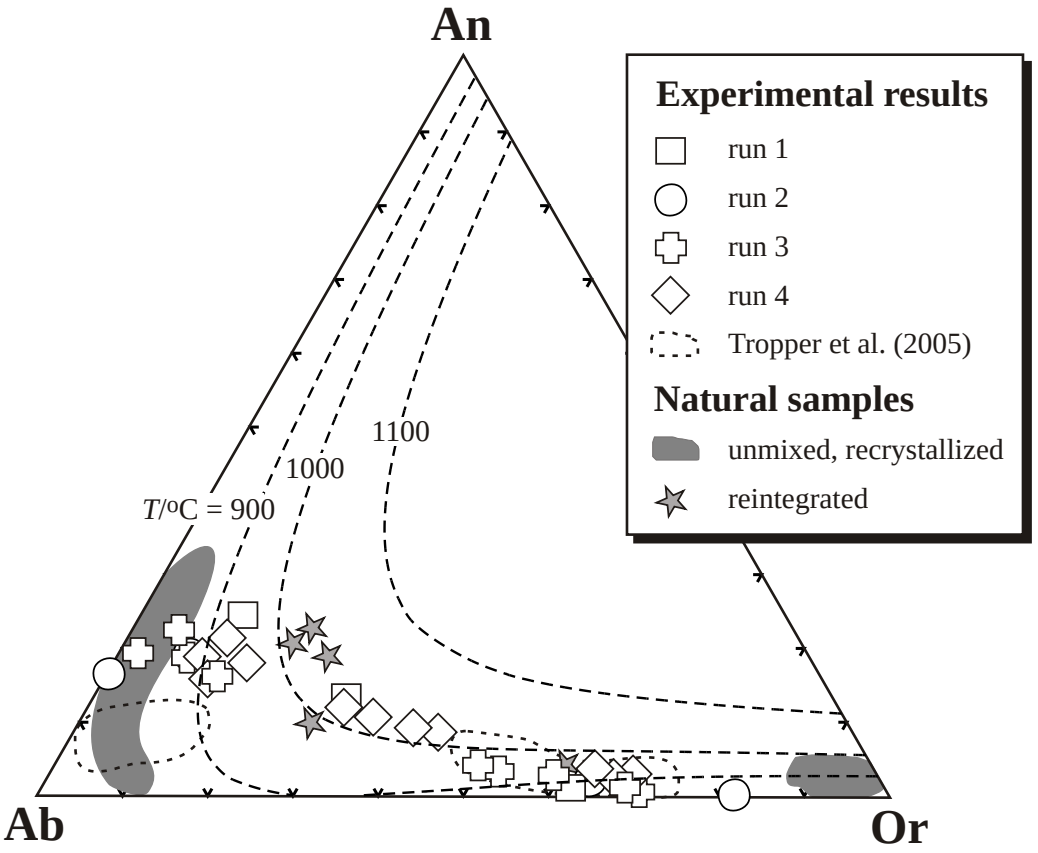
An
Ab
Or
T/oC = 900
1000
1100
Experimental results
run 1
run 2
run 3
run 4
Tropper et al. (2005)
Natural samples
unmixed, recrystallized
reintegrated

Fig. 10

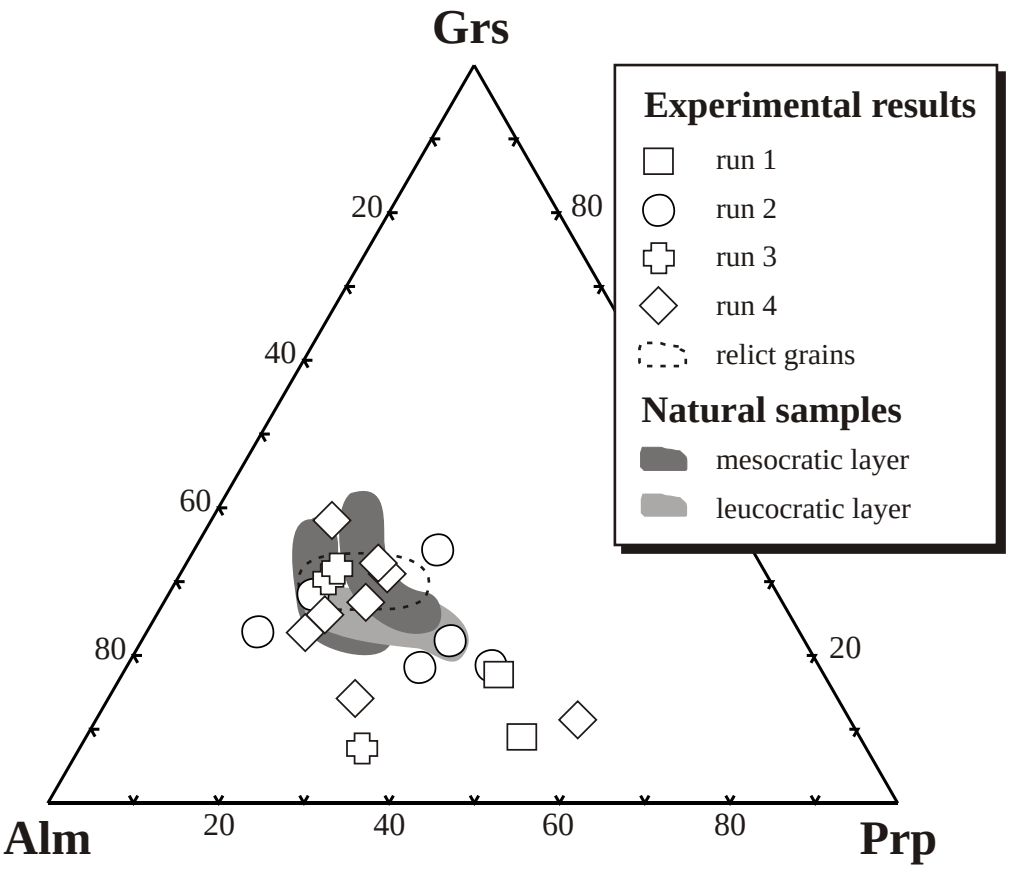
Grs
Alm
Prp
20
40
60
80
Experimental results
run 1
run 2
run 3
run 4
relict grains
Natural samples
mesocratic layer
leucocratic layer

Fig. 11

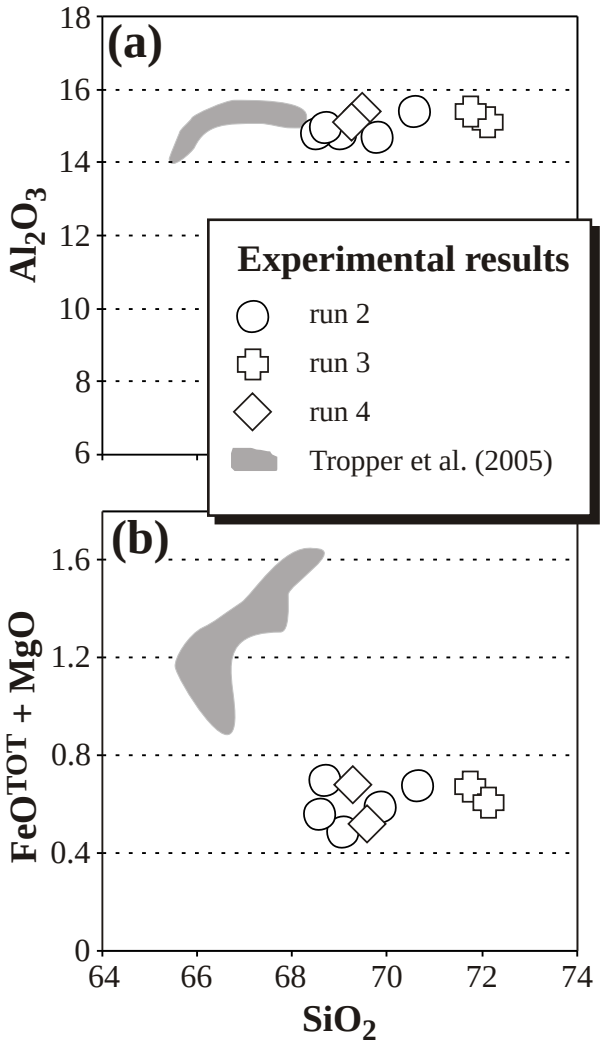
(a)
(b)
Experimental results
run 2
run 3
run 4
Tropper et al. (2005)
Al2O3
FeOTOT + MgO
SiO2
18
16
14
12
10
8
6
1.6
1.2
0.8
0.4
0
64
66
68
70
72
74

Fig. 12

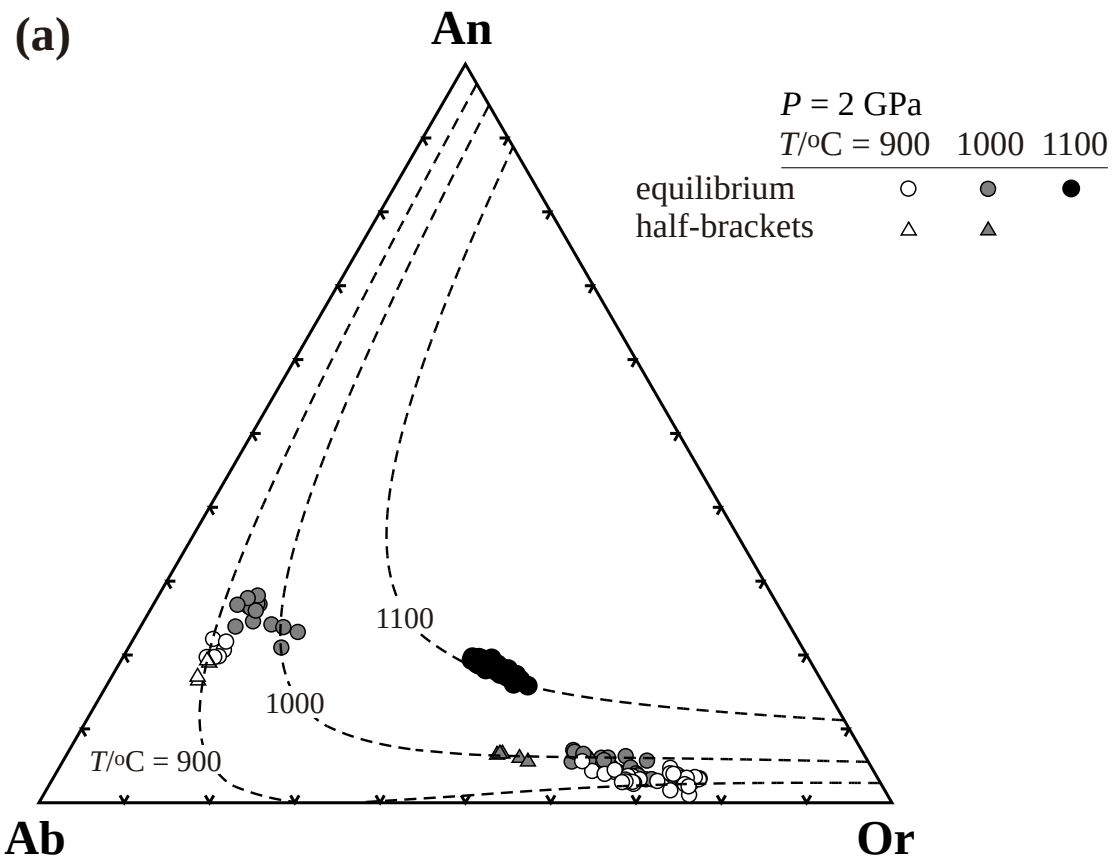
(a)
An
Ab
Or
P = 2 GPa
T/°C = 900 1000 1100
equilibrium
half-brackets
1100
1000
T/°C = 900

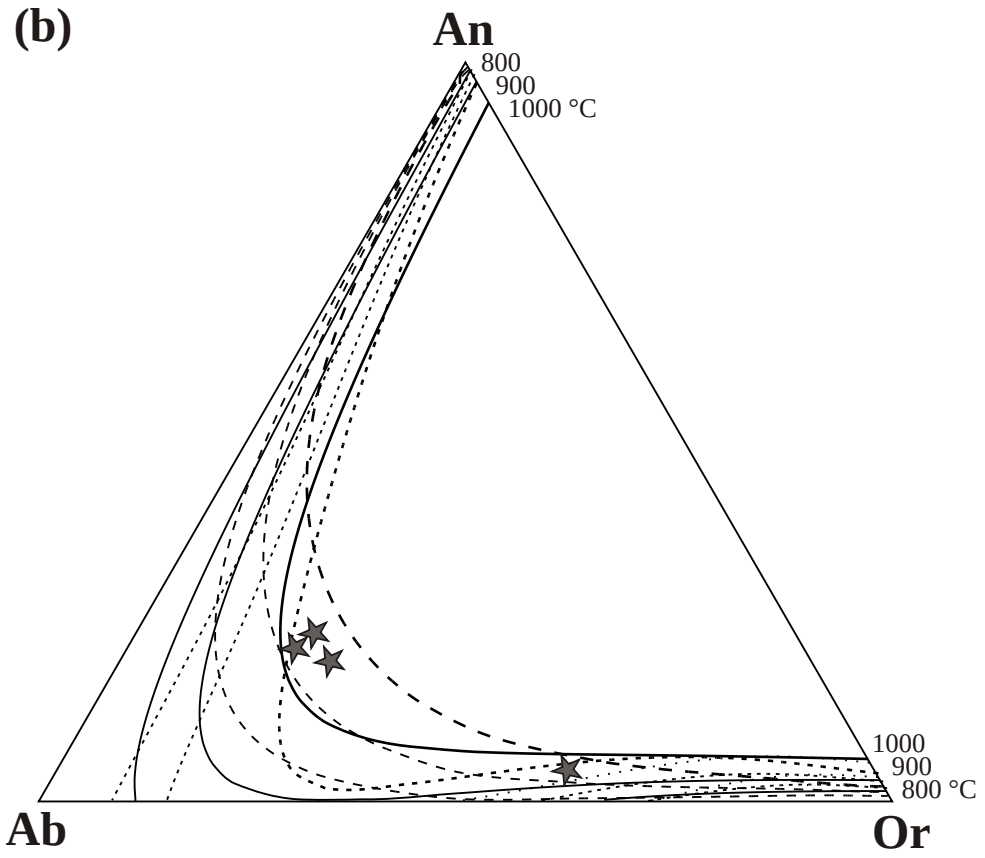
(b)
An
Ab
Or
800
900
1000 °C
1000
900
800 °C

Fig. 13

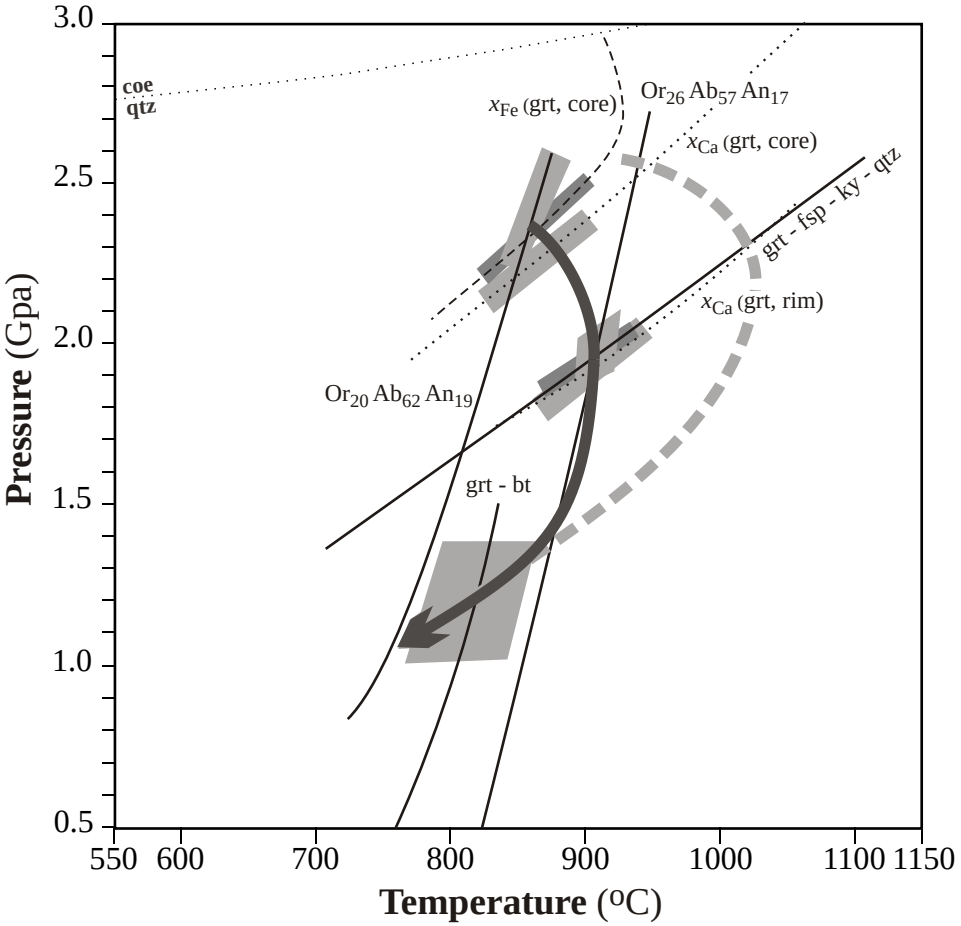
3.0
2.5
2.0
1.5
1.0
0.5
Pressure (Gpa)
550
600
700
800
900
1000
1100
1150
Temperature (°C)
coe
qtz
x_{Fe} (grt, core)
$Or_{26}\,Ab_{57}\,An_{17}$
x_{Ca} (grt, core)
grt - fsp - ky - qtz
x_{Ca} (grt, rim)
$Or_{20}\,Ab_{62}\,An_{19}$
grt - bt

Fig. 14

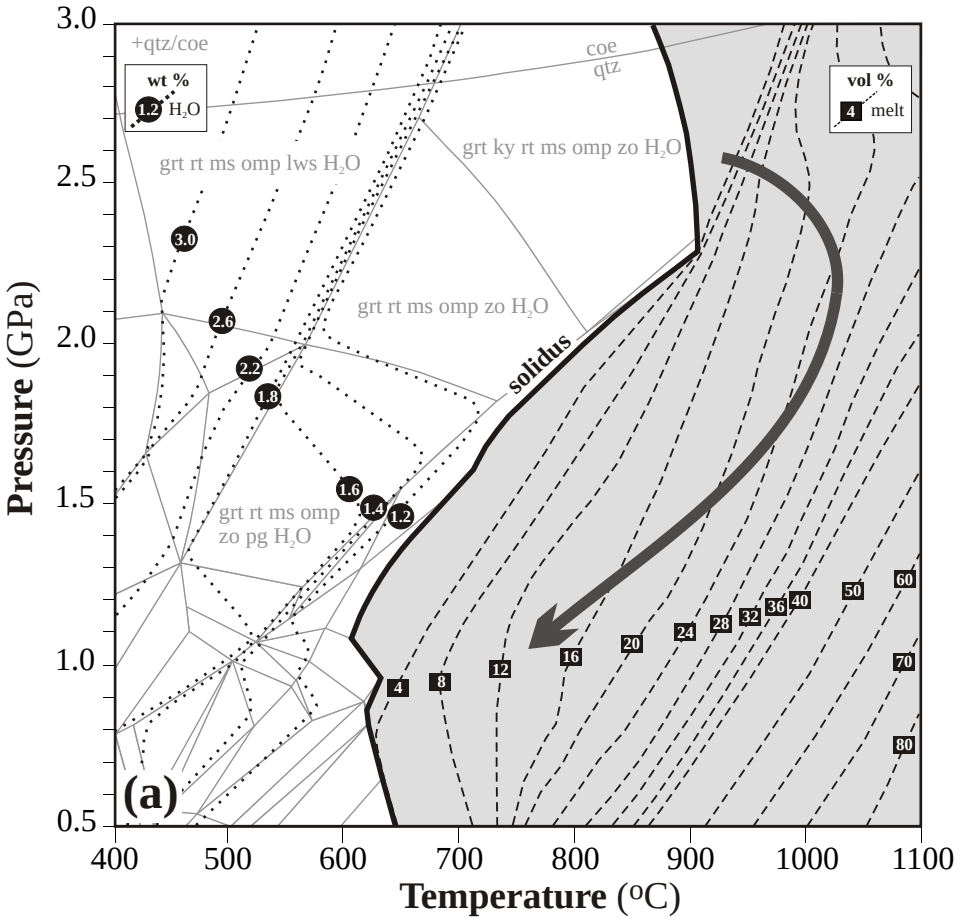
+qtz/coe
coe
qtz
wt %
1.2 H2O
vol %
4 melt
grt rt ms omp lws H2O
grt ky rt ms omp zo H2O
grt rt ms omp zo H2O
grt rt ms omp
zo pg H2O
solidus
(a)
Pressure (GPa)
Temperature (oC)
3.0
2.5
2.0
1.5
1.0
0.5
400
500
600
700
800
900
1000
1100

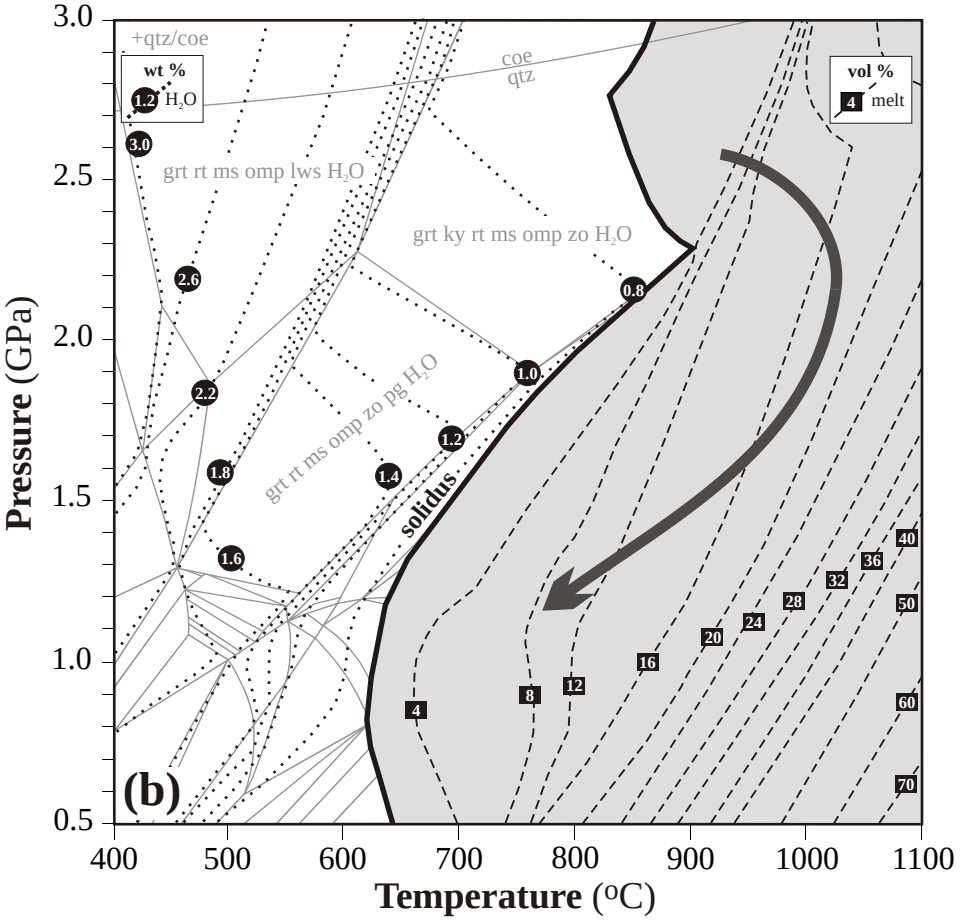
+qtz/coe
coe
qtz
wt %
1.2 H2O
vol %
4 melt
grt rt ms omp lws H2O
grt ky rt ms omp zo H2O
grt rt ms omp zo pg H2O
solidus
(b)
Pressure (GPa)
Temperature (oC)
3.0
2.5
2.0
1.5
1.0
0.5
400
500
600
700
800
900
1000
1100

Fig. 15

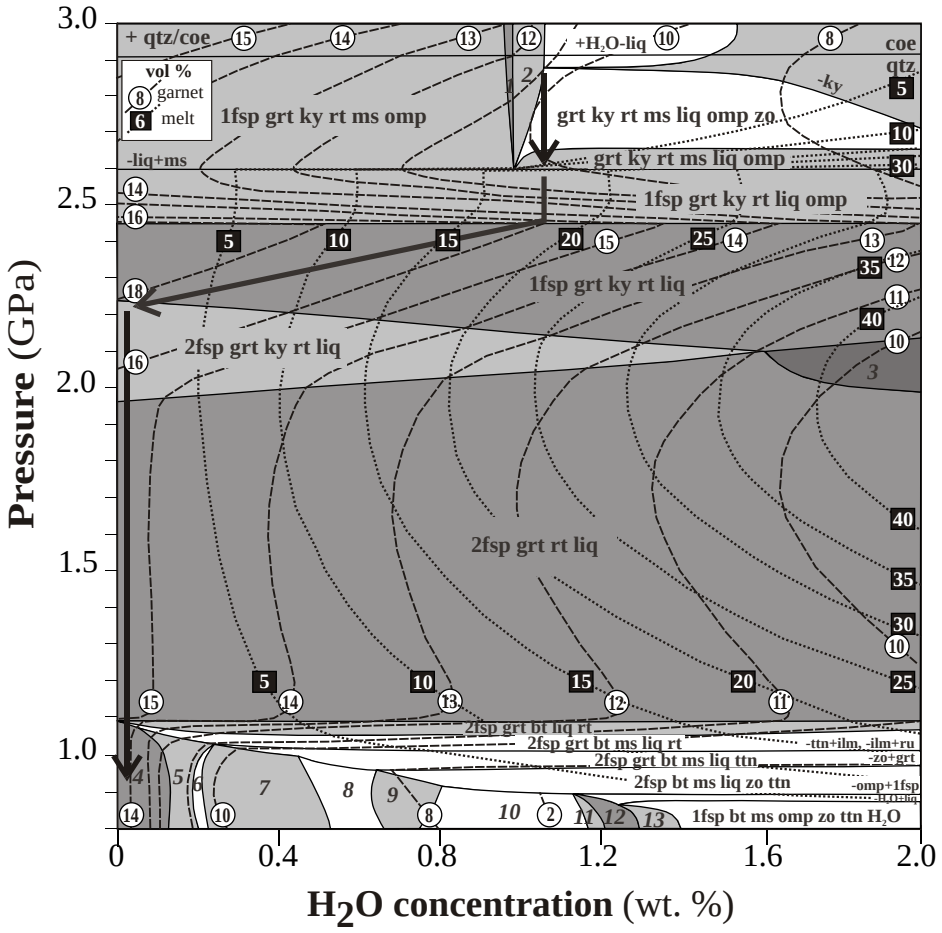
Pressure (GPa)
3.0
2.5
2.0
1.5
1.0
0
0.4
0.8
1.2
1.6
2.0
H2O concentration (wt. %)
+ qtz/coe
+H2O-liq
coe
qtz
vol %
garnet
melt
1fsp grt ky rt ms omp
grt ky rt ms liq omp zo
-ky
-liq+ms
grt ky rt ms liq omp
1fsp grt ky rt liq omp
1fsp grt ky rt liq
2fsp grt ky rt liq
2fsp grt rt liq
2fsp grt bt liq rt
2fsp grt bt ms liq rt
-ttn+ilm, -ilm+ru
2fsp grt bt ms liq ttn
-zo+grt
2fsp bt ms liq zo ttn
-omp+1fsp
-H2O=liq
1fsp bt ms omp zo ttn H2O

Fig. 16

PART I.

INCIPIENT ECLOGITE FACIES METAMORPHISM IN THE MOLDANUBIAN GRANULITES REVEALED BY MINERAL INCLUSIONS IN GARNET

We wanted to prove that the garnet inclusions (muscovite, omphacite) from prograde part of PT path in felsic granulites may transformed during high-temperature granulite facies metamorphism, partial melting and decompression to other phases, and so the original mineral can only be deduced from the inclusion morphology and reaction products. These inclusions have columnar shapes and consist of K-feldspar + kaolinite, albite + Fe-oxide, plagioclase + Fe-oxide, or albite + K-feldspar, respectively. The pseudomorphs with albite/plagioclase occur in a Ca-rich garnet that shows prograde zoning. Pressure-temperature (*PT*) evolution, derived from mineral assemblages in granulite and based on the inclusions, suggests a prograde metamorphism from amphibolite through eclogite to granulite facies conditions with subsequent amphibolite facies overprint during exhumation. The estimated *PT* trajectory for the studied granulites, which also host lenses or boudins of eclogites and garnet peridotites, allow reconstruction of the complete clockwise metamorphic path that is consistent with subduction geotherm prior to the tectonic amalgamation within the continental collisional root.

Lithos 114 (2010) 54–69

Contents lists available at ScienceDirect

Lithos

journal homepage: www.elsevier.com/locate/lithos

Incipient eclogite facies metamorphism in the Moldanubian granulites revealed by mineral inclusions in garnet

Shah Wali Faryad [a,*], Radmila Nahodilová [a,b], David Dolejš [a]

[a] Institute of Petrology and Structural Geology, Charles University, Albertov 2, 128 43 Prague 2, Czech Republic
[b] Czech Geological Survey, Klárov 3, 118 21 Prague 1, Czech Republic

ARTICLE INFO

Article history:
Received 8 December 2008
Accepted 20 July 2009
Available online 5 August 2009

Keywords:
Ti-rich muscovite
Omphacite
Prograde metamorphism
Granulite
Bohemian Massif

ABSTRACT

We investigated several mineral phases and their replacement products which occur as inclusions in garnets from felsic and mafic granulites of the Gföhl Unit in the Moldanubian Zone. The most important mineral inclusions, Ti-rich muscovite and omphacite, were used for the reconstruction of the metamorphic history of granulites. Some inclusions were transformed during high-temperature granulite facies metamorphism, partial melting and decompression to other phases, and so the original mineral can only be deduced from the inclusion morphology and reaction products. These inclusions have columnar shapes and consist of K-feldspar + kaolinite, albite + Fe-oxide, plagioclase + Fe-oxide, or albite + K-feldspar, respectively. The pseudomorphs with albite/plagioclase occur in a Ca-rich garnet that shows prograde zoning. Pressure–temperature (*PT*) evolution, derived from mineral assemblages in granulite and based on the inclusions, suggests a prograde metamorphism from amphibolite through eclogite to granulite facies conditions with subsequent amphibolite facies overprint during exhumation. The estimated *PT* trajectory for the studied granulites, which also host lenses or boudins of eclogites and garnet peridotites, allows reconstruction of the complete clockwise metamorphic path that is consistent with subduction geotherm prior to the tectonic amalgamation within the continental collisional root.

© 2009 Elsevier B.V. All rights reserved.

1. Introduction

The survival of high-/ultrahigh-pressure (HP/UHP) minerals in metamorphic rocks is often restricted to lithologies that often experienced rapid exhumation accompanied by continuous cooling. Where amphibolite or granulite facies overprint had occurred, the HP/UHP phases usually re-equilibrate and information about prograde or early high-pressure metamorphic history is lost. However, evidence for such processes can be traced from mineral inclusions preserved in phases that sustain a decompression. Garnet is a unique container that may preserve these phases, and it commonly occurs in metamorphic rocks from amphibolite through eclogite and granulite facies.

Granulite facies rocks with lenses of eclogites and garnet peridotites are abundant in the Moldanubian and Saxothuringian Zones in the Bohemian Massif (Fig. 1). UHP conditions were confirmed for some of these rocks by the presence of coesite or microdiamond in the Erzgebirge Mts. (Massonne, 2001; Nasdala and Massonne, 2000; Schmädicke and Müller, 2000) and by exchange thermobarometry in garnet peridotites and eclogites in the Moldanubian Zone (Medaris et al., 1998, 2006; Nakamura et al., 2004; Vrána and Frýda, 2003; Faryad et al., 2006a). Coesite has not yet been found in the Moldanubian Zone, although Raman spectroscopy analyses of quartz inclusions in zircon from eclogite in Nové Dvory (eastern part of the Moldanubian Zone) showed vibration peak of 512 cm^{-1} that is typical for coesite. Maximum pressure conditions of 2.0 and 2.3 GPa at 900–1000 °C for the adjacent felsic and mafic granulite were obtained in the Saxothuringian (Willner et al., 1997; O'Brien, and Rötzler, 2003; Rötzler et al., 2004) and Moldanubian Zones (Kotková and Harley, 1990; Carswell and O'Brien, 1993; O'Brien, 1999, 2008; Vrána et al., 2006).

There is, however, no information about a possible prograde stage of metamorphism from medium-temperatures or about the relationships between granulites, eclogite or garnet peridotites. In this work we present new data on mineral inclusions in garnet from granulites in the Moldanubian Zone that reveal prograde and high-pressure metamorphic history prior to the granulite facies re-equilibrium. This finding has important consequences for the interpretation of numerous eclogite and garnet peridotite bodies that either are enclosed in felsic granulites or occur adjacent to them. The HP/UHP rocks from the Saxothuringian Zone were considered as having resulted from south-eastward subduction beneath the Moldanubian Zone, and as a consequence the rocks in the Moldanubian Zone have been interpreted in different ways. In contrast to the geochemical and mineralogical similarities of granulites and garnet peridotites and eclogites in these two zones, which indicate similar petrogenetic scenarios, the origin of these rocks in the Moldanubian Zone was

* Corresponding author. Fax: +420 221 951 533.
E-mail address: faryad@natur.cuni.cz (S.W. Faryad).

0024-4937/$ – see front matter © 2009 Elsevier B.V. All rights reserved.
doi:10.1016/j.lithos.2009.07.014

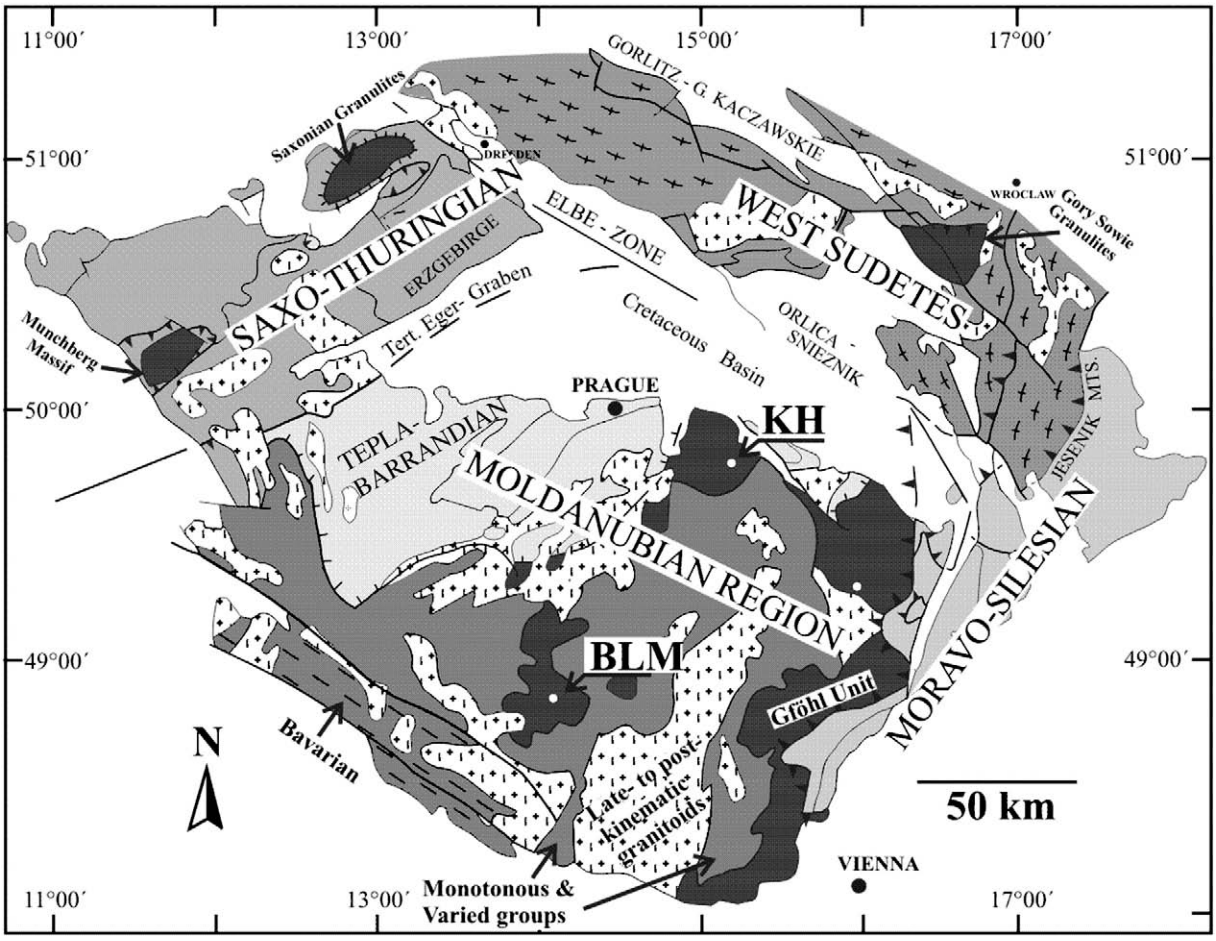

Fig. 1. Simplified geological map of the Bohemian Massif (modified after Franke, 2000). High-grade rock units in the Moldanubian Zone (Gföhl Unit) as well as in the Saxothuringian Zone (Münchberg Massif, Saxonian Granulite Mts.) and West Sudetes (Gory Sowie) are shown by dark colour. The studied localities in the Moldanubian Zone are the KHC (Kutná Hora Complex) and the BLM (Blanský Les Massif).

assumed to be related to a westward subduction beneath the Moldanubian Zone (Franke, 2000; Medaris et al., 2006; Finger et al., 2007). In another model (Schulmann et al., 2002, 2005) the rocks in the Moldanubian Zone were interpreted as fragments of lower-crust or upper-mantle exhumed by deep-level wedging (indentation) of a continental block and by buckling of crustal layers in thickened orogenic root. Therefore, the present study contributes to resolution of conflicting relationships and prograde histories of granulites, eclogites and garnet peridotites in the Variscan orogen.

2. Geological setting

Metamorphic rocks in the Moldanubian Zone of the Bohemian Massif belong to three tectonic units (the Gföhl Unit and the Varied and Monotonous Groups; Fig. 1), which differ by lithologies and metamorphic conditions (Dudek and Fediuková, 1974; Dawson and Carswell, 1990; Medaris et al., 1995; Dallmeyer et al., 1995). The Gföhl Unit, with granulites and migmatites, shows generally higher metamorphic conditions (granulite facies) when compared with the Varied and Monotonous Groups (amphibolite facies). All three units contain eclogites and peridotites, but garnet peridotites are known from the Gföhl Unit only, where they occur within or adjacent to granulites and gneisses. The estimated *PT* conditions are in the range of 1.6–2.1 GPa and 850–1000 °C for granulites, (Carswell and O'Brien, 1993; Petrakakis and Jawecki, 1995; O'Brien, 1999; Cooke, 2000; Štípská and Powell, 2005; Tajčmanová, et al., 2006; Racek et al., 2006, 2008; Franěk et al., 2006; Vrána et al., 2006; Kotková, 2007), 2–4 GPa and 800–1000 °C for eclogites (Vrána and Frýda, 2003; Nakamura et al., 2004; Medaris et al., 2006; Faryad et al., 2006b; Faryad, 2009; Štípská et al., 2006), and 3–5 GPa and 1000–1200 °C for garnet peridotites (Medaris et al., 1995; Faryad, 2009). Most granulite bodies occur along the eastern boundary of the Moldanubian Zone, but some are also exposed in the central (the Kutná Hora Complex, KHC) and southern parts (the Blanský Les Massif, BLM) near the towns of Kutná Hora and Český Krumlov, respectively (Fig. 1). Granulites from the eastern portions of the Moldanubian Zone have re-equilibrated under medium- to low-pressure conditions as documented by migmatization, replacement of kyanite by sillimanite and spinel, and breakdown of garnet to plagioclase and biotite. Granulites from the southern parts of the Moldanubian Zone have also re-equilibrated at lower pressures to variable extent but those from the Kutná Hora Complex contain no sillimanite, and the HP mineral assemblages are better preserved. A large portion of the granulites corresponds to the felsic variety but mafic granulites with diopsidic clinopyroxene and orthopyroxene are also abundant.

Geochronological studies gave ages of 370–340 Ma for the peak metamorphic conditions in high-grade rocks (Carswell and Jamtweit, 1990; Wendt et al., 1994; Svojtka et al. 2002; Kröner et al., 2000; Schulmann et al., 2005, 2008; Janoušek et al., 2006). The older ages come mostly from peridotites (Sm–Nd WR–Cpx–Grt isochron ages; Carswell and Jamtweit, 1990; Brückner et al., 1991; Beard et al., 1992; Becker, 1997). U–Pb zircon dating from granulites yielded mostly ages around 340 Ma (Kröner et al., 2000, Kotková, 2007 and references therein), but a 350-Ma Sm–Nd age from garnet in granulites has also been reported (Prince et al., 2000). Some Ar–Ar isotopic data from micas in some gneisses suggest that the final stages of exhumation

were linked to thrusting followed by cooling to ca. 300 °C at 325 Ma (Fritz et al., 1996).

Several granulite bodies with migmatites, gneisses and micaschists are present in the Kutná Hora Complex. The largest granulite body (5×10 km) at Běstvina village is characterized by the presence of garnet peridotite and eclogite boudins. Medaris et al. (1998, 2006) calculated a pressure of 5 GPa at 1100 °C for the garnet peridotite and 2 GPa at 900 °C for the eclogite at this locality, and a pressure of about 3.6 GPa was obtained for kyanite-bearing eclogite within felsic granulite (Faryad, 2009). Vrána et al. (2006) calculated a pressure of 2.2 GPa and temperature of 900 °C for this granulite.

The Blanský Les granulite (16×22 km) contains numerous bodies of serpentinite, garnet peridotite and amphibolite. Amphibolite lenses enclosed in granulite are assumed to have formed by retrogression of eclogite (Vrána, 1992), but no omphacite has been found in these rocks. Pressures of 1.3–1.8 GPa at 900–1000 °C were estimated for the Blanský Les granulite (Vrána, 1989; Owen and Dostál, 1996a,b; Kotková and Harley, 1990; O'Brien, 1999). A lower temperature of 800 °C at 1.7 GPa was estimated for the granulite facies metamorphism by Štípská and Powell (2005) who assumed that the ternary feldspar, previously interpreted to have formed at high temperature, is a relic from the igneous protolith. This model was also accepted for mafic granulite with inclusions of omphacite in garnet from St. Leonhard in Austria (Racek et al., 2006, 2008).

3. Petrology and mineral chemistry

The studied felsic granulites from both the Kutná Hora Complex and the Blanský Les Massif are composed of two feldspars, quartz, garnet and kyanite. They partly show weak foliation that varies from discrete, aligned quartz lenses to closely spaced quartz ribbons. Rutile, zircon, and apatite with monazite are the common accessories. Garnet, kyanite, and mesoperthite form disseminated, coarser grains of up to millimetre size, and ternary feldspars are also characteristic for these granulites. Mafic granulite from the Blanský Les Massif is composed of clinopyroxene, orthopyroxene, plagioclase, garnet, quartz, K-feldspar, hornblende and biotite. While mafic granulites form discrete layers and lenses in felsic granulite in the Kutná Hora Complex, their relations in the Blanský Les Massif are not very clear; according to Kodym (1972), they form lenses and boudins ranging from a few decimetres up to 250 m in size and occur within felsic granulite.

Five samples of granulites (four from felsic and one from the mafic variety) with mineral inclusions in garnet were selected for a detailed study. Textural relations and compositions of the minerals were studied by using a scanning electron microscope at Charles University and a CAMECA SX 50 electron microprobe at the Institute of Mineralogy and Crystal Chemistry, University of Stuttgart, which is equipped with four wavelength-dispersive spectrometers. The following standards were used: pyrope (Si, Al, Mg), andradite (Ca, Fe), jadeite (Na), spessartine (Mn), K-silicate glass (K), Ba-silicate glass (Ba), NaCl (Cl), as well as natural rutile (Ti) and topaz (F). The operating voltage was 15 kV using beam current between 10 and 15 nA, and the beam was focused to a 1- to 2-mm diameter except for micas, for which an 8- to 10-mm beam was used. Ferric/ferrous iron ratios of clinopyroxene were calculated using the method of Droop (1987). Crystalochemical formulae and end-member proportions are given in Tables 1–4.

3.1. Sample 28d (the Běstvina felsic granulite, the Kutná Hora Complex)

The granulite contains quartz, two feldspars (including antiperthite), garnet, biotite, kyanite, rutile and muscovite. Garnet shows a zoning profile (Fig. 2) that is characterized by a decrease of Ca and Mg and an increase of Fe from the core (Alm_{50}, Py_{32}, Grs_{17} in mol%) toward the rim (Alm_{60}, Py_{26}, Grs_{12}). Mn content is very low (less than 1 mol%) but shows a slight decrease toward the rim.

Two varieties of muscovite inclusions in garnet were observed (Fig. 2A, D). The first fresh muscovite inclusion has a high Ti content (TiO_2 = 3.0–3.1 wt.%), and it is rich in MgO (2.2–2.4 wt.%; average 0.22 Mg pfu) with FeO = 1.0–1.2 wt.% (0.06 Fe pfu) (Table 2). The second muscovite, partly replaced by biotite, has a low TiO_2 content (1.5–1.7 wt.%), with MgO = 1.7–2.7 wt.% and FeO = 0.8–1.3 wt.%. The low Ti in this muscovite is probably due to its partitioning into newly formed biotite, which has TiO_2 = 4.40 wt.%. Biotite replaces garnet, but it also occurs as individual grains in the matrix, and both varieties have high TiO_2 (4–5 wt.%) with X_{Mg} = 0.66–0.79. Plagioclase has an anorthite content of 13–20 mol%, with a very small orthoclase abundance (<2 mol%; Table 3). K-feldspars grains form both lamellae and individual grains and have albite content about 7–12 mol%.

Table 1
Representative electron microprobe analyses of garnet.

Sample	28B		27I		27H		CZG-23		H232	
Location*	c	+ms	c	r	c	+qtz	c	+sp	c	+om
SiO_2 wt.%	38.61	38.63	37.25	37.98	37.97	37.94	38.74	38.15	38.64	38.47
TiO_2	0.07	0.04	0.27	0.14	0.15	0.21	0.05	0.04	0.22	0.09
Al_2O_3	22.17	21.92	21.42	21.99	21.99	21.84	21.42	21.26	21.68	21.86
FeO	24.04	26.63	22.47	23.01	23.63	25.13	23.23	29.81	22.37	22.53
MnO	0.39	0.52	0.42	0.30	0.39	0.47	0.54	0.74	0.48	0.47
MgO	8.36	8.01	2.16	5.71	4.46	3.49	6.94	8.30	6.02	8.08
CaO	6.48	4.32	15.05	10.85	11.1	11.37	9.07	1.57	11.43	8.53
Total	100.12	100.06	99.04	99.98	99.69	100.46	100.03	99.91	100.84	100.03
Si *per 12 O*	2.964	2.984	2.955	2.947	2.932	2.933	2.991	2.979	2.967	2.957
Al	1.979	1.983	1.974	1.974	2.001	1.989	1.934	0.002	1.934	1.944
Ti	0.004	0.002	0.016	0.008	0.008	0.012	0.003	1.934	0.013	0.005
Fe^{3+}	0.013	0.013	0.000	0.011	0.000	0.011	0.058	0.056	0.041	0.045
Fe^{2+}	1.510	1.697	1.390	1.454	2.001	2.000	1.430	1.869	1.375	1.377
Mn	0.025	0.033	0.028	0.02	1.526	1.611	0.035	0.048	0.031	0.03
Mg	0.944	0.917	0.251	0.649	0.025	0.031	0.793	0.955	0.680	0.909
Ca	0.525	0.355	1.261	0.885	0.514	0.402	0.744	0.130	0.927	0.689
alm mol%	0.50	0.57	0.49	0.48	0.51	0.54	0.48	0.62	0.46	0.46
py	0.31	0.31	0.08	0.22	0.17	0.13	0.26	0.32	0.23	0.30
grs	0.17	0.12	0.42	0.29	0.31	0.31	0.25	0.04	0.31	0.23
sps	0.01	0.01	0.01	0.01	0.01	0.01	0.01	0.02	0.01	0.01

*Location indicates analysis of the grain core (c), rim (r) or at the contact with muscovite (+ms), polymorphic quartz (+qtz), spinel (+sp) and omphacite (+om).

Table 2
Representative electron microprobe analyses of micas.

Mineral	Muscovite		Biotite							
Sample	28b				271i	27h	CZG23		H232	
Location*	inc	inc	inc	mtx	mtx	mtx	mtx	+st	+opx	mtx
SiO_2 wt.%	46.93	46.84	36.53	35.31	34.85	36.78	36.04	37.25	36.51	37.12
TiO_2	3.14	3.12	4.33	4.46	3.17	4.79	6.17	4.81	5.58	7.18
Al_2O_3	30.89	30.79	16.62	19.21	19.36	17.13	14.41	16.12	13.87	13.33
Cr_2O_3	0.00	0.00	0.10	0.00	0.00	0.00	0.08	0.06	0.00	0.09
FeO	1.13	1.13	12.93	12.69	17.52	15.93	14.49	10.93	18.00	18.55
MnO	0.00	0.03	0.04	0.00	0.04	0.00	0.00	0.03	0.03	0.05
MgO	2.15	2.35	14.23	12.82	10.16	11.42	13.20	16.82	12.78	11.35
CaO	0.05	0.00	0.02	0.02	0.00	0.00	0.00	0.00	0.01	0.08
Na_2O	0.43	0.37	0.11	0.07	0.10	0.00	0.00	0.18	0.00	0.05
K_2O	10.61	9.89	9.52	9.86	9.96	9.60	10.08	9.96	9.87	9.84
BaO	0.38	0.32	0.04	0.35	0.00	0.00	0.00	0.00	0.38	0.20
F	0.42	0.49	0.52	0.61	–	–	–	–	–	–
Total	96.14	95.33	95.00	95.41	95.15	95.65	94.47	96.16	97.03	97.83
Si *per 11 O*	3.132	3.127	2.813	2.633	2.765	2.742	2.816	2.780	2.741	2.765
Al^{IV}	0.868	0.873	1.187	1.367	1.236	1.258	1.184	1.220	1.227	1.170
Al^{VI}	1.561	1.549	0.322	0.321	0.573	0.268	0.143	0.198	0.000	0.000
Ti	0.158	0.157	0.251	0.250	0.189	0.248	0.363	0.270	0.315	0.402
Cr	0.000	0.000	0.006	0.000	0.000	0.000	0.005	0.004	0.000	0.005
Fe^{2+}	0.063	0.063	0.832	0.791	1.162	0.993	0.947	0.682	1.130	1.156
Mn	0.000	0.002	0.003	0.000	0.003	0.000	0.000	0.002	0.002	0.003
Mg	0.214	0.234	1.633	1.425	1.202	1.270	1.538	1.871	1.430	1.260
Ca	0.003	0.000	0.002	0.002	0.000	0.000	0.000	0.000	0.001	0.006
Ba	0.010	0.008	0.001	0.938	0.000	0.000	0.000	0.000	0.011	0.006
Na	0.056	0.048	0.016	0.010	0.016	0.000	0.000	0.026	0.000	0.008
K	0.903	0.843	0.935	0.010	1.008	0.913	1.005	0.948	0.946	0.935
F	0.101	0.104	0.126	0.145	–	–	–	–	–	–
X_{Mg}			0.662	0.643	0.508	0.561	0.619	0.733	0.559	0.522

*Indicates location of the analysis: inc — inclusion in garnet, mtx — matrix, +st — at the contact with staurolite, +opx — at the contact with orthopyroxene.

3.2. Sample 27i (felsic granulite from the Miškovice village, the Kutná Hora Complex)

The Miškovice granulite body (0.5 × 2 km) is characterized by 1- to 5-cm-thick leucocratic bands. It consists of plagioclase, K-feldspar, quartz with abundant relics of antiperthitic feldspar, together with garnets, kyanite, and biotite. Garnet forms up to 4-mm grains, with inclusions of quartz, kyanite, and rutile, and some garnet grains contain numerous columnar-shaped inclusions of K-feldspar that sometimes have parallel orientation (Fig. 3A–E). These inclusions were found in several garnet grains, and they always occur in the central and relatively Ca-rich parts of garnet. In addition to K-feldspar, these inclusions contain kaolinite, Fe-oxide and numerous cavities. It is not clear whether the holes are after one of these phases or after another mineral that was lost during thin-section preparation. Garnet with such inclusions is mostly cross cut by biotite crystals that have random orientation and form overgrowths from the matrix side (Fig. 3A, B). This sample also contains atoll garnet filled by one or more of the minerals: quartz, K-feldspar, biotite, and antiperthite. The host garnet with the columnar-shaped inclusions is rich in Fe and Ca and has a relatively flat compositional profile in the core ($Grs_{42\text{-}37}$, $Py_{7\text{-}9}$, $Alm_{49\text{-}54}$, Sps_1), but at the rims it shows an increase in Mg and a decrease in Ca (Grs_{29}, Py_{22}, Alm_{48}, Sps_1, Fig. 3C–E, Table 1). Biotite in the matrix, including that which cross-cuts garnet, has $TiO_2 = 3.2$–4.4 wt.% and $X_{Mg} = 0.48$–0.52 (Table 2). Relics of antiperthitic plagioclase have $An_{24\text{-}16}$, but some large plagioclase grains have high Ca in the core (An_{35}), which decreases towards the rim (An_{14}). K-feldspar lamella in antiperthite has Ab = 7 mol%.

Table 3
Representative electron microprobe analyses of feldspars.

Mineral	kfs	pl	kfs	pl	pl	pl	kfs	pl
Sample	28b		27i		CZG23		H232	
Location*	P	P	A	A	inc	mtx	A	A
SiO_2 wt.%	64.41	64.72	65.43	65.84	58.72	62.60	64.65	63.20
Al_2O_3	18.62	22.25	18.28	21.37	26.08	23.60	18.57	23.28
CaO	0.14	3.37	0.00	2.78	8.66	6.02	0.12	5.03
Na_2O	1.60	9.29	0.77	9.69	6.01	7.50	0.80	8.30
K_2O	14.30	0.25	15.62	0.20	0.36	0.47	15.61	0.31
Total	99.07	99.89	100.09	99.87	99.84	100.20	99.75	100.11
per 8 (O)								
Si	2.985	2.850	3.010	2.893	2.633	2.791	2.989	2.788
Al	1.017	1.155	0.991	1.107	1.378	1.240	1.012	1.210
Ca	0.007	0.159	0.000	0.131	0.416	0.288	0.006	0.238
Na	0.143	0.793	0.068	0.825	0.523	0.648	0.072	0.709
K	0.845	0.014	0.917	0.011	0.021	0.027	0.920	0.017
ab mol%	0.144	0.821	0.069	0.853	0.545	0.673	0.072	0.736
an	0.007	0.165	0.000	0.135	0.434	0.299	0.006	0.246
or	0.849	0.015	0.931	0.012	0.022	0.028	0.922	0.018

*Indicates textural relationship of the analyzed grain: P — perthite, A — antiperthite, inc — inclusion in garnet, mtx — matrix.

Table 4
Representative electron microprobe analyses of pyroxene, amphibole and spinel.

Mineral	Pyroxene				Amphibole	Spinel
Sample	H232				CZG23	
Location*	inc		mtx	+pl	inc	inc
SiO_2 wt.%	51.99	51.64	51.57	52.24	39.21	0.23
TiO_2	0.83	0.83	0.41	0.09	1.90	0.06
Al_2O_3	11.42	11.33	3.11	2.04	17.49	60.55
Cr_2O_3	0.00	0.00	0.00	0.01	0.00	0.58
FeO	6.57	6.58	11.35	25.33	11.61	22.09
MnO	0.06	0.04	0.22	0.20	0.06	0.04
MgO	9.00	9.00	12.06	20.32	11.19	9.45
CaO	16.83	16.75	20.45	0.40	11.57	0.00
Na_2O	4.10	3.99	0.80	0.02	2.08	
K_2O					0.67	
ZnO						6.54
F					0.02	
Cl					0.25	
Total	100.79	100.16	99.97	100.648	96.54	99.54
atoms per			*6 O*		*23 O*	*4 O*
Si	1.873	1.874	1.934	1.956	5.877	0.006
Ti	0.023	0.023	0.012	0.003	0.214	0.001
Al	0.485	0.484	0.137	0.090	3.090	1.947
Cr	0.000	0.000	0.000	0.000	0.000	0.013
Fe3+	0.007	0.002	0.010	0.000	0.000	0.000
Fe2+	0.191	0.197	0.345	0.793	1.455	0.504
Mn	0.002	0.001	0.007	0.006	0.008	0.001
Mg	0.483	0.487	0.674	1.134	2.499	0.384
Ca	0.650	0.651	0.822	0.016	1.858	0.000
Na	0.287	0.281	0.058	0.001	0.604	
K					0.128	
Zn						0.132
F					0.010	
Cl					0.064	
X_{Mg}	0.72	0.71	0.67	0.59	0.63	0.43
aug mol%	60.6	58.8	81.10			
jd	28.1	28.0	3.82			
aeg	0.7	0.2	1.07			
FeMgtsc	7.2	5.5	0.00			
Titsc	3.4	3.4	1.77			
opx	0.0	2.0	11.17			

*Indicates textural relationship of the analyzed grain: inc — inclusion in garnet, mtx — matrix and +pl — at the contact with plagioclase.

3.3. Sample 27h (felsic granulite from Miškovice village, the Kutná Hora Complex)

This is a leucocratic band in felsic granulite that has relatively high proportions of quartz and feldspars. Garnet has a composition in the core (Grs_{31}, Py_{17}-$Alm_{51}Sps_1$; Table 1) close to that in the rest of the granulite (sample 27i), but the garnet rim exhibits lower Ca and higher X_{Mg} (Grs_{15}, Py_{20}, Alm_{55}, Sps_1). Inclusion of polycrystalline quartz (Fig. 3F and G) was found in garnet, which yielded high Ca content (Grs_{31}; Table 1). Cracks in garnet are not radial but rather sub-parallel in one direction. Biotite in the matrix is rich in $TiO_2 = 4.8$ wt.%, with $X_{Mg} = 0.56$.

3.4. Sample CZG23 (felsic granulite, the Blanský Les Massif)

Weakly foliated granulite contains 5- to 30-mm-wide leucocratic bands (leucosome). The main minerals in the light-gray granulite (paleosome) are feldspars, garnet and quartz, with accessory apatite and rutile. Kyanite was found as inclusions in garnet. Garnet has a composition in the range of $Alm_{48\text{-}62}$, $Prp_{26\text{-}32}$, $Grs_{25\text{-}04}$, and $Sps_{1\text{-}2}$ (Table 1) and shows prograde zoning in the central part, where Mn and X_{Fe} decrease outward but Ca remains constant (Fig. 4). The rim parts of garnet show strong retrograde zoning, with a decrease in Ca and Mg, an increase in Fe, and a slight increase in Mn. In addition to rutile, garnet contains columnar euhedral inclusions filled mostly with albite but K-feldspar and plagioclase (An_{14} and An_{43}) were also found (Fig. 5A, B). These inclusions occur in the Ca-rich internal parts of garnet (Fig. 5C, D) and usually contain a mixture of Fe-oxide + titanite with small holes. Calcic amphibole rimming apatite was also observed as inclusion in garnet (Fig. 5E). Outer, Ca-poor parts of some garnet crystals (Alm_{62}, Prp_{32}, Grs_{04}) may contain inclusions of biotite and spinel (Fig. 5F) with about 6 wt.% ZnO in the latter (Table 4).

Biotite analyzed in the matrix has a relatively high TiO_2 content (6.2 wt.%) and low X_{Mg} (0.62) compared with that overgrowing garnet or occurring with the spinel inclusion ($TiO_2 = 4.8$ and $X_{Mg} = 0.73$; Table 2). Both biotite and host garnet in contact with spinel have very low ZnO (<0.04 wt.%). The amphibole inclusion in garnet is pargasite with low F (0.02 wt.%) and Cl (0.25 wt.%; Table 4). The low halogen contents suggest that it does not represent a simple reaction product between apatite and garnet but rather it has formed by fluid-present transformation of some previous phase. With the exception of high SiO_2, the rest of the oxide constituents in a hypothetical pargasite are in the range of 0.5 host garnet + 0.5 hypothetical Mg-rich ($X_{Mg} = 0.92$) Na-clinopyroxene (Jd_{30}). Plagioclase in the matrix has An_{31}, and accessory K-feldspar is almost pure orthoclase. No antiperthite was found in the rock.

3.5. Sample H232 (mafic granulite, the Blanský Les Massif)

The granulite consists of garnet, clinopyroxene, orthopyroxene, mesoperthite, plagioclase, biotite, quartz, rutile, and ilmenite. In the field, it forms an exposure of about 6 × 15 m in size but its relation to surrounding felsic granulite is not obvious. The garnet shows a flat profile in the core, with a composition of Grs_{32}, Py_{25}, Alm_{45}, and retrograde zoning near the rim (Grs_{24}, Py_{21}, Alm_{51}). Omphacite (Jd_{28};

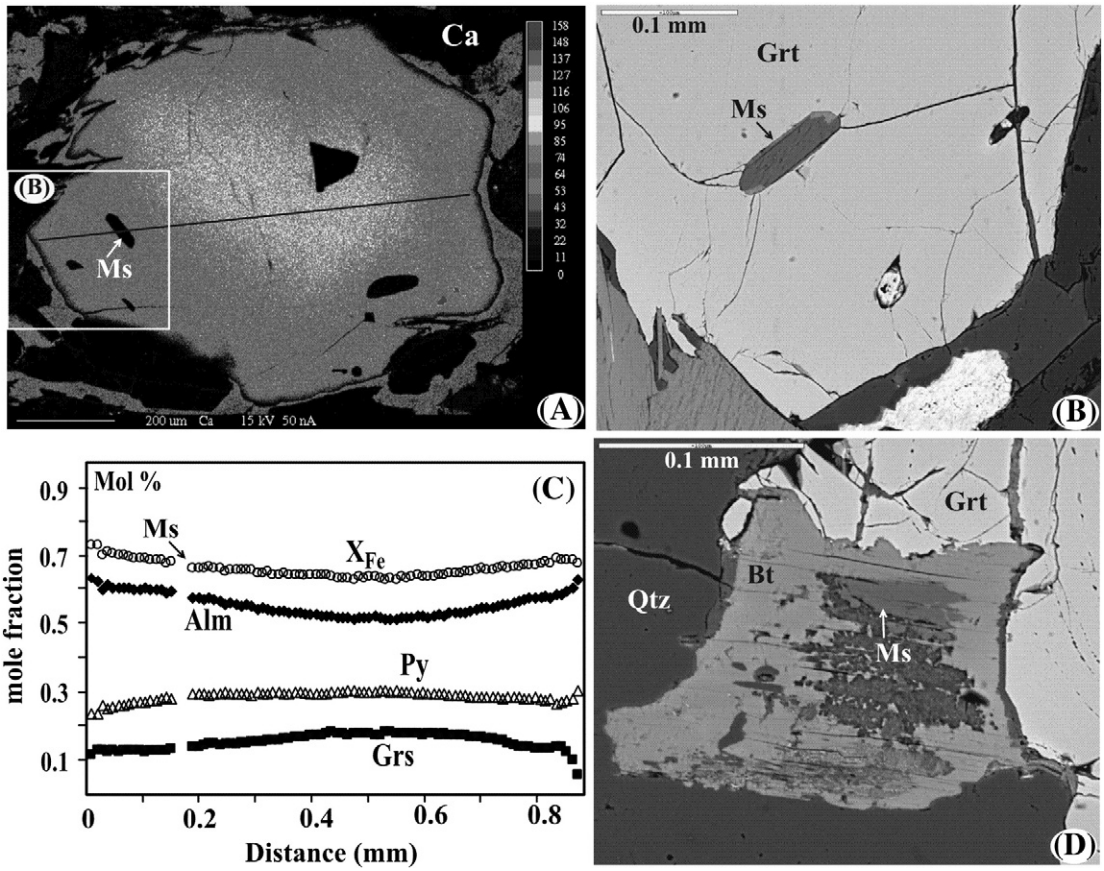

Fig. 2. Compositional map (Ca concentration) of garnet with inclusion of Ti-muscovite (A) with detailed backscattered electron image (B) and compositional profile (C) from the Běstvina felsic granulite (sample 28b in the Kutná Hora Complex). (D) shows muscovite replaced by biotite with quartz, all enclosed in garnet (sample 28b).

Table 4) was found as an inclusion in garnet (Fig. 6A), and symplectite of clinopyroxene with plagioclase is partly enclosed in the outer part of garnet. Clinopyroxene in the matrix is diopside, with X_{Mg} of about 0.78. Fig. 6B shows garnet with inclusion of antiperthite and quartz, and the garnet is partly replaced by a symplectite of orthopyroxene + plagioclase. Orthopyroxene also occurs in the corona around quartz at the contact with garnet (Fig. 6B), and its X_{Mg} values are in the range of 0.52 to 0.60. Plagioclase in the matrix has a composition of $An_{34\text{-}50}$, and that occurring in the symplectite with orthopyroxene is rich in Ca, with An_{85}. Antiperthite with An_{24} and Or_2 has a lamella of K-feldspar of Or_{92}, Ab_{07}. Biotite has $X_{Mg} = 0.55$ with $TiO_2 = 7.2$–5.6 wt.%.

4. Discussion and interpretation

4.1. Inclusions of Ti-muscovite

Most Ti-rich muscovites are known from igneous rocks (Monier et al., 1984; Speer, 1984). The HP/UHP metamorphic rocks usually contain phengite without extreme Ti contents, although several metamorphic Ti-rich muscovites (phengites) from UHP terranes have also been described (Table 5). The first two are from microdiamond-bearing gneisses and quartz-rich rocks of the Kokchetav Massif and Saxonian Erzgebirge, respectively. The third Ti-rich muscovite, with a similar composition but having slightly higher Mg content, was reported from the Archean garnetiferous quartzite in the East Athabasca, western Canadian Shield. All of these three rocks with Ti-rich muscovite show temperatures of 830–1000 °C (Table 5; the lower temperature for the Saxonian locality is after Willner et al., 1997). A minimum pressure of 1.5 GPa for the Archean garnetiferous quartzite is based on the assumption of coexisting kyanite and plagioclase but the associated peraluminous kyanite- and corundum-bearing garnet clinopyroxenite with fassaitic sodian clinopyroxene and an unusually pyrope-rich garnet suggest higher-pressure nature (Snoeyenbos et al., 1995). Two titanian phengites were reported from UHP metagranite in the western Alps. They come from the Dora Maira Massif and from Monte Mucrone, and they coexist with a mineral assemblage that indicates a temperature of about 700 °C. An average of 8 microprobe analyses from the studied Ti-rich muscovite in the Kutná Hora granulite from the Moldanubian Zone shows relatively low Fe but high Mg, which is similar to muscovite from the Saxonian Erzgebirge, Kokchetav Massif and East Athabasca.

Table 5 shows no systematic variation in Ti content in muscovite among different occurrences—only muscovites that formed at higher temperatures have lower Fe content (except for muscovite from the Saxonian locality). The main substitution in the Ti-muscovite is assumed to be $Ti^{VI} + Mg^{VI} = 2Al^{VI}$ (Monier and Robert, 1986). Because phengite without extreme Ti content is widely known from medium-temperature UHP rocks (e.g., Carswell et al., 1997; Massonne, 2003), the preservation of Ti-rich variety is likely due to its high thermal stability (Spicer et al., 2004). Therefore, it has resisted reactions or melting, and occurs as inclusions in garnet, which prevented re-equilibrium with other phases during decompression.

4.2. Inclusions of K-feldspar + kaolinite

The columnar pseudomorphs of K-feldspar with kaolinite and opaque phases in garnet from granulite (sample 27i) in the Kutná Hora Complex indicate their possible formation from muscovite by incipient melting: muscovite + quartz = K-feldspar + kyanite + melt. Kyanite was not observed, but kaolinite as alteration product provides convincing evidence for the presence of former Al-rich silicate. The lack of rutile or other titaniferous phase in the pseudomorphs

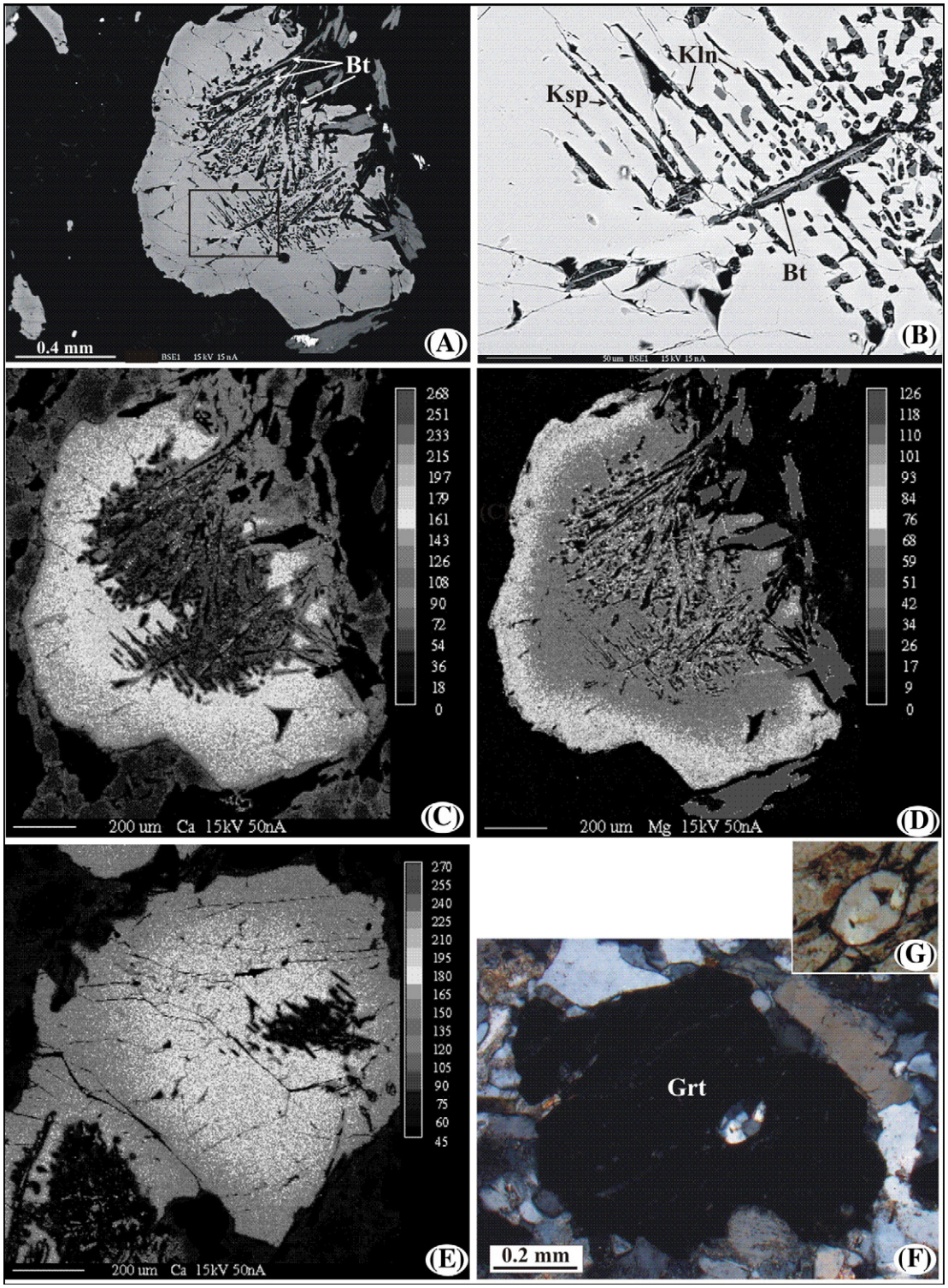

Fig. 3. Backscattered electron images (A, and detail in B) of columnar pseudomorphs of K-feldspar and kaolinite with Fe-oxides after muscovite (phengite?) from Miškovice felsic granulite (sample 27i) in the Kutná Hora Complex. Note that biotite has grown from the outside and it is perpendicular to the orientation of the columnar inclusions. (C)–(E) show compositional maps of Ca and Mg from two garnets with these inclusions. The inclusions occur in the central (Ca-rich) part of the garnet. (F) shows garnet with inclusion of polycrystalline quartz from leucocratic granulite (sample 27H). Detail in plan-polarized light is shown in the upper-right section (G).

suggests that this muscovite was Ti-poor and not stable at higher temperatures. Furthermore, preservation of Ti-rich muscovite and the presence of columnar-shaped pseudomorphs document that granulite formed from a muscovite or phengite-bearing protolith. Partial dehydration melting of such rocks is supported by the formation of leucocratic bands in the granulite, also known from HP metamorphic rocks elsewhere (e.g. Lang and Gilotti, 2007).

No coesite or its pseudomorphs have been reported from the Moldanubian eclogites or granulites but the presence of polycrystalline quartz is usually considered as evidence for the former presence of these phases (Liou et al., 1998). Kobayashi et al. (2007) analyzed quartz inclusions in zircon from eclogite in Nové Dvory by Raman spectroscopy, found peaks of quartz at 464 and 393 cm^{-1} but also a weak peak at 521 cm^{-1} and a still weaker peak at 179 cm^{-1}. Such

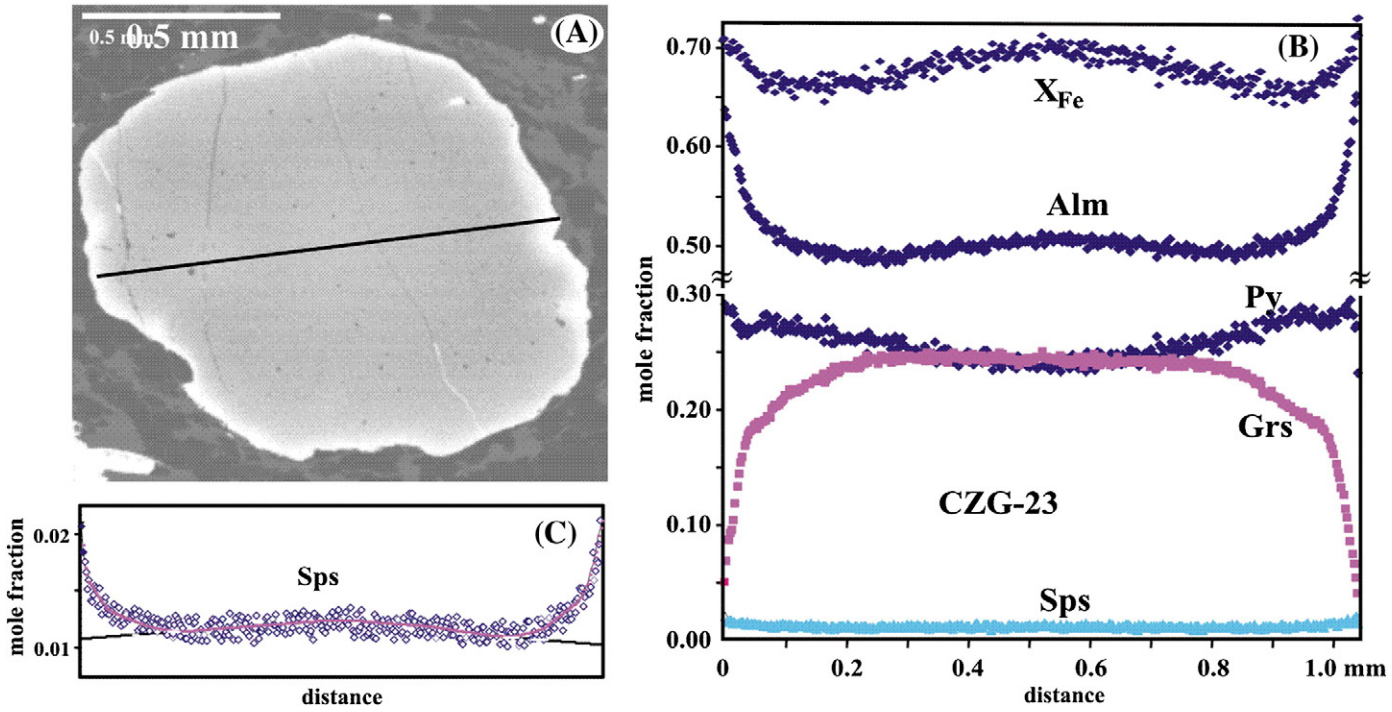

Fig. 4. Backscattered electron image (A) of garnet from paleosome part of granulite gneiss (sample CZG23). The thin line shows the position of the compositional profiles (B, C). Note the outward decrease of X_{Fe} (B) and spessartine (C) in the core (prograde zoning) and their strong backward diffusion zoning at the rim of the garnet.

peaks represent fundamental vibrations of coesite along with the typical quartz vibration as reported from quartz-transformed coesite in UHP rocks (Fulai et al., 2002). Raman spectroscopy of polycrystalline SiO_2 inclusion in garnet (Fig. 3F) showed only quartz peaks thus suggesting complete recrystallization of coesite if it had ever formed.

4.3. Inclusions of sodic plagioclase

Based on their forms and composition, the columnar inclusions filled by albite, and partly also by Ca-rich plagioclase or K-feldspar, could have formed by transformation of jadeite, paragonite, glaucophane, or, in the case of plagioclase, from a mixture of paragonite and margarite. However, the reactions producing these minerals require one or more additional reactant or product phases:

$$\text{Jadeite: } NaAlSi_2O_6 + SiO_2 = NaAlSi_3O_8 \quad (1)$$

$$\text{Paragonite: } NaAl_2AlSi_3O_{10}(OH)_2 + SiO_2 = NaAlSi_3O_8 + Al_2SiO_5 + H_2O \quad (2)$$

$$\text{Glaucophane: } 4\,Na_2(Fe_3Al_2)Si_8O_{22}(OH)_2 + 3\,O_2 = 8\,NaAlSi_3O_8 + 8\,SiO_2 + 6\,Fe_2O_3 + 4\,H_2O \quad (3)$$

$$\text{Margarite: } CaAl_2(Al_2Si_2)O_{10}(OH)_2 + SiO_2 = CaAl_2Si_2O_8 + Al_2SiO_5 + H_2O \quad (4)$$

Because no other hydrous phases except for retrograde (?) biotite are present in granulite, the formation of feldspars in these inclusions could have occurred by dehydration melting of one or more of these phases during prograde metamorphism. Subsequent retrogression and alteration could result in further transformation of the product phases, as illustrated by the presence of Fe-oxides and titanite. However, it is clear that these columnar-shaped inclusions, occurring in the central part of garnet, were once in equilibrium with the host Ca-rich garnet and can be used to trace the early metamorphic history of the rock. This is confirmed by the prograde zoning in garnet that is probably preserved due to its high Ca content and its low diffusion rate among other divalent cations in garnet (Loomis, 1978; Loomis et al., 1985; Ganguly et al., 1998; Carlson, 2006).

The presence of spinel in the Ca-poor rim part of garnet suggests its formation under granulite facies conditions. Such textures are widely known from felsic granulites elsewhere in the Bohemian Massif (Becker and Altherr, 1991; Carswell and O'Brien, 1993; Petrakakis and Jawecki 1995; Owen and Dostal 1996a,b; O'Brien, 1997), and they are assumed to be the result of kyanite breakdown, which produces spinel and/or corundum, as well as Al-rich sapphirine. These reactions are probably due to decompression breakdown of kyanite followed by growth of garnet under near-isobaric cooling.

4.4. Inclusions of omphacite

Lenses and boudins of UHP eclogites and garnet peridotites in felsic granulites have been described from the Kutná Hora Complex (Medaris et al., 2006; Faryad, 2009). Garnet peridotites with similar mineral assemblages and chemistry also occur in the Blanský Les Massif, but mafic rocks have almost completely converted to amphibolite, and their maximum pressure conditions are not clear (Vrána, 1992). The presence of omphacite inclusion in garnet from mafic granulite suggests that these rocks passed through eclogite facies prior to their granulite facies overprint. Diopside-rich clinopyroxene forms small grains within the foliated matrix. By contrast, clinopyroxene–plagioclase symplectite, which is partly enclosed by garnet, suggests replacement of omphacite during decompression. Similarly, the formation of orthopyroxene was related to decompression into the granulite facies. In contrast to garnet peridotite and eclogite, which are assumed to be tectonically emplaced in granulites, the relationship between mafic and felsic granulites is not always

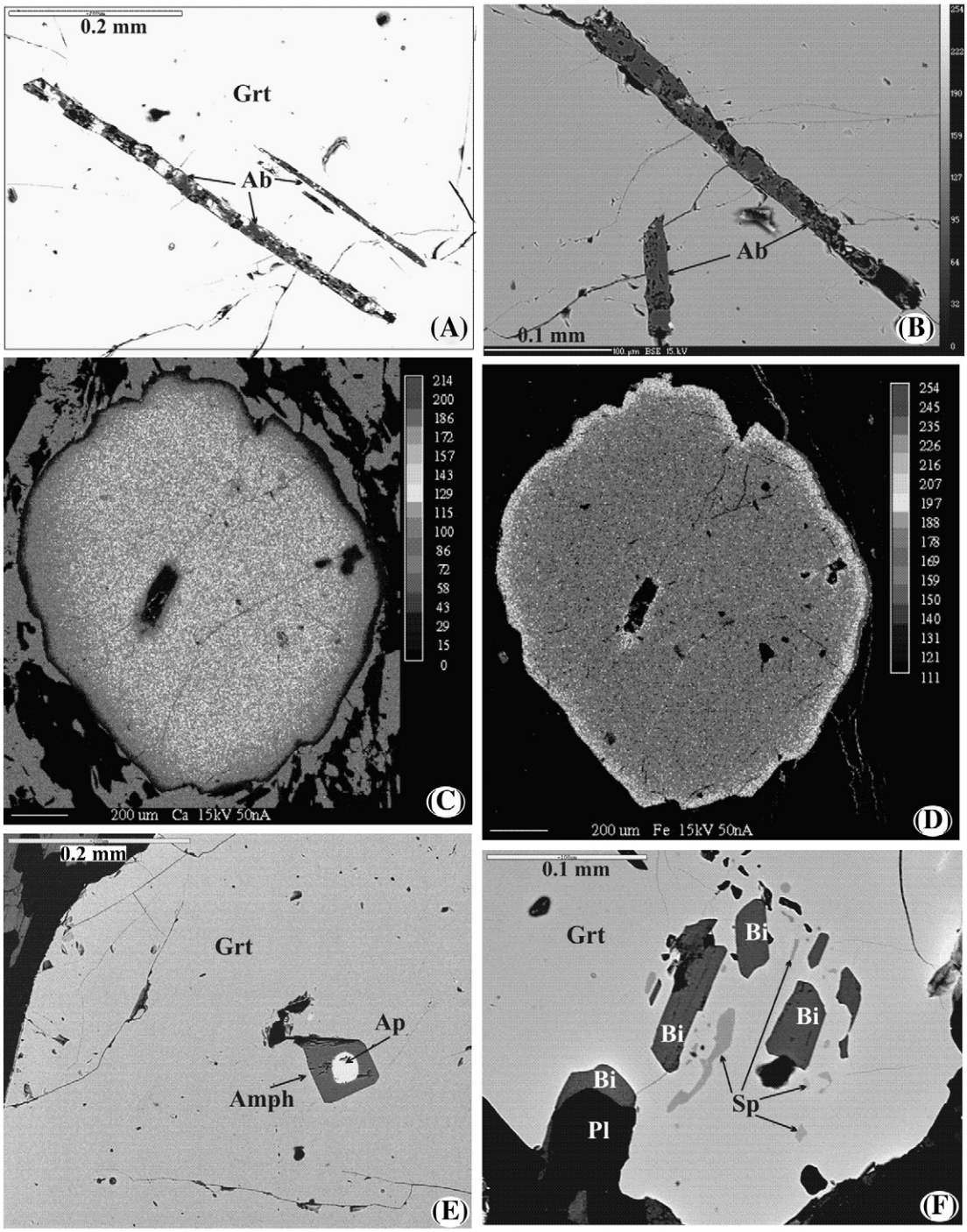

Fig. 5. Backscattered electron images (A B, E, and F) and compositional maps (C and D) of garnet crystals with inclusions from granulite gneiss in the Blanský Les Massif (sample CZG23). (A) and (B) show inclusions of albite with Fe-oxides (after clinopyroxene, Na-amphibole, or paragonite?). (C) and (D) are concentration maps (Ca and Fe) of the host garnet with columnar-shaped inclusion of albite + K-feldspar (Ksp). Note the diffusion zone of Ca around this inclusion. (C) shows amphibole inclusion around apatite in garnet, and (D) shows inclusions of Zn-spinel and biotite with some holes (dark) in the garnet rim.

clear. According to Kodym (1972) they form boudins in the Blanský Les granulite, but granulites of similar lithologies and compositions from the Münchberg Massif (Saxothuringian Zone) are characterized by 1- to 4-m-thick bands (layers) that alternate with felsic granulite along an almost 500-m deep borehole profile (Rötzler et al., 2004). The same is found in the Kutná Hora area, where mafic varieties form discrete bands and lenses within felsic granulite. The lack of clinopyroxene in felsic granulites could be due to inappropriate whole-rock composition or could be a result of extensive granulite facies overprint, as discussed further below.

4.5. Pressure–temperature stability of the observed inclusions

There is general agreement about the maximum *PT* conditions ($T = 900–1000$ °C and $P = 1.8–2.2$ GPa) reached by the granulites in the Bohemian Massif, including those in the Blanský Les Massif and in the Kutná Hora Complex (Vrána, 1989; O'Brien, 1999; Vrána et al., 2006; Kotková, 2007). In spite of possible common metamorphic history of granulites and eclogites lenses with prograde zoned garnet, most thermobarometric calculations for granulites are focused only on their exhumation and retrograde histories (see Kotková 2007 and

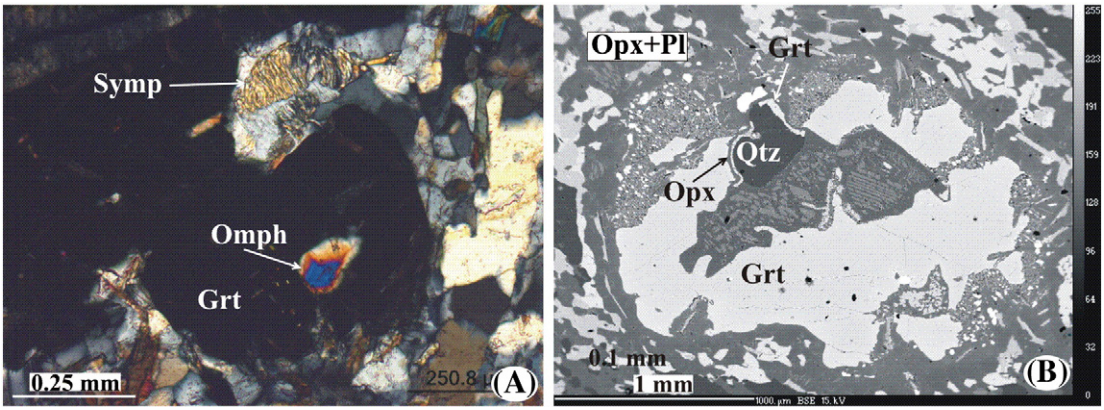

Fig. 6. Photomicrograph in crossed polarizers (A) and BSE image (B) from mafic granulite (sample H232) in the Blanský Les Massif. (A) shows omphacite (omph) inclusion in garnet, and symplectite (symp) of clinopyroxene with plagioclase, partially armatured by garnet, is also preserved. (B) shows composite antiperthite and quartz inclusion in garnet, and orthopyroxene (opx) corona around quartz at the contact with garnet is also shown. Garnet is partly replaced by symplectite of plagioclase with orthopyroxene.

references therein). To trace the *PT* stability fields of the observed inclusion phases and to examine the possible prograde history from amphibolite/eclogite to granulite facies conditions, the pseudosection method was applied to samples 28b and CZG23. The pseudosection was calculated by the Gibbs energy minimization software Perplex (Connolly, 2005) with the internally consistent thermodynamic data set of Holland and Powell (1998: 2002 upgrade). Because of the very low whole-rock Mn contents (MnO < 0.09 wt.%), the pseudosections were calculated in the NKCFMASH and NKCFMATSH systems, and the results of the NKCFMATSH system for samples 28b and CZG23 are presented in Figs. 7 and 8. Feldspar mixing models were formulated following Holland and Powell (2003), and the model used for H_2O-bearing melt was adapted from White et al. (2001). Other models that were used include orthopyroxene (Powell and Holland, 1999), garnet and clinopyroxene (Holland and Powell, 1998) and biotite and phengite (White et al., 2007).

Considering that the muscovite in sample 28b was preserved due to its high Ti content and that the columnar inclusions of K-feldspar + kaolinite (after kyanite) in garnet are products of dehydration melting after phengite/muscovite, the Kutná Hora granulite should, based on the pseudosection (Fig. 7), have crossed the muscovite breakdown reaction at 2.2 GPa while at temperatures of 900–1000 °C (Vrána, 1989; O'Brien, 1999; Vrána et al., 2006; Kotková, 2007). *PT* conditions of 900 °C/2.2 GPa for partial melting of granulite in the Kutná Hora Complex were obtained by combination of phase equilibrium modeling and experimental work (Nahodilová et al., 2008). These *PT* data fit well with the data from the adjacent kyanite-bearing eclogite lens of this locality, which contains garnet with prograde zoning and shows a maximum pressure of 3.4 GPa followed by decompression in granulite facies conditions at 900 °C (Faryad, 2009).

Pseudosection calculated for sample CZG23 (Fig. 8) contains a wide array of Na–Ca minerals (paragonite, jadeite, phengite, glaucophane, zoisite) that are suitable candidates for phases observed as inclusions in garnet. All of these phases are stable at temperatures exceeding 600 °C and pressures of up to 2.2 GPa. Phengite, similar to that in sample 28b, decomposes at 900 °C/2.2 GPa, and biotite is stable at higher temperatures. Preservation of a weak but prograde zoning in garnet in this sample suggests that its core composition was not completely modified by diffusion and may reflect *PT* conditions close to the metamorphic stage during which the phases were enclosed. This fits well with the garnet isopleths ($X_{Fe} = 0.69–0.70$ and $X_{Ca} = 0.23–0.24$) which are located in one of these fields with glaucophane, jadeite, and phengite at $T = 620$ °C and $P = 2.2$ GPa. The outer part of the garnet, with the highest pyrope content ($X_{Ca} = 0.18$ and $X_{Fe} = 0.66$), gives $T = 820$ °C and $P = 1.6$ GPa or T870 °C/1.0 GPa and may record granulite facies conditions before modification of the marginal part of garnet during cooling.

The main difference between the NKCFMASH (not shown) and NKCFMATSH models is in the stability field of kyanite in sample 28b. In the Ti-free system, kyanite is present above 2 GPa, but in the Ti-bearing system it occurs in a wide *PT* space, above 0.5 GPa and 500 °C (Fig. 7). The breakdown reaction of muscovite is slightly shifted to lower pressure in the Ti-bearing system. In the sample CZG23, biotite appears during retrogression from granulite facies conditions at $T = 800–850$ °C and $P = 0.5–1.5$ GPa in the Ti-free system, but in the Ti-bearing system biotite is present almost in the whole *PT* diagram (Fig. 8). Both the Ti-bearing and Ti-free systems show the presence of clinopyroxene in the pseudosections, although in the Ti-free system in sample 28b it appears at higher pressure (above 1.7 GPa/600 °C to 2.5 GPa/900 °C). The lack of clinopyroxene in the studied samples can be explained by one of the following alternatives: (1) the rock experienced a prograde *PT* path along the low-pressure boundary of the clinopyroxene stability field (~1.3 GPa/600 °C to 1.7 GPa/900 °C for sample 28b and 1.3 GPa/600 °C to 2.0 GPa/900 °C for sample CZG23); (2) the clinopyroxene has formed at high pressure conditions but was subsequently replaced during decompression under granulite facies conditions; or (3) the present topology of the clinopyroxene-bearing field is a result of poor thermodynamic constraints of clinopyroxene–garnet–feldspar equilibria at high pressures. The last option was discussed also by Štípská and Powell (2005), who discussed the lack of experimental data used in the calibration of ternary feldspar mixing at high pressures. The option (3) is supported by the presence of omphacite inclusion in garnet from the mafic variety of granulite at this locality (sample H232). In felsic granulite under high-pressure conditions, a jadeite-rich clinopyroxene is expected, but it could have been in scenario (2) readily converted to albite during high-temperature granulite facies overprint. Garnet–clinopyroxene thermometry applied to mafic granulite (sample H232) indicated granulite facies conditions (923 ± 20 and 948 ± 43 °C, obtained by the calibrations of Ai, 1994 and Ganguly et al., 1996,

Table 5
Composition of Ti-muscovite/phengite (atoms per 11 oxygens) from HP/UHP metamorphic rocks.

Locality	Si	Ti	Mg	Fe	*P* (GPa)	*T* (°C)	Source
Kokchetav Massif	3.22	0.28	0.18	0.07	UHP	1000	1
Saxonian Erzgebirge	3.19	0.14	0.29	0.14	UHP	830, 1000	2, 3
East Athabasca	3.17	0.21	0.53	0.04	min 1.5	1000	4
Dora Maira	3.37	0.19	0.28	0.13	UHP	700	5
Monte Mucrone	3.39	0.14	0.36	0.12	UHP	700	6
Moldanubian Zone	3.14	0.15	0.28	0.06	min. 2.2	900	7

Literature sources: 1 — Vavilov et al. (1991), 2 — Willner et al. (1997), 3 — Massonne (2003), 4 — Snoeyenbos et al. (1995), 5 — Bino and Compagnoni (1992), 6 — Koons (1987), 7 — this study.

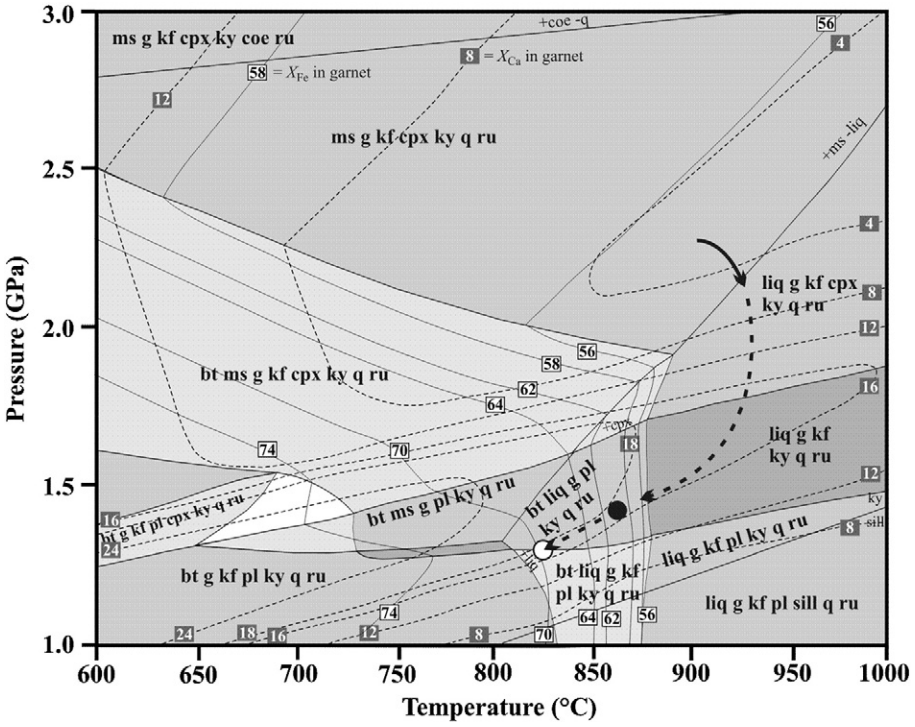

Fig. 7. Pseudosection for a felsic granulite with muscovite inclusion in garnet from the Kutná Hora Complex (sample 28b; whole-rock composition: SiO_2 72.86, TiO_2 0.35, Al_2O_3 10.36, FeO 5.35, MgO 4.24, CaO 2.42, Na_2O 2.17, K_2O 2.08, H_2O 1.50 in mol%). Phase abbreviations are as follows: bt — biotite, cd — cordierite, coe — coesite, cpx — clinopyroxene, g — garnet, ilm — ilmenite, ky — kyanite, liq — liquid, ms — muscovite, opx — orthopyroxene, q — quartz, ru — rutile, sill — sillimanite. Solid and open circles indicate the intersections of isopleths for the core and rim composition of garnet, respectively.

respectively), which are comparable to those in the Kutná Hora Complex. Omphacite was not found in the Kutná Hora mafic granulite yet but diopside and plagioclase are present in the matrix.

4.6. Omphacite–garnet–feldspar equilibria at the eclogite–granulite facies transition

The mineral inclusion relics observed in garnet and the subsequent granulite facies overprint are in a close relationship to preservation of some mineral assemblages during the eclogite–granulite facies transition. Here we discuss the clinopyroxene–garnet–feldspar equilibria, which mark the decompression into the granulite facies and the potential for preservation of eclogite–facies mineral assemblages and composition.

The evolution of granulite facies assemblage, particularly the formation of feldspar by omphacite and garnet breakdown, can be described by the Na_2O–CaO–Al_2O_3–SiO_2 (NCAS) and Na_2O–CaO–MgO–Al_2O_3–SiO_2 (NCMAS) systems. With increasing pressure, plagioclase breaks down to jadeite and grossular-rich garnet according to equilibria:

$$NaAlSi_3O_8\,(\text{albite}) = NaAlSi_2O_6\,(\text{jadeite}) + SiO_2\,(\text{quartz}) \quad (5)$$

$$3\,CaAl_2Si_2O_8\,(\text{anorthite}) = Ca_3Al_2Si_3O_{12}\,(\text{grossular}) + 2\,Al_2SiO_5\,(\text{kyanite}) + SiO_2\,(\text{quartz}) \quad (6)$$

The end-member equilibria are shifted by 0.35–0.55 GPa (Fig. 9). During decompression, jadeite component in clinopyroxene and grossular component in garnet become depleted in favour of newly formed plagioclase. The breakdown first appears in felsic granulites with high Na/Ca whole-rock ratios whereas the depletion in Ca of garnet commences at lower pressures in particular for mafic granulites. In other words, the formation of early, sodium-rich plagioclase provides evidence for its origin during the decompression into the granulite facies.

Fig. 10 illustrates the role of omphacite by expanding the composition space from the NCAS to NCMAS system. At medium-temperature eclogite facies, clinopyroxene is ordered into jadeit rich, omphacite and diopside-rich compositions which undergo progressive disordered and miscibility as temperature increases (Green et al., 2007). Simultaneously, orthopyroxene becomes unstable in the presence of kyanite and is replaced by garnet. The assemblage of omphacitic clinopyroxene and Ca-bearing garnet is, therefore, characteristic for the high-temperature eclogite facies. Phase compositions in this high-variance assemblage are sensitive to whole-rock Na_2O, CaO and MgO contents. In felsic granulites, Na-rich omphacites coexist with Ca-poor garnets whereas in mafic protoliths, both omphacite and garnet are comparably rich in Ca (Fig. 10).

During decompression from eclogite to granulite facies series of phase compatibilities occurs as a consequence of combination of feldspar-forming equilibria (Eqs. (5) and (6)) with breakdown of Na-rich clinopyroxene and omphacite according to the reaction:

$$2\,Na_{0.5}Ca_{0.5}Mg_{0.5}Al_{0.5}Si_2O_6 + SiO_2 = NaAlSi_3O_8 + CaMgSi_2O_6 \quad (7)$$

As temperature increases and pressure decreases, newly formed plagioclase becomes progressively more calcic, clinopyroxene becomes nearly pure diopside whereas garnet is depleted in the grossular component. This divariant equilibrium can be deduced from compatibility triangles (Fig. 10) and it first occurs in felsic granulites which consist of Ca-poor garnet and plagioclase at high-temperature eclogite facies conditions but is recorded later by mafic granulites which may preserve relics of diopsidic clinopyroxene.

The results of phase equilibrium modeling are consistent with petrographic observations from felsic and mafic granulites from the Kutná Hora Complex and the Blanský Les Massif. In felsic granulites, breakdown of sodic clinopyroxene must have occurred relatively early in favour of sodic plagioclase coexisting with garnet. In mafic granulites, the transition to plagioclase-bearing assemblage occurs at lower pressures, and in very Ca-rich protoliths diopside-rich

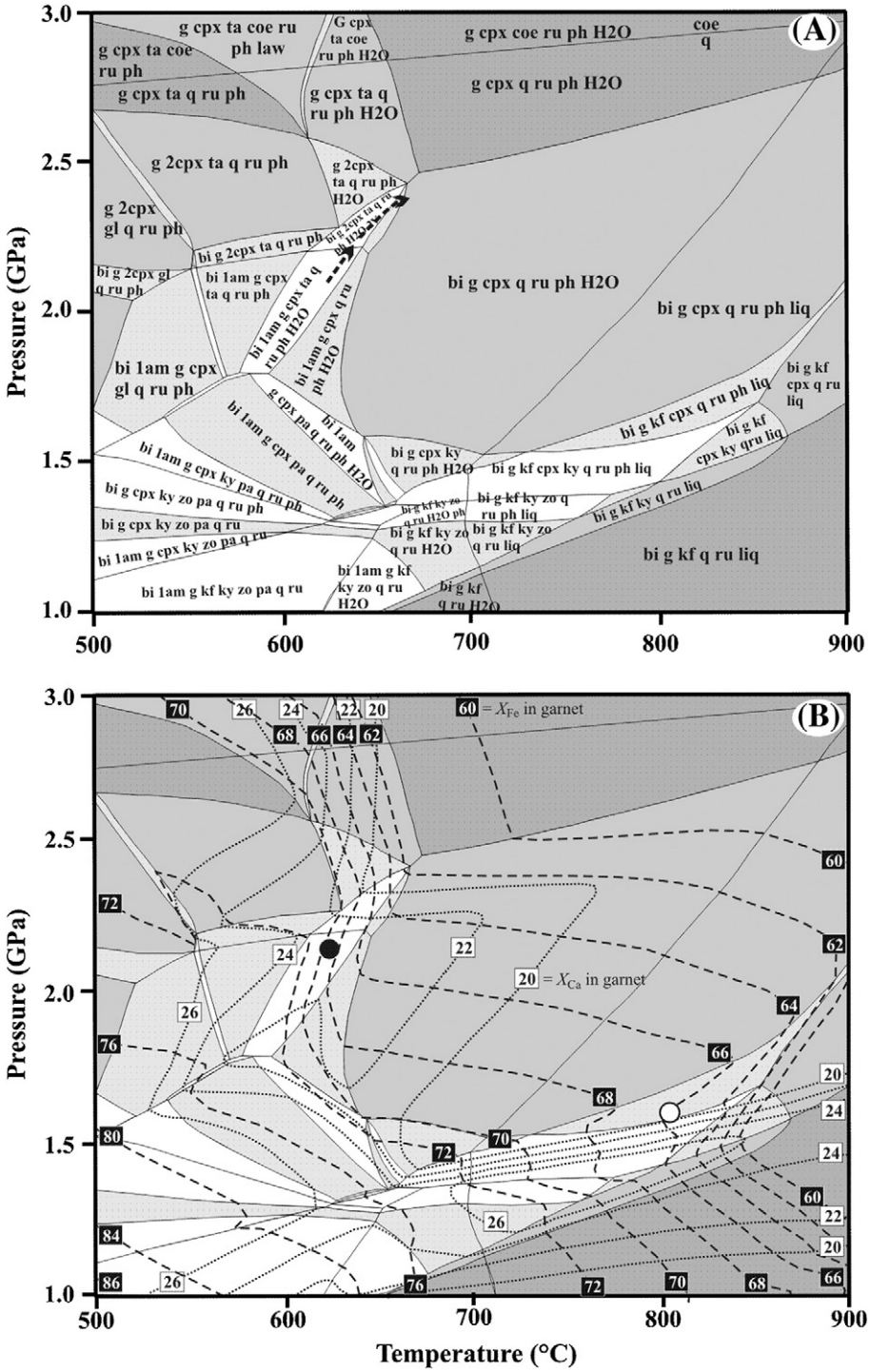

Fig. 8. Pseudosection (A) and garnet composition isopleths (B) for a granulite with inclusions of feldspars in garnet from the Blanský Les Massif (sample CZG23; whole-rock composition: SiO_2 60.64, TiO_2 0.95, Al_2O_3 16.60, FeO 7.08, MgO 3.83, MnO 0.11, CaO 4.10, Na_2O 2.78, K_2O 2.05, H_2O 1.01 in wt.%). Phase abbreviations are as follows: amp — amphibole, pa — paragonite, ph — phengite, ta — talc, for others see Fig. 7. Dotted arrows in (A) show a possible prograde PT path derived from inclusions and compositional zoning in garnet. Filled and open circles in (B) are intersections of the garnet X_{Ca} and X_{Fe} isopleths.

clinopyroxene coexists with calcic plagioclase and Ca-depleted garnet. These observations suggest that jadeite-rich clinopyroxene cannot be preserved in felsic rocks into the granulite facies but the prograde and decompression *PT* path can still be reconstructed from their pseudomorphs as inclusions in garnet as well as from the intragranular variations in garnet composition. By contrast, the composition of plagioclase in matrix is likely to reflect the re-equilibriation at granulite facies conditions owing to much more rapid diffusional exchange. However, inclusions of albite, which have probably formed from Na-rich phase like jadeite isolated in garnet, can preserve the original composition.

4.7. Geodynamic setting of the granulite facies overprint

The most debated questions regarding metamorphism of the Gföhl Unit in the Moldanubian Zone concern the origin of and relationships between granulites and associated eclogites and garnet peridotites. The formation of eclogites and garnet peridotites is usually related to a

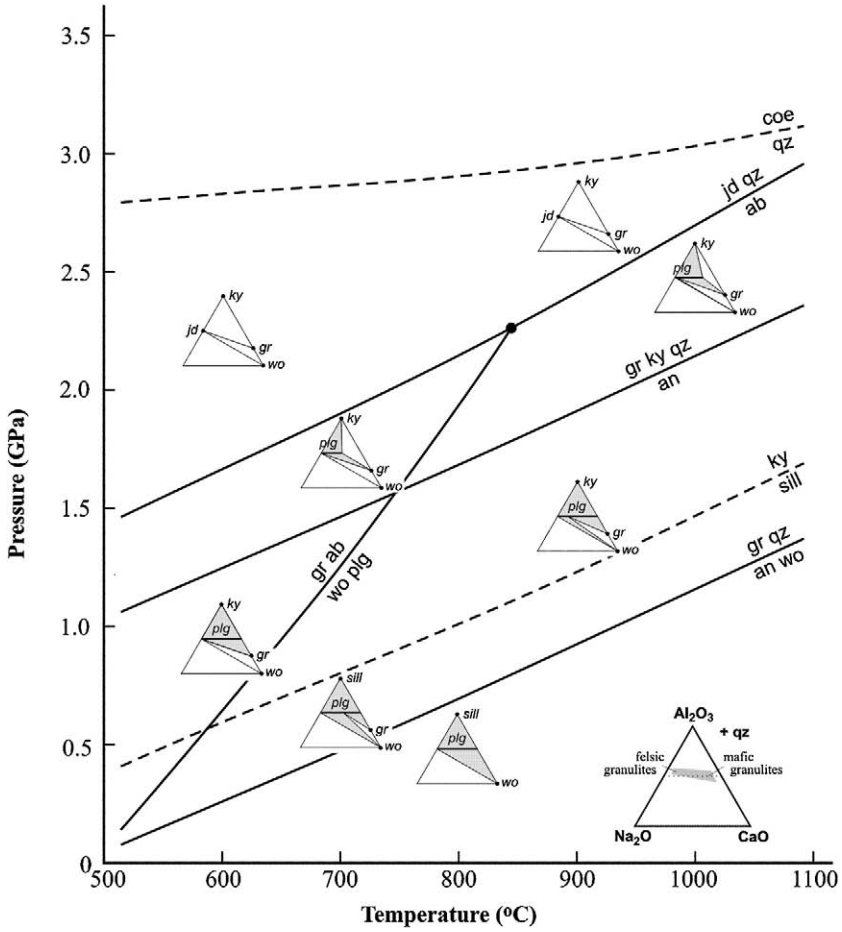

Fig. 9. Pressure–temperature projection of the Na_2O–CaO–Al_2O_3–SiO_2 system illustrating mineral equilibria and phase compatibilities at the eclogite–granulite facies transition. Phase abbreviations are: ab — albite, an — anorthite, coe — coesite, gr — grossular, jd — jadeite, ky — kyanite, plg — plagioclase, qz — quartz, sill — sillimanite, wo — wollastonite.

subduction-zone setting (Medaris et al., 2005; Vrána, 1992; Finger et al., 2007; Kotková et al., 1997) but they are also assumed to represent fragments of the upper-mantle that, together with granulites (lower continental crust), were exhumed during thickening of the continental crust in the orogenic root (Schulmann et al., 2002, 2005). Answering this question as well as explaining the relationships between eclogites/garnet peridotites and granulites, will require integration of petrological, geochemical, geochronological, structural, and geophysical data. Fig. 11 summarizes the *PT* equilibria of granulites and the host eclogite, which forms a lens in the Kutná Hora granulite. In spite of granulite facies recrystallization, this eclogite preserves garnet with prograde zoning, omphacite and kyanite recording a pressure of 3.6 GPa at $T = 900$ °C (Faryad, 2009). Consistent with the data from literature (Carswell and O'Brien, 1993; O'Brien, 1999, 2008; Vrána et al., 2006), these results confirm that eclogites/garnet peridotites and granulites share the same *PT* loop at least from HP granulite facies (minimum 2.2 GPa) conditions. The lack of coesite constrains maximum pressure of about 2.8 GPa at 850 °C reached by the granulite. The granulites could have reached the coesite field, but the coesite must have been decomposed, when the rocks were decompressed at higher temperatures of the granulite facies. Alternatively, coesite has not formed due to kinetic overstepping or a rapid prograde path (Spear, 1993).

Preservation of pre-granulite (amphibolite to eclogite) facies mineral inclusions or their replacement products in garnet, as well as the presence of prograde zoning garnet in granulite, are indicative of a prograde metamorphism accompanied by very fast burial and subsequent exhumation rates of the rocks. The corresponding model for such rapid cycling is usually assumed to result from syn-subduction exhumation of detached slab fragments or exhumation along the subduction channel (Chemenda et al., 1996; Cloos and Shreve, 1988; Gerya et al., 2002; Froitzheim et al., 2003). In addition to the west-dipping subduction zone (Medaris et al., 2005; Finger et al., 2007), the close similarities in lithology, whole-rock composition, age relations, mineral composition, and *PT* conditions of granulites, eclogites and garnet peridotites between the Moldanubian and Saxothuringian Zones (Janoušek et al., 2006; Massonne and O'Brien, 2003 and references therein) would suggest their formation under similar conditions, that is, along a subduction zone. In addition to the possible common granulite facies metamorphic history of the HP/UHP rocks in the Bohemian Massif, the results of this work demonstrate that mineral inclusions in garnet or in other rock-forming phases can be used as a fruitful tool for investigating high-pressure rocks overprinted in granulite facies conditions.

5. Conclusions

1. Mineral inclusions in garnets from felsic granulites of the Gföhl Unit in the Kutná Hora Complex and in the Blanský Les Massif indicate a prograde PT path from eclogite facies conditions prior to granulite facies metamorphism.
2. Passage through the eclogite facies is further supported by the presence of omphacite inclusion or its pseudomorphs in garnet from mafic granulite that occur as discrete lenses in felsic granulites. The composition of Ti-rich muscovite inclusion in garnet from felsic granulite is comparable to that known from other UHT and UHP terranes, and its presentation is interpreted to be due to high Ti content.

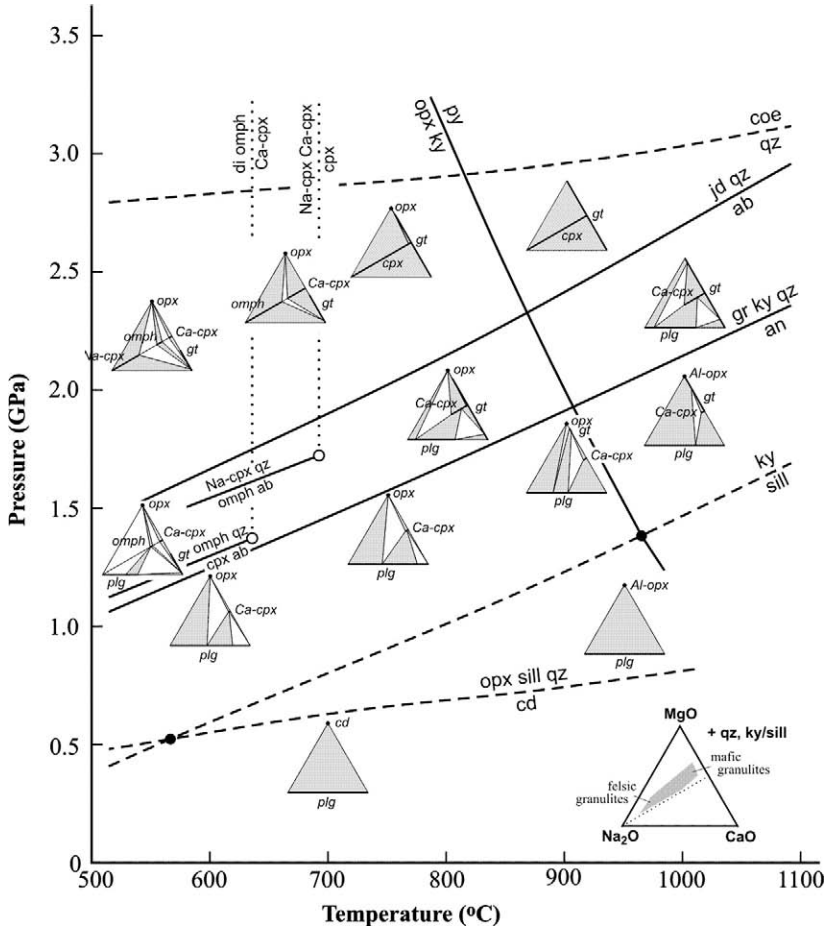

Fig. 10. Pressure–temperature projection of the Na_2O–CaO–MgO–Al_2O_3–SiO_2 systems illustrating mineral equilibria and phase compatibilities at the eclogite–granulite facies transition. Phase abbreviations are: cd — cordierite, cpx — clinopyroxene, omph — omphacite, opx — orthopyroxene, py — pyrope, for others see Fig. 9.

3. Granulite has formed from a muscovite-bearing hence hydrous protolith as evidenced by the presence of mica inclusions and their pseudomorphs in garnet.
4. The relationship of granulite to LT/HP metamorphism, consistent with subduction geothermal regime, is supported by (1) the presence of UHP eclogite that has locally preserved garnet with prograde zoning, and (2) the *PT* trajectory of granulite obtained using the pseudosection method with stability fields of mineral inclusions in garnet.

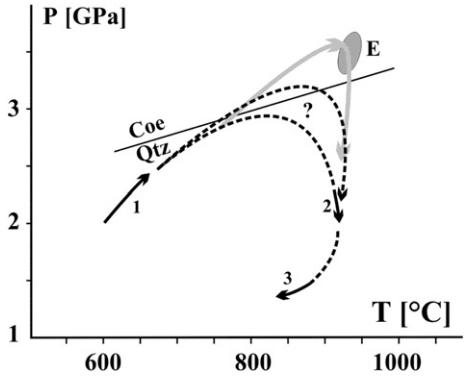

Fig. 11. Summary of the *PT* conditions and interpreted *PT* paths (dashed curves) for the studied granulites in the Moldanubian Zone. Arrows in points 1 and 2 are locations of the stability field and breakdown reactions (Figs. 7 and 8) of phases enclosed in garnet, respectively. Point 3 shows the intersection of isopleths for near-rim composition of garnet in sample CZG23. The *PT* path (gray curve) for the eclogite lens (E; Faryad, 2009) in the Kutná Hora granulite (sample 28d) is also indicated.

Acknowledgments

This study was supported by the research projects of Ministry of Education of the Czech Republic MSM 0021620855 and the Czech Science Foundation 205/06/0688. Sample CZG23 was kindly provided by J. Košler. T. Theye (Stuttgart) and K. Ettinger (Graz) are thanked for their help with microprobe analyses. The first version of this paper has benefited from discussions and suggestions of P. O'Brien. We thank Ch. Hauzenberger for his careful and thorough review of the manuscript.

References

Ai, Y., 1994. A revision of the garnet–clinopyroxene Fe^{2+}–Mg exchange geothermometer. Contributions to Mineralogy and Petrology 115, 467–473.

Beard, B.L., Medaris, L.G., Johnson, C.M., Brückner, H.K., Mísař, Z., 1992. Petrogenesis of Variscan high-temperature group A eclogites from the Moldanubian Zone of the Bohemian Massif, Czechoslovakia. Contributions to Mineralogy and Petrology 111, 468–483.

Becker, R.H., 1997. Sm–Nd garnet ages and cooling history of high-temperature garnet peridotite massifs and high-pressure granulites from Lower Austria. Contributions to Mineralogy and Petrology 127, 224–236.

Becker, H., Altherr, R., 1991. Al-rich sapphirine in a high-P charnockite: reaction textures and *P–T* evolution. Terra Abstracts 3, 437.

Bino, G.G., Compagnoni, R., 1992. Very-high-pressure metamorphism of the Brossasco coronite metagranite, Southern Dora-Maira Massif, Western Alps. Schweizerische Mineralogische und Petrographische Mitteilungen 72, 347–363.

Brückner, H.K., Medaris, L.G., Bakun-Czubarow, N., 1991. Nd and Sr age and isotope patterns from Variscan eclogites of the eastern Bohemian Massif. Neues Jahrbuch für Mineralogie, Abhandlungen 163, 169–196.

Carlson, W.D., 2006. Rates of Fe, Mg, Mn, and Ca diffusion in garnet. American Mineralogist 91, 1–11.

Carswell, D.A., Jamtweit, B., 1990. Variscan Sm–Nd ages for the high-pressure metamorphism in the Moldanubian Zone of the Bohemian Massif. Neues Jahrbuch für Mineralogie, Abhandlungen 162, 69–78.

Carswell, D.A., O'Brien, P.J., 1993. Thermobarometry and geotectonic significance of high-pressure granulites—examples from the Moldanubian Zone of the Bohemian Massif in lower Austria. Journal of Petrology 34, 427–459.
Carswell, D.A., O'Brien, P.J., Wilson, R.N., Zhai, M., 1997. Thermobarometry of phengite-bearing eclogites in the Dabie Mountains of central China. Journal of Metamorphic Geology 15, 239–252.
Chemenda, A.I., Mattauer, M., Bokun, A.N., 1996. Continental subduction and a mechanism for the exhumation of high-pressure metamorphic rocks: new modelling and field data from Oman. Earth and Planetary Science Letters 143, 173–182.
Cloos, M., Shreve, R.L., 1988. Subduction-channel model of prism accretion, melange formation, sediment subduction, and subduction erosion at convergent plate margins. Pure and Applied Geophysics 128, 455–499.
Connolly, J.A.D., 2005. Computation of phase equilibria by linear programming: a tool for geodynamic modeling and its application to subduction zone decarbonation. Earth and Planetary Science Letters 236, 524–541.
Cooke, R.A., 2000. High-pressure/temperature metamorphism in the St. Leonhard Granulite Massif, Austria: evidence from intermediate pyroxene-bearing granulites. International Journal of Earth Sciences 89, 631–651.
Dallmeyer, R.D., Franke, W., Weber, K. (Eds.), 1995. Pre-Permian Geology of Central and Eastern Europe. Springer-Verlag, Berlin, pp. 1–593.
Dawson, J.B., Carswell, D.A., 1990. High temperature and ultra-high pressure eclogites. In: Carswell, D.A. (Ed.), Eclogite Facies Rocks. Glasgow, Blackie, pp. 315–349.
Droop, G.T.R., 1987. A general equation for estimating Fe^{3+} concentrations in ferromagnesian silicates and oxides from microprobe analyses, using stoichiometric criteria. Mineralogical Magazine 51, 431–435.
Dudek, A., Fediuková, E., 1974. Eclogites of the Bohemian Moldanubicum. Neues Jahrbuch für Mineralogie, Abhandlungen 121, 127–159.
Faryad, S.W., 2009. The Kutná Hora Complex (Moldanubian Zone, Bohemian Massif), a composite of crustal and mantle rocks subducted to HP/UHP conditions. Lithos 109, 193–208.
Faryad, S.W., Nahodilová, R., Machek, M., 2006a. HP/UHP metamorphism with granulite facies overprint from the Moldanubian Zone (European Variscides). Geochimica et Cosmochimica Acta 70, A16.
Faryad, S.W., Perraki, M., Vrána, S., 2006b. *P–T* evolution and reaction textures in retrogressed eclogites from Světlík, the Moldanubian Zone (Czech Republic). Mineralogy and Petrology 88, 297–319.
Finger, F., Gerdes, A., Janoušek, V., René, M., Riegier, G., 2007. Resolving the Variscan evolution of the Moldanubian sector of the Bohemian Massif: the significance of the Bavarian and the Moravo–Moldanubian tectonometamorphic phases. Journal of Geosciences 52, 9–28.
Franěk, J., Schulmann, K., Lexa, O., 2006. Kinematic and rheological model of exhumation of high-pressure granulites in the Variscan orogenic root: example of the Blanský les granulite, Bohemian Massif, Czech Republic. Mineralogy and Petrology 86, 253–276.
Franke, W., 2000. The mid-European segment of the Variscides: tectonostratigraphic units, terrane boundaries and plate tectonic evolution. In: Franke, W. (Ed.), Orogenic Processes: Quantification and Modelling in the Variscan Belt. Special Publication, vol. 179. Geological Society London, pp. 35–61.
Fritz, H., Dallmeyer, R.D., Neubauer, F., 1996. Thick-skinned versus thin-skinned thrusting: rheology controlled thrust propagation in the Variscan collisional belt (the Southeastern Bohemian Massif, Czech Republic–Austria). Tectonics 15, 1389–1413.
Froitzheim, N., Pleuger, J., Roller, S., Nagel, T., 2003. Exhumation of high- and ultrahigh-pressure metamorphic rocks by slab extraction. Geology 31, 925–928.
Fulai, L., Zhiqin, X., Liou, J., Katayama, I., Masago, H., Maruyama, S., Jingsui, Y., 2002. Ultrahigh-pressure mineral inclusions in zircons from gneissic core samples of the Chinese Continental Scientific Drilling Site in eastern China. European Journal of Mineralogy 14, 499–512.
Ganguly, J., Cheng, W., Tirone, M., 1996. Thermodynamics of alumosilicate garnet solid solution: new experimental data, an optimized model, and thermodynamic application. Contributions to Mineralogy and Petrology 126, 137–151.
Ganguly, J., Cheng, W., Chakraborty, S., 1998. Cation diffusion in aluminosilicate garnets: experimental determination in pyroxene–almandine diffusion couples. Contributions to Mineralogy and Petrology 131, 171–180.
Gerya, T.V., Stöckhert, B., Perchuk, A.L., 2002. Exhumation of high-pressure metamorphic rocks in a subduction channel: a numerical simulation. Tectonics 21, 1–19.
Green, E.C.R., Holland, T.J.B., Powell, R., 2007. An order-disorder model for omphacitic pyroxenes in the system jadeite-diopside-hedenbergite-acmite, with applications to eclogite rocks. American Mineralogist 92, 1181–1189.
Holland, T.J.B., Powell, R., 1998. An internally consistent thermodynamic data set for phases of petrological interest. Journal of Metamorphic Geology 16, 309–343.
Holland, T.J.B., Powell, R., 2003. Activity–composition relations for phases in petrological calculations: an asymmetric multicomponent formulation. Contributions to Mineralogy and Petrology 145, 492–501.
Janoušek, V., Gerdes, A., Vrána, S., Finger, F., Erban, V., Friedl, G., Braithwaite, C.J.R., 2006. Low-pressure granulites of the Líšov Massif, southern Bohemia: Viséan metamorphism of Late Devonian plutonic arc rocks. Journal of Petrology 47, 705–744.
Kobayashi, T., Hirajima, T., Hiro, N., Svojtka, M., 2007. Raman and cathodoluminescence (CL) study of zircon inclusions derived from Gfohl felsic rocks in the Moldanubian Zone, Czech Republic. Geochimica et Cosmochimica Acta 71, A499.
Kodym, O., 1972. Multiphase deformation in the Blanský les granulite Massif (South Bohemia). Krystalinikum 9, 91–105.
Koons, P.O., 1987. The effects of disequilibrium and deformation on the mineralogical evolution of quartz diorite during metamorphism in the eclogite facies. Journal of Petrology 28, 679–700.
Kotková, J., 2007. High-pressure granulites of the Bohemian Massif: recent advances and open questions. Journal of Geosciences 52, 45–71.
Kotková, J., Harley, S.L., 1990. Formation and evolution of high-pressure leucogranulites: experimental constraints and unresolved issues. Physics and Chemistry of the Earth, Part A—Solid Earth 24, 299–304.
Kotková, J., Harley, S.L., Fišera, M., 1997. A vestige of very high-pressure (ca. 28 kbar) metamorphism in the Variscan Bohemian Massif, Czech Republic. European Journal of Mineralogy 9, 1017–1033.
Kröner, A., O'Brien, P.J., Nemchin, A.A., Pidgeon, R.T., 2000. Zircon ages for high-pressure granulites from South Bohemia, Czech Republic, and their connection to Carboniferous high-temperature processes. Contributions to Mineralogy and Petrology 138, 127–142.
Lang, H.M., Gilotti, J.A., 2007. Partial melting of metapelites at ultrahigh-pressure conditions, Greenland Caledonides. Journal of Metamorphic Geology 25, 129–147.
Liou, J.G., Zhang, R.Y., Ernst, W.G., Rumble, D., Maruyama, S., 1998. High-pressure minerals from deeply subducted metamorphic rocks. In: Hemley, R.J. (Ed.), Ultrahigh-Pressure Mineralogy: Physics and Chemistry of the Earth's Deep Interior: Reviews in Mineralogy, vol. 37, pp. 33–96.
Loomis, T.P., 1978. Multicomponent diffusion in garnet: II comparison of models with natural data. American Journal of Science 278, 1119–1137.
Loomis, T.P., Ganguly, J., Elphick, S.C., 1985. Experimental determination of cation diffusivities in aluminosilicate garnets II. Multicomponent simulation and tracer diffusion coefficients. Contributions to Mineralogy and Petrology 90, 45–51.
Massonne, H.-J., 2001. First find of coesite in the ultrahigh-pressure metamorphic area of the central Erzgebirge, Germany. European Journal of Mineralogy 13, 565–570.
Massonne, H.-J., 2003. A comparison of the evolution of diamondiferous quartz-rich rocks from the Saxonian Erzgebirge and the Kokchetav Massif: are so-called diamondiferous gneisses magmatic rocks? Earth and Planetary Science Letters 216, 347–364.
Massonne, H.-J., O'Brien, P.J., 2003. The Bohemian Massif and the NW Himalayas. In: Carswell, D.A., Compagnoni, R. (Eds.), Ultrahigh Pressure Metamorphism, EMU Notes in Mineralogy, 5, European Mineralogical Union. Eötvös University Press, Budapest, pp. 145–187.
Medaris, L.G., Jelínek, E., Mísař, Z., 1995. Czech eclogites—terrane settings and implications for Variscan tectonic evolution of the Bohemian Massif. European Journal of Mineralogy 7, 7–28.
Medaris, L.G., Fournelle, J.H., Ghent, E.D., Jelínek, E., Mísař, Z., 1998. Prograde eclogite in the Gföhl Nappe, Czech Republic: new evidence on Variscan high-pressure metamorphism. Journal of Metamorphic Geology 16, 563–576.
Medaris, L.G., Wang, H., Jelínek, E., Mihaljevič, M., Jakeš, P., 2005. Characteristics and origins of diverse Variscan peridotites in the Gföhl Nappe, Bohemian Massif, Czech Republic. Lithos 82, 1–23.
Medaris, L.G., Ghent, E.D., Wang, H.F., Fournelle, J.H., Jelínek, E., 2006. The Spačice eclogite: constraints on the *P–T–t* history of the Gföhl granulite terrane, Moldanubian Zone, Bohemian Massif. Mineralogy and Petrology 86, 203–220.
Monier, G., Robert, J.L., 1986. Evolution of the miscibility gap between muscovite and biotite solid solutions with increasing lithium content: an experimental study in the system K_2O–Li_2O–MgO–FeO–Al_2O_3–SiO_2–H_2O–HF. Mineralogical Magazine 50, 641–651.
Monier, G., Mergoil-Daniel, J., Labernardiere, H., 1984. Generations successives de muscovites et feldspaths potassiques dans les leucogranite du massif de Millevaches (Massif Central Francais). Bulletin de Mineralogie 107, 55–68.
Nahodilová, R., Faryad, S.W., Tropper, P., Konzett, J., 2008 High- to ultra-high pressure partial melting in orogenic belts: Implications for the formation of felsic granulites from the Bohemian Massif. 33rd International Geological Conference, Oslo, UHP-03, (abstract), CD-ROM.
Nakamura, D., Svojtka, M., Naemura, K., 2004. Very high-pressure (>4 GPa) eclogite associated with the Moldanubian Zone garnet peridotite (Nové Dvory, Czech Republic). Journal of Metamorphic Geology 22, 593–603.
Nasdala, L., Massonne, H.-J., 2000. Microdiamonds from the Saxonian Erzgebirge, Germany: in situ micro-Raman characterisation. European Journal of Mineralogy 12, 495–498.
O'Brien, P.J., 1997. Garnet zoning and reaction textures in overprinted eclogites, Bohemian Massif, European Variscides: a record of their thermal history during exhumation. Lithos 41, 119–133.
O'Brien, P.J., 1999. Asymmetric zoning profiles in garnet from HP–HT granulite and implications for volume and grain-boundary diffusion. Mineralogical Magazine 63, 227–238.
O'Brien, P.J., 2008. Challenges in high-pressure granulite metamorphism: reaction textures, compositional zoning, ages and tectonic interpretation with examples from the Bohemian Massif. Journal of Metamorphic Geology 26, 235–251.
O'Brien, P.J., Rötzler, J., 2003. High-pressure granulites: formation, recovery of peak conditions, and implications for tectonics. Journal of Metamorphic Geology 21, 3–20.
Owen, J.V., Dostál, J., 1996a. Prograde metamorphism and decompression of the Gföhl gneiss, Czech Republic. Lithos 38, 259–270.
Owen, J.V., Dostál, J., 1996b. Contrasting corona structures in mafic granulite from the Blanský les complex, Bohemian Massif, Czech Republic. Canadian Mineralogist 34, 959–966.
Petrakakis, K., Jawecki, C., 1995. High-grade metamorphism and retrogression of Moldanubian granulites, Austria. European Journal of Mineralogy 7, 1183–1203.
Powell, R., Holland, T.J.B., 1999. Relating formulations of the thermodynamics of mineral solid solutions: activity modelling of pyroxenes, amphiboles and micas. American Mineralogist 84, 1–14.
Prince, C.I., Košler, J., Vance, D., Günter, D., 2000. Comparison of laser ablation ICP-MS and sotope dilution REE analyses—implications for Sm–Nd garnet geochronology. Chemical Geology 168, 255–274.
Racek, M., Štípská, P., Pitra, P., Schulmann, K., Lexa, O., 2006. Metamorphic record of burial and exhumation of orogenic lower and middle crust: a new tectonothermal

model for the Drosendorf window (Bohemian Massif, Austria). Mineralogy and Petrology 86, 221–251.
Racek, M., Štípská, P., Powell, R., 2008. Garnet–clinopyroxene intermediate granulites in the St Leonhard Massif of the Bohemian Massif: ultrahigh-temperature metamorphism or not? Journal of Metamorphic Geology 26, 253–271.
Rötzler, J., Romer, R.L., Budzinski, H., Oberhänsli, R., 2004. Ultrahigh-temperature high-pressure granulites from Tirschheim, Saxon Granulite Massif, Germany: *P–T–t* path and geotectonic implications. European Journal of Mineralogy 16, 917–937.
Schmädicke, E., Müller, W.F., 2000. Unusual exsolution phenomena in omphacite and partial replacement of phengite by phlogopite plus kyanite in an eclogite from the Erzgebirge. Contributions to Mineralogy and Petrology 139, 629–642.
Schulmann, K., Schaltegger, U., Ježek, J., Thompson, A.B., Edel, J.B., 2002. Rapid burial and exhumation during orogeny: thickening and synconvergent exhumation of thermally weakened and thinned crust (Variscan orogen in Western Europe). American Journal of Science 302, 856–879.
Schulmann, K., Kröner, A., Hegner, E., Wendt, I., Konopásek, J., Lexa, O., Štípská, P., 2005. Chronological constraints on the pre-orogenic history, burial and exhumation of deep-seated rocks along the eastern margin of the Variscan orogen, Bohemian Massif, Czech Republic. American Journal of Science 305, 407–448.
Schulmann, K., Lexa, O., Štípská, P., Racek, M., Tajčmanová, L., Konopásek, J., Edel, J.-B., Peschler, A., Lehmann, J., 2008. Vertical extrusion and horizontal channel flow of orogenic lower crust: key exhumation mechanisms in large hot orogens? Journal of Metamorphic Geology 26, 273–297.
Snoeyenbos, D.R., Williams, M.L., Hanmer, S., 1995. Archean high-pressure metamorphism in the western Canadian Shield. European Journal of Mineralogy 7, 1251–1272.
Spear, F.S., 1993. Metamorphic Phase Equilibria and Pressure–Temperature–Time Paths. Mineralogical Society of America, Washington, D.C. 799 pp.
Speer, J.A., 1984. Micas in igneous rocks. Reviews in Mineralogy 13, 299–356.
Spicer, E.M., Stevens, G., Buick, I.S., 2004. The low-pressure partial-melting behaviour of natural boron-bearing metapelites from the Mt. Stafford area, central Australia. Contributions to Mineralogy and Petrology 148, 160–179.
Štípská, P., Powell, R., 2005. Does ternary feldspar constrain the metamorphic conditions of high-grade meta-igneous rocks? Evidence from orthopyroxene granulites, Bohemian Massif. Journal of Metamorphic Geology 23, 627–647.
Štípská, P., Pitra, P., Powell, R., 2006. Separate or shared metamorphic histories of eclogites and surrounding rocks? An example from the Bohemian Massif. Journal of Metamorphic Geology 24 (3), 219–240.
Svojtka, M., Košler, J., Venera, Z., 2002. Dating granulite–facies structures and the exhumation of lower crust in the Moldanubian Zone of the Bohemian Massif. International Journal of Earth Sciences 91, 373–385.
Tajčmanová, L., Konopásek, J., Schulmann, K., 2006. Thermal evolution of the orogenic lower crust during exhumation within a thickened Moldanubian root of the Variscan belt of Central Europe. Journal of Metamorphic Geology 24, 119–134.
Vavilov, M.A., Sobolev, N.V., Shatskiy, V.S., 1991. Micas in diamond-bearing metamorphic rocks of northern Kazakhstan. Doklady Akademii Nauk SSSR 319, 466–470.
Vrána, S., 1989. Perpotassic granulites from southern Bohemia—a new rock type derived from partial melting of crustal rocks under upper mantle conditions. Contributions to Mineralogy and Petrology 103, 510–522.
Vrána, S., 1992. The Moldanubian Zone in southern Bohemia: polyphase evolution of imbricated crustal and upper mantle segments. In: Kukal, Z. (Ed.), International Conference on Bohemian Massif. Czech Geol Surv, Prague, pp. 331–336.
Vrána, S., Frýda, J., 2003. Ultrahigh-pressure grossular-rich garnetite from the Moldanubian Zone, Czech Republic. European Journal of Mineralogy 15, 43–54.
Vrána, S., Štědrá, V., Fišera, M., 2006. Petrology and geochemistry of the Běstvina granulite body metamorphosed at eclogite facies conditions, Bohemian Massif. Journal of the Czech Geological Society 50, 81–94.
Wendt, J.I., Kröner, A., Fiala, J., Todt, W., 1994. U–Pb zircon and Sm–Nd dating of Moldanubian HP/HT granulites from South Bohemia, Czech Republic. Journal of the Geological Society London 151, 83–90.
White, R.W., Powell, R., Holland, T.J.B., 2001. Calculation of partial melting equilibria in the system Na_2O-CaO-K_2O-FeO-MgO-Al_2O_3-SiO_2-H_2O (NCKFMASH). Journal of Metamorphic Geology 19, 139–153.
White, R.W., Powell, R., Holland, T.J.B., 2007. Progress relating to calculation of partial melting equilibria for metapelites. Journal of Metamorphic Geology 25, 511–527.
Willner, A.P., Rötzler, K., Maresch, W.V., 1997. Pressure–temperature and fluid evolution of quartzo-feldspathic metamorphic rocks with a relic high-pressure, granulite–facies history from the Central Erzgebirge (Saxony/Germany). Journal of Petrology 38, 307–336.

PART II.

MAGMATICS FABRICS AND EMPLACEMENT OF CONE-SHEET BEARING KNÍŽECÍ STOLEC DURBACHITIC PLUTON (MOLDANUBIAN UNIT, BOHEMIAN MASSIF): IMPLICATIONS FOR MID-CRUSTAL REWORKING GRANULITIC LOWER CRUST IN THE CENTRAL EUROPEAN VARISCIDES

Except other, in this paper we analysed metamorphic evolution of Křišťanov granulite body and we try to estimate the *PT* conditions of fabric formation as a indicator of emplacement conditions of Knížecí Stolec durbachite pluton.

The ~340 Ma Knížecí Stolec durbachite pluton (located in southwestern part of the Moldanubian Unit) was emplaced into the centre of Křišťanov granulite body which was already juxtaposed against the mid-crustal metamorphic rocks of the Drosendorf Unit. The pluton evolved from a deep-seated cone-sheet-bearing complex followed by the nested intrusion of large magma pulses into the center of the outer sheeted complex.

The steep sub-concentric HP-HT metamorphic foliation in the granulite probably recorded intense ductile folding during its retrograde metamorphism. Subsequently, the durbachite pluton intruded discordantly into the granulite at around ~340 Ma. The steep margin-parallel magmatic fabrics in the durbachite may have recorded intrusive strain during emplacement. After the emplacement but prior to final solidification, the pluton was overprinted by the orogenic flat-lying fabric recorded also in the host granulite and in the nearby Drosendorf Unit.

Except of petrological observation, we apllied thermodynamic modelling to infer granulite *PT* evolution in the Na_2O-CaO-K_2O-FeO-MgO-Al_2O_3-SiO_2-H_2O (NCKFMASH) system using the THERMOCALC software. The mineral succession suggests that the early metastable garnet-kyanite-biotite plagioclase-K-feldspar-quartz mineral assemblage (S1 fabric) has been replaced by the stable garnet-sillimanite-biotite-plagioclase-K-feldspar-quartz assemblage (S2 fabric). According to Ky-Grt-Melt (+Kfs+Pl+Qtz) stability field in pseudosection we estimated the max. *PT* conditions at about 1.0 – 1.5 GPa and 780 – 850 °C. Further *PT* evolution is characterized by the appearance of sillimanite as a result of overstepping the Ky = Sill curve due to decompression and the crystallization of biotite around the garnet suggests transition to the Bt-Sill-Grt-Melt (+Kfs+Pl+Qtz) stability field during cooling. The *PT* conditions of this late stable mineral assemblage were calculated by means of the ‘‘Average *PT*’’ method (Powell and Holland 1990) using the activities for particular end-member components of the garnet rim, matrix biotite, recrystallized feldspars

and H_2O. Sillimanite and quartz were considered as pure end-member phases. The calculation of the *PT* conditions for the formation of the flat-lying foliation yielded a temperature of 765 ± 53 °C and pressure of 0.76 ± 0.15 GPa. We suggest that these *PT* conditions for the formation of the flat-lying foliation S2 in granulite also represent the *PT* conditions of Knížecí Stolec durbachite emplacement.

Int J Earth Sci (Geol Rundsch) (2008) 97:19–33
DOI 10.1007/s00531-006-0153-z

ORIGINAL PAPER

Magmatic fabrics and emplacement of the cone-sheet-bearing Knížecí Stolec durbachitic pluton (Moldanubian Unit, Bohemian Massif): implications for mid-crustal reworking of granulitic lower crust in the Central European Variscides

Kryštof Verner · Jiří Žák · Radmila Nahodilová · František V. Holub

Received: 10 March 2006 / Accepted: 2 December 2006 / Published online: 9 January 2007
© Springer-Verlag 2007

Abstract The ~340 Ma Knížecí Stolec durbachitic pluton was emplaced as a deep-seated cone-sheet-bearing ring complex into the Křišťanov granulite body (Moldanubian Unit, Bohemian Massif). Prior to the emplacement of the durbachitic magma, the steep sub-concentric metamorphic foliation in the granulite formed due to intense ductile folding during high-grade retrograde metamorphism. Subsequently, the durbachitic pluton intruded discordantly into the granulite at around ~340 Ma. The steep margin-parallel magmatic fabric in the durbachitic rocks may have recorded intrusive strain during emplacement. After the emplacement, but prior to the final solidification, the pluton was overprinted by the regional flat-lying fabric under lower pressure–temperature conditions (T = 765 ± 53°C; P = 0.76 ± 0.15 GPa). Based on this study and comparison with other ultrapotassic plutons, we suggest that the flat-lying fabrics, widespread throughout the exhumed lower to middle crust (Moldanubian Unit), exhibit major variations in character, intensity, kinematics, and shape of the fabric ellipsoid. These fabrics may have formed at different structural levels and in different parts of the root prior to ~337 Ma. Therefore, we suggest that this apparently ''single'' orogenic fabric recorded multiple deformation events and heterogenous finite deformation rather than reflecting a single displacement field within the orogenic root.

Keywords Durbachite · Emplacement · Exhumation · Granulite · Moldanubian Unit · Pluton

K. Verner (✉) · J. Žák · R. Nahodilová
Czech Geological Survey, Klárov 3, Prague 11821
Czech Republic
e-mail: verner@cgu.cz

K. Verner · F. V. Holub
Institute of Petrology and Structural Geology,
Charles University, Albertov 6, Prague 12843,
Czech Republic

J. Žák
Institute of Geology and Paleontology, Charles University,
Albertov 6, Prague 12843, Czech Republic

Introduction

In the Central European Variscides, formed during the Devonian to Carboniferous collision of Gondwana-derived crustal segments with the Baltica (northern European plate; Franke 1989; Pharaoh 1999; Winchester 2002), major crustal thickening was followed by the exhumation of lower- and mid-crustal rocks. Excess crustal thickness was maintained until around ~340 Ma, when large volumes of lower- to mid-crustal rocks, referred to as the Moldanubian Unit and interpreted to represent an orogenic root system, were rapidly exhumed within a few million years (Willner et al. 2002 and references therein).

Interestingly, the ~340 Ma event, which represents one of the most dramatic changeovers during the evolution of the Variscan orogen, overlaps the time span of emplacement of ultrapotassic plutons (Fig. 1; ~343–335 Ma; Holub et al. 1997; Schaltegger 1997). Elsewhere, potassic to ultrapotassic intrusions occur preferentially in the thickened continental crust during or immediately after continental collision as, for example, in the Tibetan Plateau (e.g., Hou et al. 2006 and references therein) or in the thickened continental crust at convergent (Andean-type) margins (e.g.,

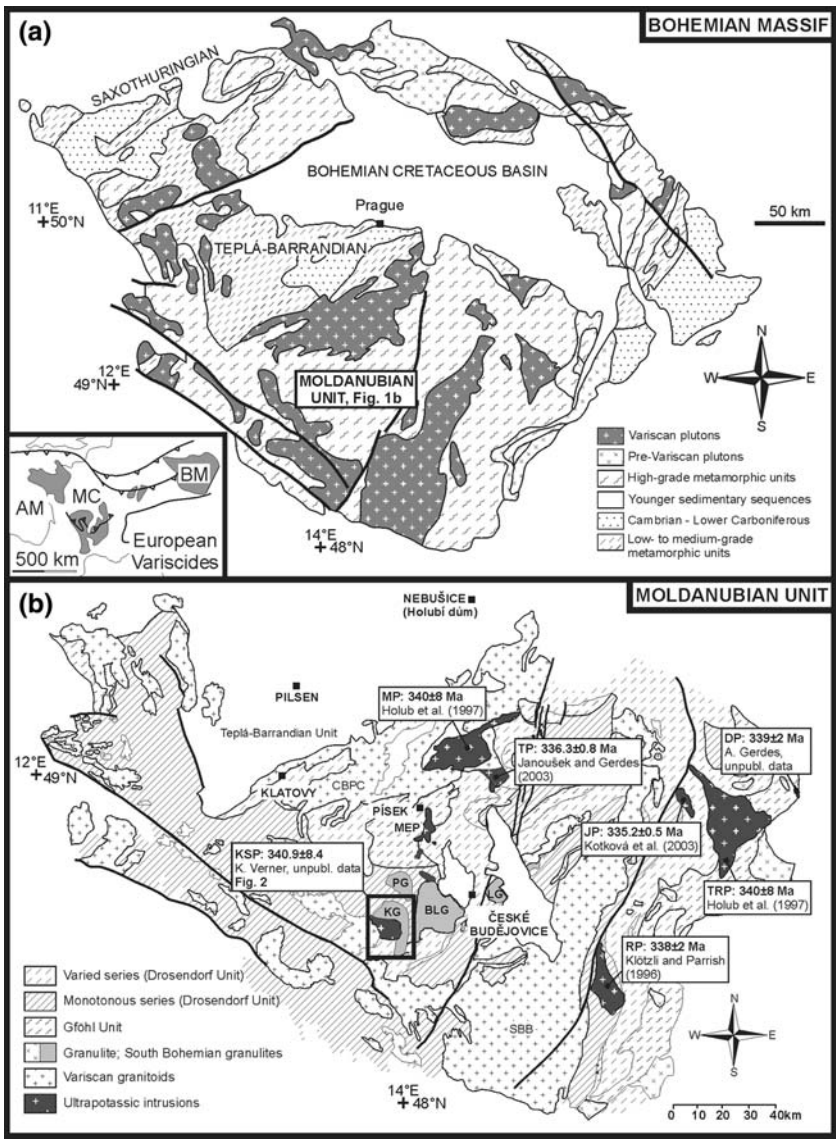

Fig. 1 **a** Geological sketch map of the Bohemian Massif and its position in the European Variscides (*inset*). The Moldanubian Unit forms the southern part of the Bohemian Massif. *AM* Armorican Massif, *BM* Bohemian Massif, *MC* Massif Central. **b** Geological map of the Moldanubian Unit showing location of the study area (*bold rectangle*) and locations and radiometric ages of ultrapotassic plutons and granulite bodies in the Moldanubian Unit. *CBPC* Central Bohemian Plutonic Complex, *DP* Drahonín pluton, *KSP* Knížecí Stolec pluton, *MEP* Mehelník pluton, *MP* Milevsko pluton, *SBB* South Bohemian Batholith, *TP* Tábor pluton, *TRP* Třebíč pluton. South Bohemian granulites: *BLG* Blanský les granulite, *KG* Křišťanov granulite, *LG* Lišov granulite, *PG* Prachatice granulite

Carlier et al. 2005). Potassic-ultrapotassic intrusions are thus a key feature for better structural-kinematic, petrological and geochemical understanding of the deep (''orogenic root'') processes during continental collision and the re-organisation of the continental crust during or after orogenic events.

From this perspective, as a growing body of data indicates that the internal fabrics of plutons may track kinematic history, evolution of regional strain fields and exhumation paths of pluton host rocks (e.g., Benn et al. 2001; Callahan and Markley 2003; Gleizes et al. 1997, 2001; Paterson et al. 1998; Schofield and D'Lemos 1998; Verner et al. 2006; Žák et al. 2005), we were interested in determining whether examining of structural relations in and around these ultrapotassic plutons may place some constraints not only on the ~340 Ma orogenic event but also on the exhumation of their host lower- to mid-crustal metamorphic complexes in the Variscan orogen.

The present paper examines the emplacement-related structures and internal fabrics of one of these ultrapotassic plutons in the Central European Variscides in relation to the tectonometamorphic evolution of their host rocks. As a case example, we investigated the Knížecí Stolec durbachitic pluton, which intruded a granulite body in the southwestern flank of the Moldanubian Unit (Bohemian Massif; Fig. 1b). In this work, we first outline the regional geological setting and then describe structural data from the pluton and the host granulites. In addition, we present petrological data to estimate metamorphic evolution and the *P–T* conditions of the host granulites prior to and during

pluton emplacement. Finally, we integrate these data sets to address the following issues: (1) emplacement of the Knížecí Stolec durbachite pluton; (2) interpretation of magmatic fabrics in the pluton with respect to the deformation and metamorphic evolution of the host granulites; (3) the significance and timing of regional orogenic fabrics in the Moldanubian Unit.

Regional geological setting

Moldanubian Unit

The Moldanubian Unit (also referred to as the Moldanubian Zone or Moldanubicum) exhumed lower- to middle-crust, interpreted to represent an orogenic root system in the internal part of the Variscan orogenic belt in central Europe (Fig. 1a, b). In general, the Moldanubian Unit has undergone polyphase metamorphism and has a complex deformational history. Its overall structure resulted from stacking of several major lithotectonic units at ~350–330 Ma (e.g., Vrána 1979, 1988; Vrána et al. 1995; Petrakakis 1997), followed by HT-LP metamorphism and anatexis dated at ~337–323 Ma (Friedl et al. 1993; Gerdes et al. 2000; Kalt et al. 2000), and later (~Permian) wrench tectonics (Brandmayr et al. 1995; Edel et al. 2003). However, the exact time constraints for these tectonic events may vary within the orogenic root and are still open to discussion.

The Moldanubian Unit (Fig. 1b) comprises two major sub-units with contrasting tectonometamorphic evolution and exhumed from different depths: the mid-crustal Drosendorf and the lower-crustal Gföhl Units (see Vrána 1988 for review; Urban and Synek 1995 and references therein). The Drosendorf Unit is structurally the lowermost unit and consists of metasedimentary sequences Paleozoic; Kröner 1988; Drábek and Stein 2003) dominated by sillimanite-biotite (±cordierite) paragneisses and migmatites (referred to as the Monotonous Group) or paragneisses with abundant bodies of metaquartzites, marbles, calc-silicate rocks, graphite-bearing schists and amphibolites (altogether referred to as the Varied Group). Estimated *P–T* conditions of regional metamorphism of the Drosendorf Unit range from 630–720°C and 0.3–0.6 GPa (Petrakakis 1997; Vrána et al. 1995; Linner 1996).

The high-grade Gföhl Unit, the protolith ages of which range from Precambrian to Lower Paleozoic (Friedl 1993; Petrakakis 1997; Schulmann et al. 2005), is structurally the uppermost unit and is composed of orthogneisses, felsic migmatites, granulites, eclogites and peridotites. Estimations of *P–T* conditions of peak metamorphism in the Gföhl Unit are ~950–1,050°C and ~1.4–2.0 GPa (in crustal peridotites) dated at ~351 ± 6 (Carswell and O'Brien 1993; Wendt et al. 1994; Medaris et al. 2005) and ~345 ± 5 (Van Breemen et al. 1982) followed by retrograde metamorphism (*T*~600–800°C and ~0.6–0.8 GPa; Owen and Dostal 1996) at ~337–333 Ma (Friedl et al. 1993; Wendt et al. 1994; Gebauer and Friedl 1994).

Granulite bodies in the Moldanubian Unit

Several separate bodies of HP-HT granulites (peak metamorphic conditions $P > 1.5$ GPa and $T > 900$°C; Kröner et al. 2000; O'Brien and Rötzler 2003) with associated mantle rocks occur throughout the Moldanubian Unit (Fig. 1b; also see Fig. 1 in Janoušek et al. 2006 and references therein). The granulites of the Moldanubian Unit vary in composition from felsic, garnet-kyanite-bearing granulites (approximately more than 80% of the exposed Moldanubian granulites), through intermediate to mafic, pyroxene-bearing granulites (Fiala et al. 1987). The nature of protolith (metamorphosed Lower Paleozoic calc-alkaline granitoids vs. high-pressure melts), tectonic significance and exhumation mechanisms of these granulite bodies have been a matter of longstanding controversy (Fiala et al. 1987; Wendt et al. 1994; Janoušek et al. 2004, 2006; Janoušek and Holub 2006; Vrána 1989; Kotková and Harley 1999; Franěk et al. 2006; Svojtka et al. 2002).

After the HP-HT metamorphism, the granulites of the Gföhl Unit were rapidly exhumed into mid-crustal levels and juxtaposed against rocks of the Drosendorf Unit (van Breemen et al. 1982; Kröner et al. 2000; Svojtka et al. 2002). At mid-crustal levels, the felsic Moldanubian granulites experienced MP-HT metamorphic overprint (0.8–1.2 GPa, 800–900°C; Cooke 2000). The structures reflecting their emplacement into the middle crust were largely obscured by retrogression and later deformations (Rajlich et al. 1986).

Ultrapotassic plutons in the Moldanubian Unit

During the later stages of the Variscan Orogeny, the Moldanubian Unit was intruded by the ultrapotassic (melasyenitic, melagranitic or monzonitic) plutons exposed in the Vosges, Black Forest, Variscan basement of the Alps and mainly in the Bohemian Massif (Foley et al. 1987; Holub 1997; Pagel and Leterrier 1980; Schaltegger 1997; Schaltegger and Corfu 1992; Wenzel et al. 1997). These ultrapotassic magmatic rocks are geochemically very specific, characterized by high contents of MgO, K_2O, Cr, Ni, Rb, Cs, U, Th. In the Bohemian Massif, these plutons comprise two rock

groups differing in assemblages of mafic minerals: (1) amphibole-biotite rocks dominated by the durbachite series (mostly K-feldspar-phyric melasyenites to melagranites; e.g. the Knížecí Stolec pluton) are the most widespread, and (2) biotite-two-pyroxene rocks making up two smaller bodies (Fig. 1b; see Holub 1997 for review). These ultrapotassic plutons extend over the entire orogenic root (Fig. 1b). The radiometric ages of these ultrapotassic plutons range from 343 to 335 Ma (Fig. 1b). The petrogenesis and geochemistry of these plutons has been interpreted as being a result of mixing of magmas generated from anomalous domains of the sub-continental upper mantle with melts from the lower continental crust (Holub 1997; Gerdes et al. 2000; Janoušek and Holub 2006).

The Knížecí Stolec pluton

Field relationships

The Knížecí Stolec pluton (dated at 340.9 ± 8.4 Ma using U–Th–Pb electron-microprobe dating on monazite and uraninite; K. Verner, unpublished data) intrudes the southwestern half of the Křišťanov granulite body in the southwestern flank of the Moldanubian Unit (Figs. 1b, 2). The pluton is made up chiefly of durbachite (mafic K-feldspar-phyric amphibole-biotite melasyenite to melagranite). Scattered mafic microgranular enclaves occur throughout the pluton but become particularly abundant along the pluton margins to form enclave swarms. The durbachites of the Knížecí Stolec pluton are compositionally very homogeneous, and their chemical composition (major oxides) varies within narrow ranges (Verner and Pertoldová 2004; K. Verner, unpublished data). The durbachites are relatively rich in SiO_2 (56–62 wt.%) but are magnesian (MgO 5–9 wt.%, commonly 6–8 wt.%; 100 Mg/(Mg + Fe_{tot}) 51–54) and ultrapotassic (K_2O 6–7%, typical K_2O/Na_2O ~4).

In the map view, the pluton has roughly elliptical shape with its longest axis (10.3 km) oriented ~E–W and its shortest axis (5.5 km) oriented ~N–S (Fig. 2). Significant mountainous relief (720–1,226 m above sea level) provides a ~500 m vertical section through the pluton with several segments of its roof exposed at the highest elevations (Fig. 3). The pluton floor is not exposed, leaving the vertical extent and exact three-dimensional shape of the pluton unknown. The geometry and characteristics of the exposed outer pluton contact vary greatly. A major part of the contact against the host granulite is intrusive (Fig. 4a, b). Multiple durbachite sheets or smaller durbachite bodies are also scattered around or extend from the main pluton, in particular to the south east and south. At the present-day exposure level, the sheets and thin screens of host granulites between the sheets are oriented parallel to the outer pluton margin (Fig. 2). Where the outer pluton contact changes its orienta-

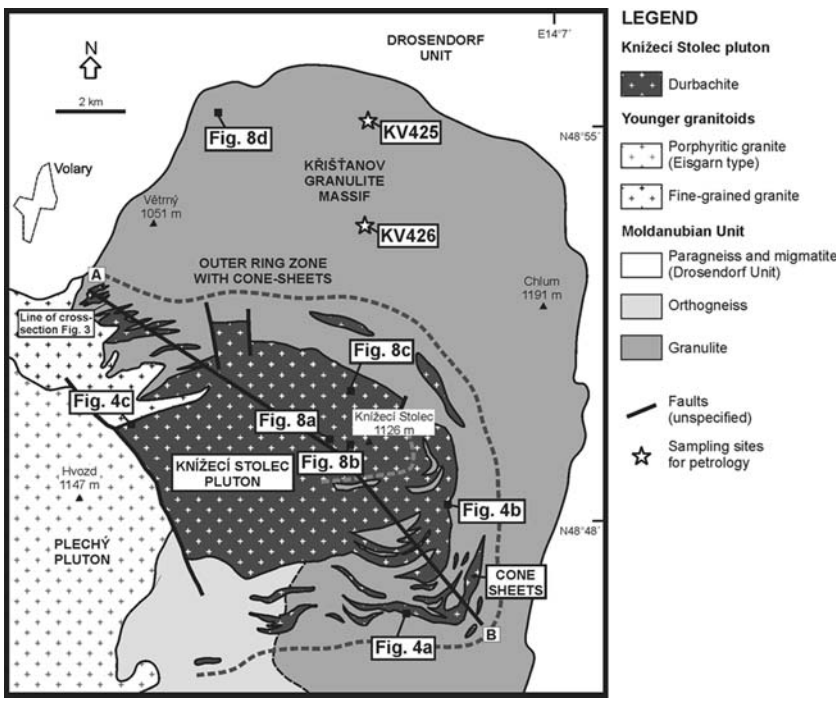

Fig. 2 Simplified geological map of the Knížecí Stolec pluton and nearby units. The pluton intrudes inner arc of horseshoe-like shaped granulite body. Note the outer ring zone with cone-sheets around the pluton. The eastern margin of the pluton was intruded by younger granitoids

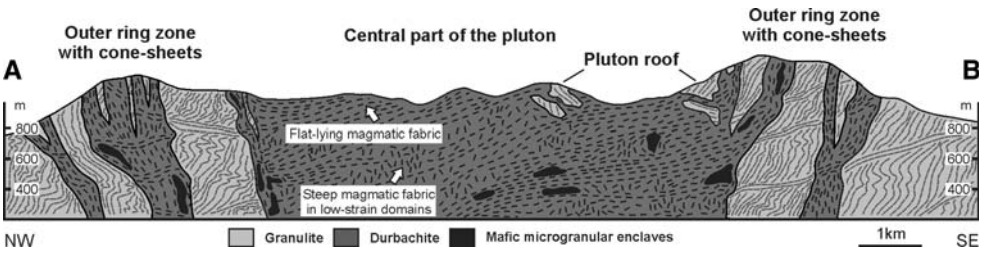

Fig. 3 Schematic cross-section along line A–B (see Fig. 2 for location) across the Knížecí Stolec pluton. The outer ring zone passes into more homogeneous pluton interior. The pluton roof is exposed at the highest elevations

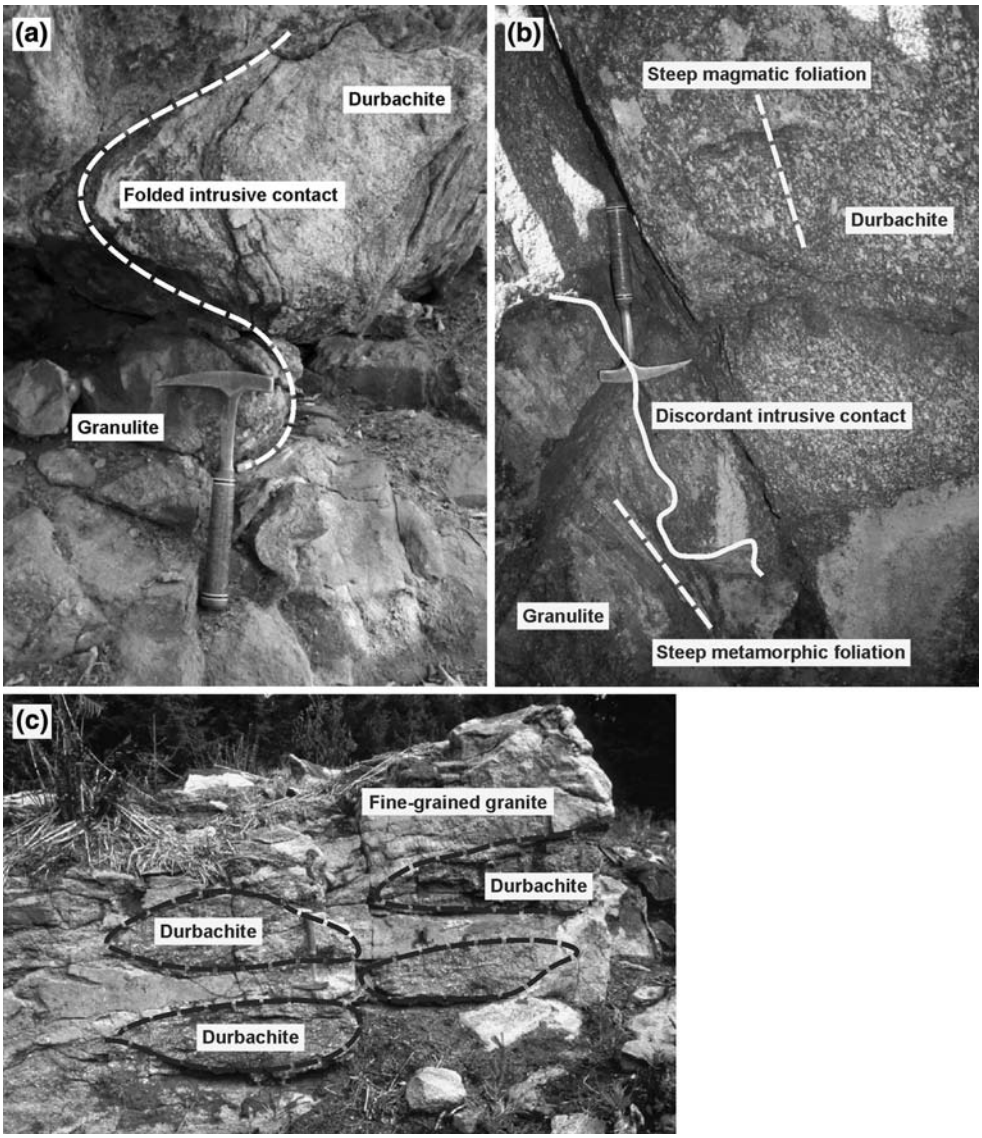

Fig. 4 Field photographs to show intrusive relationships of the durbachite to its host granulite and younger granitoids (see Fig. 2 for locations). **a** Originally steep intrusive contact between the durbachite and the granulite folded during sub-vertical contraction; hammer for scale. **b** Slightly discordant intrusive durbachite/granulite contact truncating the metamorphic foliation the host granulite; hammer for scale. **c** Sub-horizontal sheets of fine-grained younger granitoids cutting across the durbachite along sharp intrusive contacts; hammer for scale

tion, the sheets are arcuate or curved parallel to the generally elliptical outline of the pluton. Our field mapping revealed that the sheets and the intrusive contacts between the sheets and the host granulites dip moderately to steeply inwards (55–80° dip). Where exposed, the outer contact of the main body of the pluton also dips steeply inwards (70° dip) beneath the pluton (Figs. 2, 3). Therefore, these features resemble inward dipping cone-sheets and define a ring zone around the central part of the pluton (Figs. 2, 3; see Johnson et al. 1999 and Johnson et al. 2002 for definitions and discussion of cone-sheet-bearing complexes). In some places, the originally steep intrusive pluton/granulite contacts have been reoriented due to post-emplacement folding during regional sub-vertical contraction (Fig. 4a).

The segments of pluton roof are represented by thin screens of granulite that are also arcuate curved parallel to the outer pluton margins. The metamorphic foliations in these intra-pluton screens are concordant to the foliations in the host granulite outside of the pluton, suggesting that they were not significantly rotated or displaced during the melasyenite emplacement.

The southwestern margin of the pluton has been intruded by younger granitoids and affected by post-emplacement brittle faulting, both of which obliterate the original intrusive contacts. The younger granitoids presumably represent late stages of magmatic activity in the Moldanubian Unit during the Variscan Orogeny (~320–310 Ma; Finger et al. 1997; Schaltegger 1997; and references therein) and comprise a smaller body of fine-grained leucogranite and porphyritic granitoids of the Plechý pluton. These younger plutons lack evidence for solid-state deformation and intrude discordantly to the structures in the Knížecí Stolec pluton and its host granulite (Fig. 4c).

Magmatic fabrics

Two different pluton-wide magmatic foliations with associated lineations were distinguished in the Knížecí Stolec pluton (Figs. 5, 6) on the basis of their different orientation, overprinting relationships, and intensity (for definitions and discussion on multiple magmatic fabrics see Paterson et al. 1989, 1998, 2003; Vernon 2000; Žák et al. 2007). Each of the two foliations and lineations are defined by planar and linear shape-preferred orientation of K-feldspar and plagioclase phenocrysts (2–4 cm in length) and alignment of biotite and amphibole aggregates. In a micro-scale, the two fabrics share similar characteristics. All individual mineral grains (amphibole, biotite, plagioclase, K-feldspar) have euhedral to subhedral shapes, generally with lack of evidence for sub-solidus deformation (Fig. 7).

(1) The steep magmatic foliation and lineation have been preserved particularly along the outer pluton/host rock contacts, in the cone-sheets around the pluton, and locally (presumably in low-strain domains) also within the younger fabric throughout the pluton. The foliation dips steeply to moderately to the ~W to ~NNW and ~SSE and thus is roughly parallel to the outer pluton contact (Figs. 5, 6). The magmatic lineation associated with this steep foliation has variable trends and moderate plunges. The steep foliation generally intensifies towards the outer pluton margin, where it grades into highly localized narrow, up to ~1 m wide zones of sub-solidus deformation. Along the pluton margin, abundant mafic microgranular enclaves are also aligned sub-parallel to the steep magmatic foliation. The steep foliation is discordant to the steep metamorphic foliation in the host granulites on both map and outcrop scales (Fig. 4b).

(2) The other, flat-lying magmatic fabric is the dominant magmatic structure particularly in the central part of the pluton. This fabric is defined by intensely developed magmatic foliation (Fig. 8a, b) that dips to the ~NW to ~N at a low angle (less than 30°) and bears gently plunging ~N to ~NNE magmatic lineation. No evidence for sub-solidus deformation was observed in association with this fabric.

In many places all over the pluton, relative temporal relationships of the two magmatic fabrics can be established. We have observed cases where the sub-vertical foliation surrounding steeply oriented mafic microgranular enclaves was pervasively overprinted by the flat-lying magmatic foliation in the host durbachite (Fig. 8c). In the central part of the pluton, the enclaves (up to ~1 m in size) are reoriented with their longest axes parallel to the magmatic lineation and the shortest axes perpendicular to the flat-lying foliation in the host durbachite (Fig. 8b).

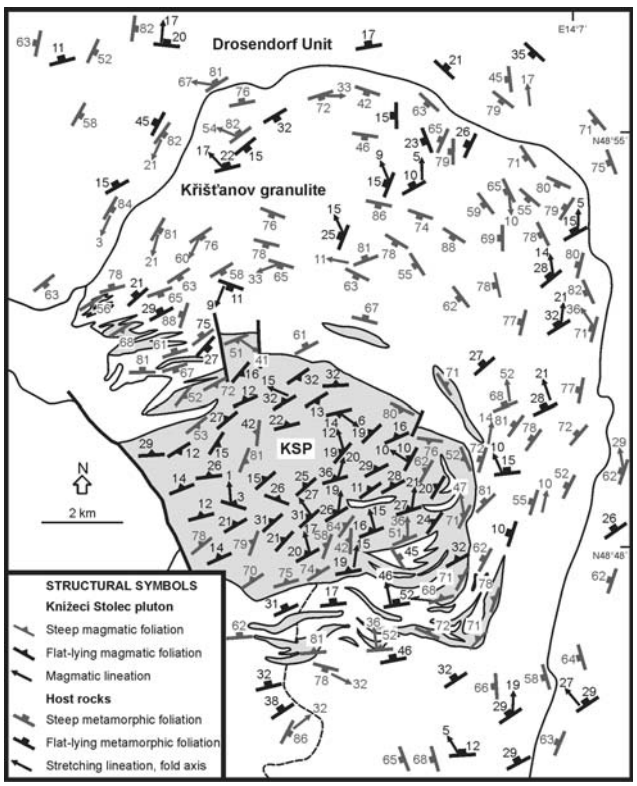

Fig. 5 Structural map of the Knížecí Stolec pluton and surrounding units to show two magmatic fabrics (*steep* and *flat-lying*) in the pluton and two metamorphic fabrics (*steep* and *flat-lying*) in the host granulite. *KSP* Knížecí Stolec pluton

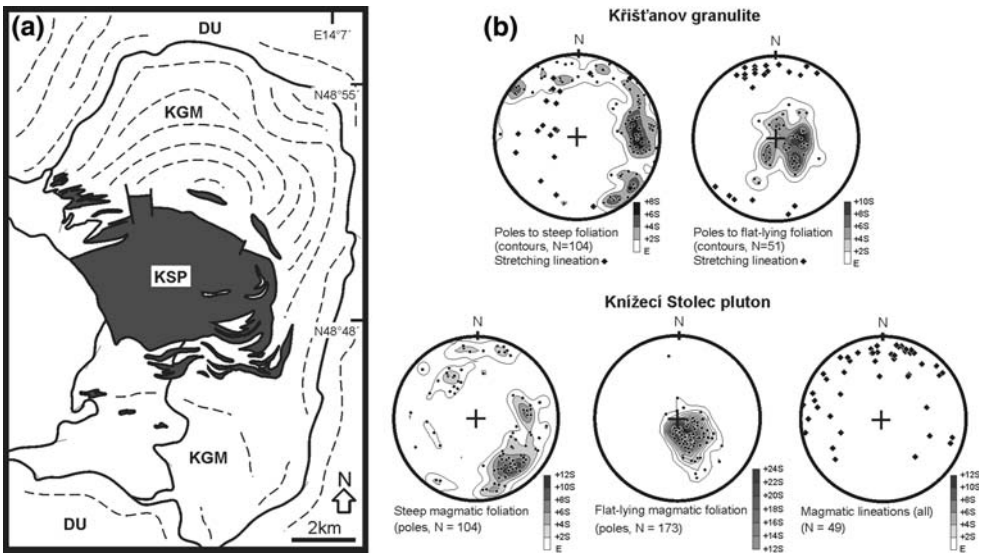

Fig. 6 **a** Simplified map of trajectories of the steep foliations in the Křišťanov granulite. *DU* Drosendorf Unit, *KGM* Křišťanov granulite massif, *KSP* Knížecí Stolec pluton. **b** Stereonets (lower hemisphere, equal area projection) of multiple foliations and lineations both from the pluton and the host granulite

In some places, thin aplite dikes discordantly cut across the enclaves and host durbachites. Where the sheets dip steeply to moderately at a high angle to the flat-lying foliation, they have been folded into asymmetric, gently inclined, open magmatic folds. The axial planes of these magmatic folds tend to be parallel to the flat-lying magmatic foliation in the durbachites (Fig. 8b). In other cases, where the dikes are sub-horizontal, they have been magmatically boudinaged or form pinch-and-swell structures (Fig. 8b).

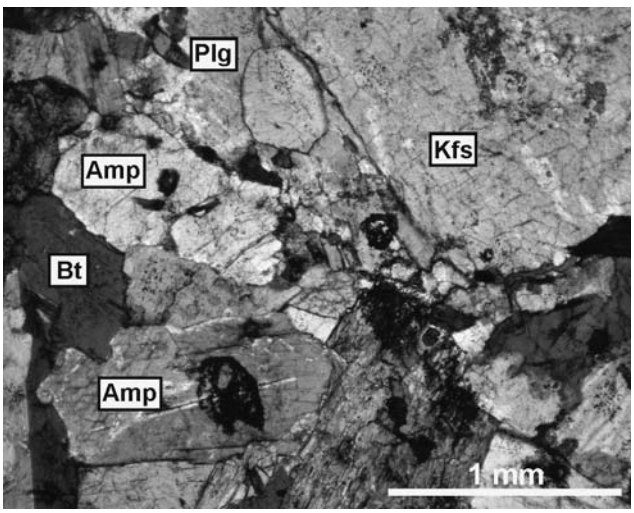

Fig. 7 Micrograph of a typical sample of the durbachite from the Knížecí Stolec pluton. The texture is magmatic with no evidence for subsolidus deformation. Mineral grains have euhedral to subhedral shapes

Pluton host rock: the Křišťanov granulite

Geology and structural pattern

The Křišťanov granulite massif (Fig. 2; Jakeš 1969) is one of the five large granulite bodies of the Moldanubian Unit in the southern part of the Bohemian Massif (together referred to as the South Bohemian granulites; Fig. 1b). These granulite bodies represent lower-crustal segments emplaced into the middle crust.

In the map view, the Křišťanov granulite body has an asymmetric horseshoe-like shape with the longest N–S dimension ~22 km and E–W dimension ~16 km (Fig. 2). Gravimmetric studies indicate that the granulite body may extend downward to depths of at least ~5 km below the present-day erosion surface (Vrána and Šrámek 1999). The Křišťanov granulite is surrounded by migmatized paragneisses of the Drosendorf Unit to the east, north and northwest. To the south, the granulite is in contact with fine-grained orthogneiss of unknown age and with uncertain relationship to the granulite (dashed contact line in Fig. 2). The inner arc of the granulite body was intruded by the durbachite and by a small body of younger fine-grained granitoids further to the west.

The structural pattern of the granulite is defined by two superimposed regional metamorphic foliations (Fig. 8d) with associated stretching (mineral) lineations. (1) The earlier, steep to moderately dipping foliation is parallel to the outer contacts of the granulite and in the map view defines a sub-concentric arcuate pattern (Figs. 5, 6). The steep foliation bears moderately plunging mineral lineation of variable trends that define a curvilinear pattern. Domains with

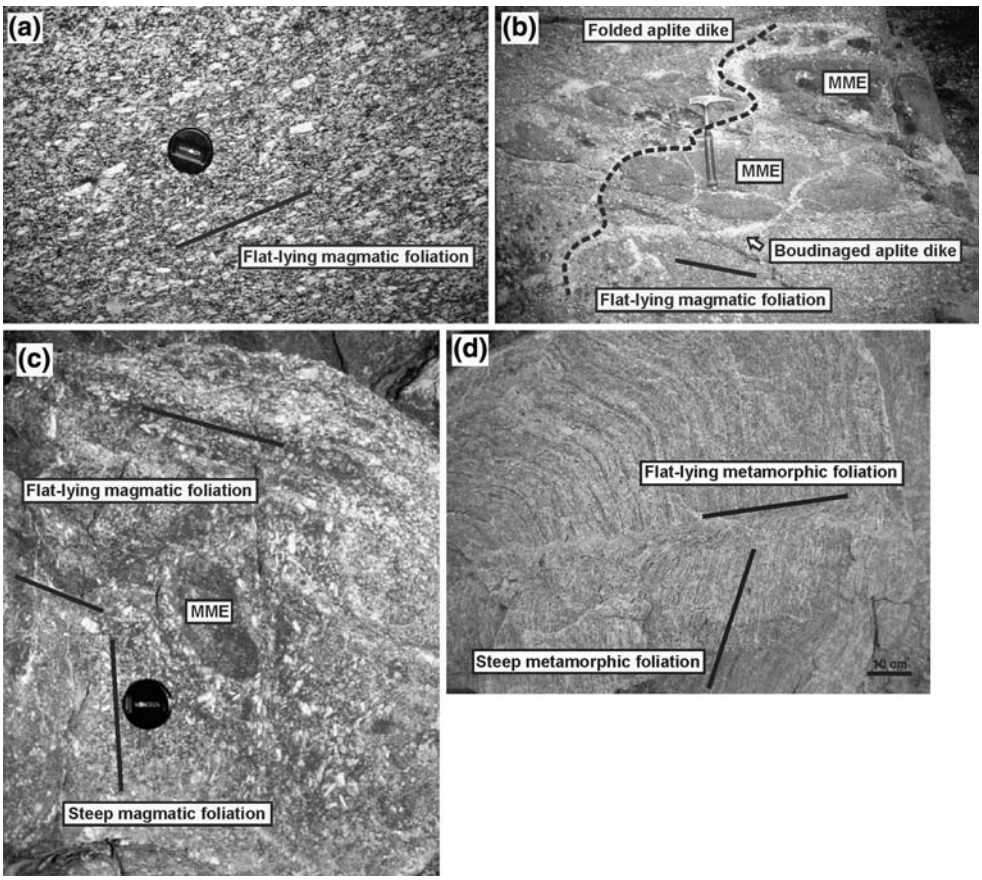

Fig. 8 Field photographs to show fabric relationships (see Fig. 2 for locations). **a** Strong flat-lying magmatic foliation defined by K-feldspar phenocrysts in the durbachite; lens cap for scale. **b** Strong flat-lying magmatic foliation in the durbachite defined by microgranular enclaves and K-feldspar phenocrysts. Aplite dikes oriented at high angle to the foliation are folded into asymmetric magmatic folds whereas dikes sub-parallel to the foliation are magmatically boudinaged; hammer for scale. **c** Outcrop-scale overprinting relationships between the two magmatic foliations in the pluton. The steep magmatic foliation defined by enclave and K-feldspar phenocrysts is overprinted by flat-lying magmatic foliation defined by K-feldspar alignment; lens cap for scale. **d** Outcrop-scale overprinting relationships between the two metamorphic foliations in the granulite. The penetrative steep foliation starts to reorient into the localized flat-lying foliation. *MME* mafic microgranular enclave

preserved minor rootless isoclinal folds of pre-existing anatectic foliation are locally enclosed within the steep foliation. This steep fabric is dominant in the granulite and is truncated by intrusive contacts with the durbachite (Fig. 4b). (2) The above structures are overprinted in some places by regional flat-lying foliation associated with shallowly plunging ~N–S stretching lineation (Figs. 5, 6). In terms of orientation, this metamorphic fabric corresponds to the flat-lying magmatic fabric in the durbachite.

In the migmatized paragneisses of the Drosendorf Unit, a steep metamorphic foliation in approximately ~1 km wide zone wraps around the granulite body (Figs. 5, 6). Further away from the granulite, the steep foliation reorients into a regional ~NNE–SSW strike. This older metamorphic foliation is heterogeneously reworked into flat-lying metamorphic foliation bearing the ~N–S trending mineral lineation.

Metamorphic evolution of the granulite

Two samples of the Křišťanov granulite (KV425 and KV426; see Fig. 2 for sample locations) were analysed to characterize metamorphic evolution of the granulite and to estimate the *P–T* conditions of fabric formation (Figs. 9, 10). Sample KV426 was taken from an outcrop with preserved earlier steep fabric (Fig. 9a), whereas sample KV425 was collected from a domain with well-developed younger flat-lying fabric (Fig. 9c).

Mineral assemblage in the granulite from sample KV426 is characterized as follows. Garnet has subhedral shape (Fig. 9b), is up to 300 μm in size, contains rare inclusions of kyanite, biotite and quartz, and shows weak zoning from core to rim ($Grs_{0.1–0.02}$ $Py_{0.18–0.20}$ $Alm_{0.66–0.73}$ $Spes_{0.02–0.02}$; Fig. 9d). Kyanite (up to 500 μm in size) occurs either as relics in the matrix commonly overgrown by aggregates of prismatic silli-

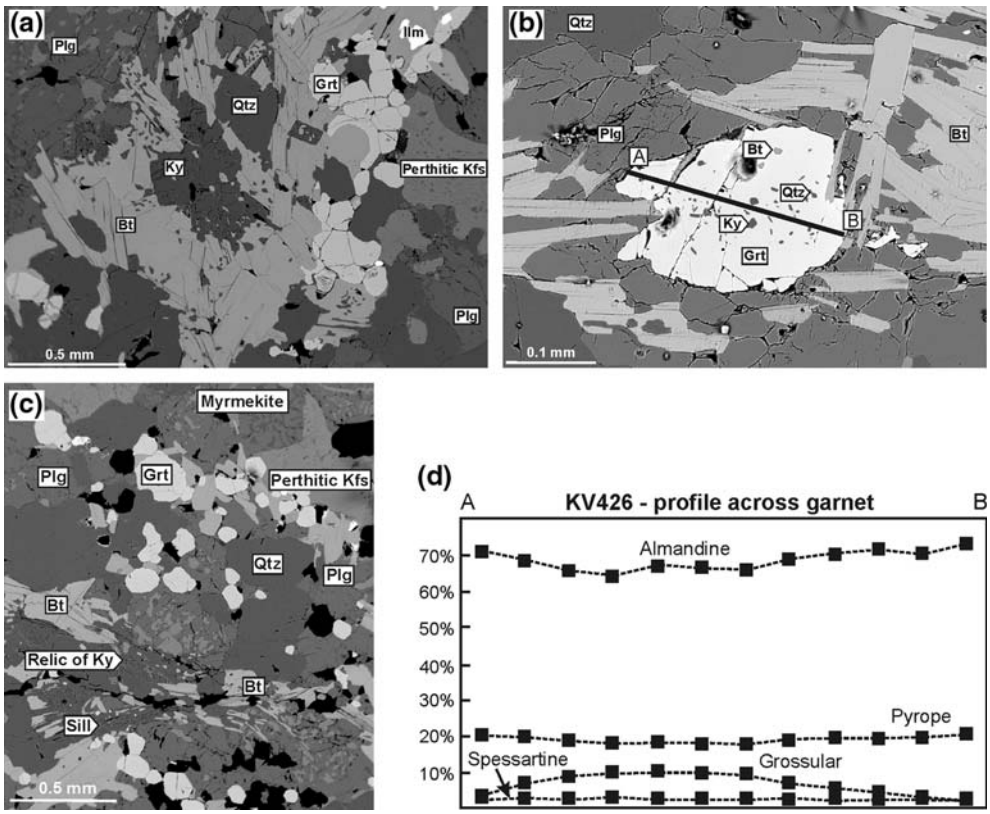

Fig. 9 **a** Early steeply dipping foliation with preserved relics of HP-HT assemblage Ky–Grt–Kfs–Plg–Bt–Qtz. **b** Larger grains of garnet contain rare inclusions of biotite, kyanite and quartz. Secondary biotite grows in pressure shadows around the garnet. **c** The growth of sillimanite fibrolitic aggregates together with biotite within the flat-lying foliation and recrystallization of feldspars and quartz indicate the late metamorphic overprint. **d** The garnet is almandine with higher pyrope component. It shows weak zoning from core to rim

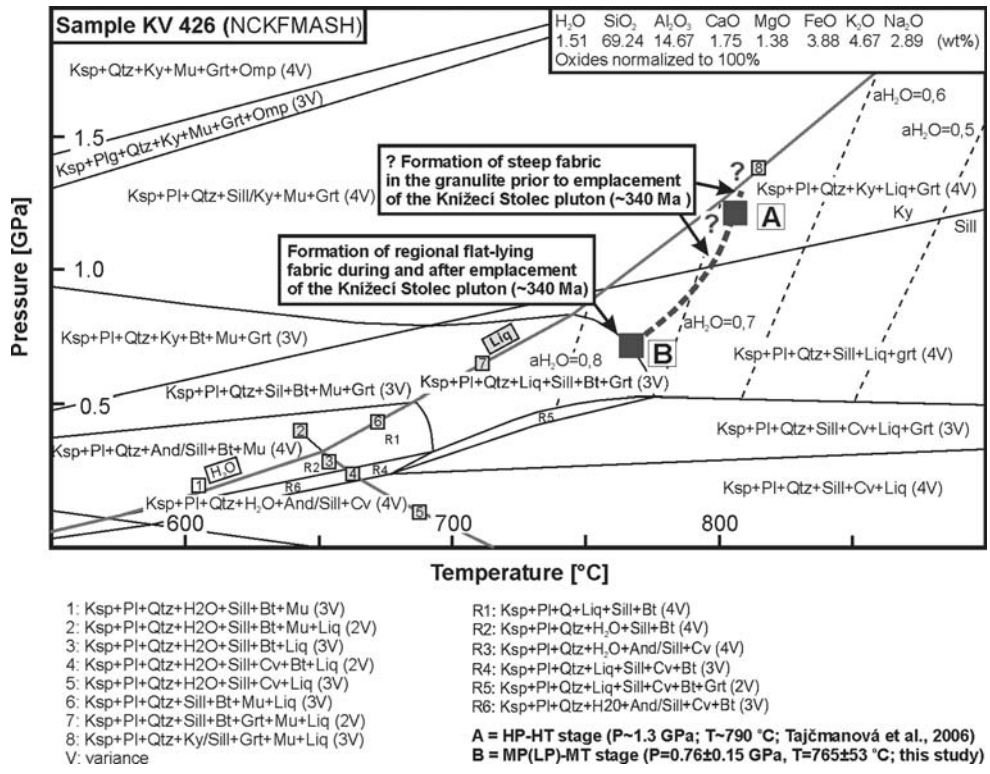

Fig. 10 Pseudosection calculated in the NCKFMASH system with pressure–temperature conditions calculated for the flat-lying fabric in the Křišťanov granulite. The durbachite emplacement took place at around 340 Ma after the formation of the steep metamorphic foliation in the granulite under HP-HT conditions, but prior to the formation of the regional flat-lying fabric under MP(LP)-MT conditions. Abbreviations used for mineral names are after Kretz (1983)

manite, or is enclosed in larger plagioclase grains (core → rim: $Ab_{0.75} \rightarrow_{0.74}$ $An_{0.24} \rightarrow_{0.25}$ $Or_{0.01} \rightarrow_{0.01}$). Feldspar grains, up to 1–2 mm in size, are rarely present in the matrix. Feldspars are typically mesoperthitic, except for cases where some parts of grains are replaced by fine-grained myrmekites.

In the sample KV425, biotite aggregates (xMg = 0.50–0.56) form the foliation bands or crystallize together with sillimanite around garnet in pressure shadows. The composition of garnet is approximately homogeneous (with no prominent zoning) and corresponds to $Grs_{0.02}$ $Py_{0.20}$ $Alm_{0.73}$ $Spes_{0.02}$. Feldspar aggregates (100–200 μm in size) indicate a higher degree of recrystallization and have compositions corresponding to orthoclase ($Ab_{0.11–0.17}$ $An_{0–0.01}$ $Or_{0.89–0.82}$) and plagioclase ($Ab_{0.70}$ $An_{0.29}$ $Or_{0.01}$).

The mineral succession suggests that the early metastable garnet-kyanite-plagioclase-K-feldspar-biotite-quartz mineral assemblage (preserved in the sample KV426) has been replaced by the stable garnet-biotite-sillimanite-plagioclase-K-feldspar-quartz assemblage (sample KV425). In order to semi-quantitatively characterize the P–T conditions of formation of the flat-lying fabric in the granulite, the stable mineral assemblage was modelled thermodynamically in the Na_2O-CaO-K_2O-FeO-MgO-Al_2O_3-SiO_2-H_2O (NCKFMASH) system using the THERMOCALC software (Powell et al. 1988; 2003 update of Holland et al. 1998). The NCKFMASH chemical system uses the mineral and liquid/melt activity-composition models and the non-ideal interaction parameters of White et al. (2001). Oxides are normalized to 100%. System composition was taken from the whole-rock analysis of sample KV426. The mineral assemblages for particular P–T ranges are presented in the form of a pseudosection in Fig. 10. The metastable assemblage (see above) corresponds to the Ksp + Plg + Qtz + Grt + Ky + liq field (Fig. 10, point 1). Further P–T evolution is characterized by the appearance of sillimanite as a result of overstepping the Ky = Sill curve due to decompression (Fig. 10, point 2) and the crystallization of biotite around the garnet suggests transition in the Ksp + Plg + Bt + Sill + Qtz + Grt + liq field (Fig. 10, point 3) during cooling.

The P–T conditions responsible for the stabilization of the late stable mineral assemblage garnet-biotite-sillimanite-plagioclase-K-feldspar-quartz were calculated by means of the ''Average PT'' method (Powell and Holland 1990) using the activities for particular end-member components of the garnet rim, matrix biotite, recrystallized feldspars and H_2O. The water activity (aH_2O = 0.8) in the melt phase was calculated from the melt-mixing model of White et al. (2001) using the ''calc aH_2O'' routine implemented in the THERMOCALC software set. Sillimanite and quartz were considered as pure end-member phases. The calculation of the P–T conditions for the formation of the flat-lying foliation (sample KV425) yielded a temperature of 765 ± 53°C and pressure of 0.76 ± 0.15 GPa (Fig. 10).

Discussion

Emplacement of the Knížecí Stolec pluton

Our mapping revealed the presence of numerous durbachite cone-sheets (arcuate on the map, inward-dipping) around the pluton. In addition, several arcuate-shaped screens of granulite have been preserved inside the pluton, particularly along its southeastern margin (Figs. 2, 3). These sheets are predominantly discordant to the steep metamorphic fabric in the host granulite. The central part of the pluton, with a few preserved segments of pluton roof, is relatively structurally homogeneous in contrast to the outer sheeted domains. The pluton margins and the sheets are generally discordant to the steep foliation in the granulite. These field relations indicate that the durbachite emplacement may have started as an outer cone-sheet-bearing ring complex. The individual cone-sheets were presumably emplaced by a magma wedging mechanism along foliation planes or into magma-driven conical fractures discordant to host foliation. Lateral and downward displacement of thin granulite screens between the sheets occurred during sheet emplacement. This cone-sheet stage was probably followed by intrusion of large magma pulse(s) into the center of the outer ring complex to form the homogenous pluton interior (Fig. 3). Largely discordant contact relationships, lack of significant emplacement-related ductile strain around the pluton and the lack of evidence for syn-emplacement faults or shear zones all indicate that magmatic stoping may have also been an important process during final emplacement of the pluton in the exposed upper parts beneath the pluton roof.

If this is true, the Knížecí Stolec pluton is a spectacular case example of rather rare and yet largely unexplored deep-seated ring complexes in the middle crust. Ring complexes most commonly develop above large magma chambers in shallow-level volcano-plutonic environments (Johnson et al. 1999, 2002). However, Johnson et al. (2002) proposed that ring complexes may even extend down to depths ~18 km and perhaps may act as vertically extensive magma plumbing systems in the crust. From this point of view, the Knížecí Stolec pluton may be viewed as a frozen-in deep-seated pathway for durbachitic magmas trapped during their ascent to the upper structural levels.

Interpretation of fabric patterns in and around the Knížecí Stolec pluton

Two pluton-wide magmatic fabrics have been preserved in the durbachite and two regional metamor-

phic fabrics in the host granulite (Figs. 5, 6, 8). Our further considerations will therefore focus on examining the relationships between the magmatic fabrics in the pluton and the superposed fabrics in the host granulite, as well as on the relative timing of fabric formation with respect to the pluton emplacement. The interpretations developed below are largely based on firmly established field relationships and structural data; the results of petrological modelling are taken only as additional constraints.

We interpret that the steep margin-parallel fabric, as well as the asymmetric horseshoe-like shape of the granulite body, may have recorded intense ductile folding along steeply plunging axes at greater depths. Except for the few local low-strain domains preserving rootless isoclinal folds with no consistent regional pattern, this steep fabric in the granulite represents the oldest recognized regional-scale fabric that pervasively obliterates earlier structural events. The metastable character of the early mineral assemblage in the Křišt'anov granulite (sample KV426) prevented estimation of the *P–T* conditions for the formation of the steep fabric (sub-concentric foliation bearing moderately plunging mineral lineation). By comparison, *P–T* estimations of early re-equilibration of the high-pressure assemblage (garnet-kyanite-plagioclase-K-feldspar-biotite-quartz) in the steep fabric in other Moldanubian granulites yielded temperatures of ~790°C and pressures of ~1.3 GPa (Tajčmanová et al. 2006 and references therein). These metamorphic conditions for the fabric formation would correspond to paleodepths of about ~40–45 km within the thickened orogenic root (Moldanubian Unit; see Fig. 3 in Konopásek and Schulmann 2005).

Subsequently, the Knížecí Stolec durbachite pluton intruded the granulite at around ~340 Ma. Largely discordant intrusive contacts indicate that the pluton was emplaced after the formation of the steep fabric in the host granulite. The steep margin-parallel magmatic fabrics in the durbachite may have recorded intrusive strain during its emplacement. After the emplacement but prior to the final solidification of the pluton, all units recorded increments of regional tectonic deformation characterized by sub-vertical contraction and ~N–S stretching. This regional sub-vertical contraction produced folding (vertical collapse) of intrusive contacts, inclined magmatic folds, flat-lying magmatic foliation in the durbachite, and localized flat-lying metamorphic foliation in the host granulite and in the migmatized paragneisses of the Drosendorf Unit (Figs. 4, 5, 6, 8). Strain partitioning due to rheological contrast among the crystallizing durbachites, host granulites and paragneisses may have caused differences in the intensity of development of the flat-lying foliations in the three units. The results of our thermodynamic modelling (Fig. 10) suggest that the metamorphic conditions of this deformation may correspond to a temperature of 765 ± 53°C and pressure of 0.76 ± 0.15 GPa (~28 km paleodepth in the thickened root; see Fig. 3 in Konopásek and Schulmann 2005). This is consistent with similar estimations of MP-MT overprint in the Blanský les and Prachatice granulite bodies obtained by Kröner et al. (2000).

Implications for the interpretation of orogenic fabrics in the Moldanubian Unit

Several studies attempted to correlate regional fabrics across the Moldanubian Unit and to assign the superposed fabrics to successive deformation phases with respect to the large-scale development of the orogenic root domain (Lobkowicz et al. 1996; Rajlich et al. 1986; Svojtka et al. 2002; Vrána 1979; Vrána and Bártek 2005). The interpretations and correlations of the orogen-scale fabrics and inferred finite deformation patterns have been particularly controversial for the flat-lying to ~NE–SW foliations dipping to the ~NW and bearing ~N–S to ~NW–SE stretching lineations (S_{H2} and S_{G3} of Franěk et al. 2006; S_2 of Rajlich et al. 1986; S_2 of Svojtka et al. 2002; S_3 of Vrána 1979; S_3 of Lobkowicz et al. 1996). These regional foliations and lineations are widespread throughout the Moldanubian Unit and were variously interpreted as being a result of: (1) simple shear deformation during N–S- to NW–SE-directed thrusting at ~341 Ma (Rajlich et al. 1986); (2) extensional shear deformation with top-to-the-NW transport prior to ~330 Ma (Lobkowicz et al. 1996); (3) extensional collapse of the vertically extruded orogenic root at ~318 Ma (Svojtka et al. 2002); (4) extensional shearing prior to the intrusion of the Eisgarn granite (Vrána and Bártek 2005), which was dated by others at ~330–320 Ma (Gerdes et al. 2000) and at ~320–314 Ma (Breiter and Scharbert 1998); (5) flow of hot material into horizontal channel developed between the upper boundary of a lithospheric indenter and the overlying orogenic lid along the eastern margin of the Bohemian Massif (Schulmann et al. 2006).

In contrast to the above interpretations, other studies emphasized that the correlation of superposed fabrics and inferred succession of deformation phases in multiply deformed regions may be rather problematic in general (e.g., Burg 1999; Luneburg and Lebit 1998; Miller et al. 2005; Tobisch and Paterson 1988; Williams 1985). The correlations, which traditionally rely on fabric orientation, styles of superposed folding and outcrop-scale overprinting

relationships, assume constant boundary conditions, isotropic materials, and homogeneity and synchroneity of regional deformation. Moreover, the effects of heterogeneous and progressive deformation and strain partitioning are ignored. An additional complexity to this issue is represented by composite structures, where multiple tectonic events may result in the formation of a single structure (Luneburg and Lebit 1998; Miller et al. 2005) and also by possible formation of steady-state foliations (Means 1981; Twiss and Moores 1992, p 287).

The above considerations along with our investigations of fabric patterns in and around the ultrapotassic plutons (this study, Verner et al. 2006; Žák et al. 2005; K. Verner, unpublished data) prompted us to challenge the significance of the above-discussed flat-lying to NW-dipping orogenic fabric in the Moldanubian Unit. Our field observations suggest that this fabric exhibits large variations in character, intensity, and shape of the fabric ellipsoid. This fabric indicates sub-vertical to inclined finite contraction and N–S to NE–SW finite stretch, but shows no regionally consistent kinematics. Moreover, simple shear and pure shear components of finite deformation during the formation of this fabric are difficult to evaluate and have also been largely a matter of speculation.

Additionally, structural relations around ultrapotassic plutons place constraints on the timing of the fabric development, which is at variance with some of the above-mentioned models. We have shown that development of this orogenic fabric was broadly synchronous with the emplacement of the deep-seated Knížecí Stolec pluton (this study) and the upper-crustal Milevsko pluton (Žák et al. 2005), but predated the emplacement of the mid- to upper-crustal ~337 Ma Tábor and ~335 Ma Jihlava plutons (see Fig. 1b for locations; Verner et al. 2006; Žák et al. 2005). At least some of these foliations may thus have formed at different structural levels in different parts of the orogenic root prior to the emplacement of the youngest ultrapotassic plutons (dated at ~335 Ma; Kotková et al. 2003).

Therefore, we propose that the difficulties and ambiguities in correlation, interpreting kinematics, and formation of the flat-lying to NW-dipping orogenic fabric in the Moldanubian Unit may have arisen from blending together multiple deformation events in different segments of the orogenic root at different times. From this perspective, the above discussed orogenic fabric(s) in the Moldanubian Unit should be viewed rather as being a result of heterogeneous finite deformation over broader timescales rather than reflecting a single displacement field within the orogenic root. Deciphering and further understanding the significance of these orogenic fabrics thus remain a major challenge for future studies.

Conclusions

The ~340 Ma Knížecí Stolec durbachite pluton was emplaced into the Křišťanov granulite body after the granulite was juxtaposed against the mid-crustal rocks of the Drosendorf Unit. The pluton evolved from a deep-seated cone-sheet-bearing complex followed by the nested intrusion of large magma pulse(s) into the center of the outer sheeted complex, and thus may represent a frozen-in pathway for durbachitic magmas trapped during ascent to the upper structural levels.

The steep sub-concentric HP-HT metamorphic foliation in the granulite probably recorded intense ductile folding during its retrograde metamorphism. Subsequently, the durbachite pluton intruded discordantly into the granulite at around ~340 Ma. The steep margin-parallel magmatic fabrics in the durbachite may have recorded intrusive strain during emplacement. After the emplacement but prior to final solidification, the pluton was overprinted by the orogenic flat-lying fabric recorded also in the host granulite (calculated temperature of 765 ± 53°C and pressure of 0.76 ± 0.15 GPa) and in the nearby Drosendorf Unit.

Finally, based on this study and comparison with other ultrapotassic plutons, we suggest that the flat-lying orogenic fabric(s) in the Moldanubian Unit may have formed at different structural levels and in different parts of the orogenic root prior to the emplacement of the Tábor and Jihlava plutons (dated at ~337 and ~335 Ma, respectively). This fabric, which records sub-vertical to inclined finite contraction and N–S to NE–SW finite stretch, exhibits large variations in character, intensity, shape of the fabric ellipsoid, no regionally consistent kinematics and uncertain simple shear and pure shear components of finite deformation. Therefore, it is likely that this apparently ''single'' orogenic fabric recorded multiple deformation events and heterogeneous finite deformation rather than reflecting a single displacement field within the orogenic root.

Acknowledgements The thorough reviews and constructive comments by Alfons Berger, Jens C. Grimmer and Rainer Altherr helped to improve the manuscript and are gratefully acknowledged. We also thank Jaroslava Pertoldová for her great support of our work, and Jiří Konopásek and Stanislav Vrána for helpful discussions. The Armed Forces of the Czech Republic and Headquarters of the Boletice Military Training Area are thanked for allowing us to access the field area. This research was

funded by Grant No. 271/2005/B-GEO/PrF of the Charles University Grant Agency (to K. Verner), Czech Geological Survey Internal Research Project No. 3233 (to K. Verner), Czech Geological Survey Internal Research Project No. 6201 (to J. Babůrek), and in part also by Grant No. 205/02/0514 of the Grant Agency of the Czech Republic (to F.V. Holub).

References

Benn K, Paterson SR, Lund SP, Pignotta GS, Kruse S (2001) Magmatic fabrics in batholiths as markers of regional strains and plate kinematics: example of the Cretaceous Mt. Stuart batholith. Phys Chem Earth 26:343–354

Brandmayr M, Dallmeyer RD, Handler R, Wallbrecher E (1995) Conjugate shear zones in the Southern Bohemian Massif (Austria): implications for Variscan and Alpine tectonothermal activity. Tectonophysics 248:97–116

Breiter K, Scharbert S (1998) Latest intrusions of the Eisgarn Pluton (South Bohemia–Northern Waldviertel). Jahr Geol Bund 141:25–37

Burg JP (1999) Ductile structures and instabilities: their implication for Variscan tectonics in the Ardennes. Tectonophysics 309:1–25

Callahan CN, Markley MJ (2003) A record of crustal-scale stress: igneous foliation and lineation in the Mount Waldo Pluton (Waldo County, Maine). J Struct Geol 25:541–555

Carlier G, Lorand JP, Liegeois JP, Soler P, Carlotto V, Cardenas J (2005) Potassic-ultrapotassic mafic rocks delineate two lithospheric mantle blocks beneath the southern Peruvian Altiplano. Geology 33:601–604

Carswell DA, O'Brien PJ (1993) Thermobarometry and geotectonic significance of high-pressure granulites—examples from the Moldanubian zone of the Bohemian Massif in lower Austria. J Petrol 34:427–459

Cooke RA (2000) High-pressure/temperature metamorphism in the St. Leonhard Granulite Massif, Austria evidence from intermediate pyroxene-bearing granulites. Int J Earth Sci 89:631–651

Drábek M, Stein H (2003) The age of formation of a marble in the Moldanubian Varied group using Re–Os dating of molybdenite (Bohemian massif, Czech Republic). Miner Explor Sus Dev 973–976

Edel JB, Schulmann K, Holub FV (2003) Anticlockwise and clockwise rotations of the Eastern Variscides accommodated by lithospheric wrenching: palaeomagnetic and structural evidence. J Geol Soc London 160:209–218

Fiala J, Matějovská O, Vaňková V (1987) Moldanubian granulites: source material and petrogenetic considerations. Neu Jb Miner Abh 157:133–165

Finger F, Roberts MP, Haunschmid B, Schermaier A, Steyrer HP (1997) Variscan granitoids of central Europe: their typology, potential sources and tectonothermal relations. Mineral Petrol 61:67–96

Foley SF, Venturelli G, Green DH, Toscani L (1987) The ultrapotassic rocks: characteristics, classification and constraints for petrogenetic models. Earth Sci Rev 24:81–134

Franěk J, Schulmann K, Lexa O (2006) Kinematic and rheological model of exhumation of high pressure granulites in the Variscan orogenic root: example of the Blanský les granulite (Bohemian Massif, Czech Republic). Mineral Petrol 86:253–276

Franke W (1989) Variscan plate tectonics in Central Europe—current ideas and open questions. Tectonophysics 169:221–228

Friedl G, von Quadt A, Ochsner A, Finger F (1993) Timing of the Variscan orogeny in the Southern Bohemian Massif (NE-Austria) deduced from new U–Pb and monazite dating. Terra abstracts 5:235–236

Gebauer D, Friedl G (1994) A 1.38 Ga protolith age for the Dobra orthogneiss (Moldanubian zone of the southern Bohemian Massif, NE-Austria): evidence from ion-microprobe (SHRIMP) dating of zircon. J Czech Geol Soc 39:34–35

Gerdes A,Wörner G, Henk A (2000) Post-collisional granite generation and HT-LP metamorphism by radiogenic heating: the Variscan South Bohemian Batholith. J Geol Soc London 157:577–587

Gleizes G, Leblanc D, Bouchez JL (1997) Variscan granites of the Pyrenees revisited: their role as syntectonic markers of the orogen. Terra Nova 9:38–41

Gleizes G, Leblanc D, Olivier P, Bouchez JL (2001) Strain partitioning in a pluton during emplacement in transpressional regime: the example of the Neouvielle granite (Pyrenees). Int J Earth Sci 90:325–340

Holland TJB, Powell R (1998) An internally consistent thermodynamic data set for phases of petrological interest. J Metamorph Geol 16:309–343

Holub FV (1997) Ultrapotassic plutonic rocks of the durbachite series in the Bohemian Massif: petrology, geochemistry, and petrogenetic interpretation. Bull Geol Sci Econ Geol Mineral 31:5–26

Holub FV, Rossi P, Cocherie A (1997) Radiometric dating of granitic rocks from the Central Bohemian plutonic complex (Czech Republic): constraints on the chronology of thermal and tectonic events along the Moldanubian-Barrandian boundary. CR Geosci 325:19–26

Hou Z, Tian S, Yuan Z, Xie Y, Yin S, Yi L, Fei H, Yang Z (2006) The Himalayan collision zone carbonatites in western Sichuan, SW China: petrogenesis, mantle source and tectonic implication. Earth Planet Sci Lett 244:234–250

Jakeš P (1969) Retrogressive changes of granulite-facies rocks—an example from the Bohemian Massif. Spec Publ Geol Soc Australia 2:367–374

Janoušek V, Gerdes A (2003): Timing the magmatic activity within the Central Bohemian Pluton, Czech Republic: conventional U–Pb ages for Sázava and Tábor intrusions and their geotectonic significance. J Czech Geol Soc 48:70–71

Janoušek V, Finger F, Roberts M, Frýda F, Pin C, Dolejš D (2004) Deciphering the petrogenesis of deeply buried granites: whole-rock geochemical constraints on the origin of largely undepleted felsic granulites from the Moldanubian Zone of the Bohemian Massif. T Roy Soc Edin Earth Sci 95:141–159

Janoušek V, Gerdes A, Vrána S, Finger F, Erban V, Friedl G, Braithwaite C (2006) Low-pressure granulites of the Lišov massif, Southern Bohemia: Viséan metamorphism of Late Devonian plutonic arc rocks. J Petrol 47:705–744

Janoušek V, Holub FV (2006) The causal link between HP-HT metamorphism and ultrapotassic magmatism in collisional orogens: case study from the moldanubian Zone of the Bohemian Massif. Proc Geol Assoc (in press)

Johnson SE, Paterson SR, Tate MC (1999) Structure and emplacement history of a multiple-center, cone-sheet–bearing ring complex: the Zarza intrusive complex, Baja California, Mexico. Geol Soc Am Bull 111:607–619

Johnson SE, Schmidt KL, Tate MC (2002) Ring complexes in the Peninsular Ranges Batholith, Mexico and the USA: magma plumbing systems in the middle and upper crust. Lithos 61:187–208

Kalt A, Corfu F, Wijbrans JR (2000) Time calibration of a *P–T* path from a Variscan high-temperature low-pressure metamorphic complex (Bayerische Wald, Germany), and the detection of inherited monazite. Contrib Mineral Petrol 138:143–163

Klötzli US, Parrish RR (1996) Zircon U/Pb and Pb/Pb geochronology of the Rastenberg granodiorite, South Bohemian Massif, Austria. Mineral Petrol 58:197–214

Konopásek J, Schulmann K (2005) Contrasting Early Carboniferous field geotherms: evidence for accretion of a thickened orogenic root and subducted Saxothuringian crust (Central European Variscides). J Geol Soc London 162:463–470

Kotková J, Harley SL (1999) Formation and evolution of high-pressure leucogranulites: experimental constrains and unresolved issues. Phys Chem Earth 24:299–304

Kotková J, Schaltegger U, Leichmann J (2003) 338–335 Ma old intrusions in the E Bohemian Massif—a relic of the orogen-wide durbachitic magmatism in European Variscides. J Czech Geol Soc 48:80–81

Kretz (1983) Symbols for rock-forming minerals. Am Mineral 68:277–279

Kröner A, Wendt I, Liew TC, Compston W, Todt W, Fiala W, Vaňková V, Vaněk J (1988) U–Pb zircon and Sm–Nd model ages of high-grade Moldanubian metasediments, Bohemian Massif, Czechoslovakia. Contrib Mineral Petrol 99:257–266

Kröner A, O'Brien PJ, Nemchin AA, Pidgeon RT (2000) Zircon ages for high pressure granulites from South Bohemia, Czech Republic, and their connection to Carboniferous high temperature processes. Contrib Mineral Petrol 138:127–142

Linner M (1996) Metamorphism and partial melting of paragneisses of the Monotonous Group, SE Moldanubicum (Austria). Mineral Petrol 58:215–234

Lobkowicz M, Štědrá V, Schulmann K (1996) Late-Variscan extensional collapse of the thickened Moldanubian crust in the southern Bohemia. J Czech Geol Soc 43:123–138

Luneburg CM, Lebit HDW (1998) The development of a single cleavage in an area of repeated folding. J Struct Geol 20:1531–1548

Means WD (1981) The concept of steady-state foliation. Tectonophysics 78:179–199

Medaris G, Wang H, Jelínek E, Mihaljevič M, Jakeš P (2005) Characteristics and origins of diverse Variscan peridotites in the Gföhl nappe, Bohemian Massif, Czech Republic. Lithos 82:1–23

Miller RB, Paterson SR, Lebit HDW, Alsleben H, Lüneburg C (2005) Significance of composite lineations in the mid- to deep crust: a case study from the North Cascades, Washington. J Struct Geol 28:302–322

O'Brien PJ, Rötzler J (2003) High-pressure granulites: formation, recovery of peak conditions and implications for tectonics. J Metamorph Geol 21:3–20

Owen JV, Dostal J (1996) Prograde metamorphism and decompression of the Gföhl gneiss, Czech Republic. Lithos 38:259–270

Pagel M, Leterrier J (1980) The subalkaline potassic magmatism of the Ballons massif (Southern Vosges, France): shoshonitic affinity. Lithos 13:1–10

Paterson SR, Vernon RH, Tobisch O (1989) A review of criteria for identification of magmatic and tectonic foliations in granitoids. J Struct Geol 11:349–363

Paterson SR, Fowler TK, Schmidt KL, Yoshinobu AS, Yuan ES, Miller RB (1998) Interpreting magmatic fabric patterns in plutons. Lithos 44:53–82

Paterson SR, Onezime J, Teruya L, Žák J (2003) Quadruple-pronged enclaves: their significance for the interpretation of multiple magmatic fabrics in plutons. J Virt Explor 10:15–30

Petrakakis K (1997) Evolution of Moldanubian rocks in Austria: review and synthesis. J Metam Geol 15:203–222

Pharaoh TC (1999) Palaeozoic terranes and their lithospheric boundaries within the Trans-European Suture Zone (TESZ): a review. Tectonophysics 314:17–41

Powell R., Holland TJB (1988) An internally consistent dataset with uncertainties and correlations; 3, applications to geobarometry, worked examples and a computer program. J Metamorph Geol 6:173–204

Powell R, Holland T (1990) Calculated mineral equilibria in the pelite system, KFMASH. Am Mineral 75:367–380

Rajlich P, Synek J, Šarbach M, Schulmann K (1986) Hercynian-thrust related shear zones and deformation of the varied group on the contact of granulites southern Moldanubian, Bohemian Massif. Geol Rundsch 75:665–683

Schaltegger U (1997) Magma pulses in the Central Variscan Belt: episodic melt generation and emplacement during lithospheric thinning. Terra Nova 9:242–245

Schaltegger U, Corfu F (1992) The age and source of late Hercynian magmatism in the central Alps: evidence from precise U–Pb ages and initial Hf isotopes. Contrib Mineral Petrol 111:329–344

Schofield DI, D'Lemos RS (1998) Relationships between syntectonic granite fabrics and regional PTtd paths: an example from the Gander-Avalon boundary of NE Newfoundland. J Struct Geol 20:459–471

Schulmann K, Kröner A, Hegner E, Wendt I, Konopásek J, Lexa O, Štípská P (2005) Chronological constraints on the pre-orogenic history, burial and exhumation of deep-seated rocks along the eastern margin of the Variscan orogen, Bohemian Massif, Czech Republic. Am J Sci 305:407–448

Schulmann K, Lexa O, Thompson AB, Štípská P, Edel JB (2006) Lower crustal channel flow in hot orogens in space and time exemplified by the Variscan Eastern margin. Geolines 20:118–119

Svojtka M, Košler J, Venera Z (2002) Dating granulite—facies structures and the exhumation of lower crust in the Moldanubian Zone of the Bohemian Massif. Int J Earth Sci 91:373–385

Tajčmanová L, Konopásek J, Schulmann K (2006) Thermal evolution of the orogenic lower crust during exhumation within a thickened Moldanubian root of the Variscan belt of Central Europe. J Metamorph Geol 24:119–134

Tobisch OT, Paterson SR (1988) Analysis and interpretation of composite foliations in areas of progressive deformation. J Struct Geol 10:745–754

Twiss RJ and Moores EM (1992) Structural geology. Freeman, San Francisco, pp 1–532

Urban M, Synek J (1995) Moldanubian Zone: Structure. In: Dallmeyer D, Franke W and Weber K (eds) Pre-Permian Geology of the Central and Western Europe. Springer, Berlin, pp 429–424

Van Breemen O, Aftalion M, Bowes DR, Dudek A, Mísař Z, Povondra P, Vrána S (1982) Geochronological studies of the Bohemian Massif (Czechoslovakia) and their significance in the evolution of Central Europe. T Roy Soc Edin, Earth Sci 73:89–108

Verner K, Pertoldová J (2004) Structural and petrological relations among granitoids near Nová Pec (Moldanubian Zone, Bohemian Forest). Geolines 17:98–99

Verner K, Žák J, Hrouda F, Holub FV (2006): Magma emplacement into exhumed lower- to mid-crustal orogenic root: the Jihlava melasyenite pluton, Moldanubian Zone, Bohemian Massif. J Struct Geol 28:1553–1567

Vernon RH (2000) Review of microstructural evidence of magmatic and solid-state flow. El Geosci 5: DOI:10.1007/s10069-000-0002-3

Vrána S (1979) Polyphase shear folding and thrusting in the Moldanubicum of southern Bohemia. Bull Geol Surv Prague 54:75–86

Vrána S (1988) The Moldanubian Zone in Southern Bohemia: polyphase evolution of imbricated crustal and upper mantle segments. Proceedings of the 1st International Conference on the Bohemian Massif, Czech Geological Survey, Prague pp 331–336

Vrána S (1989) Perpotassic granulites from Southern Bohemia: a new rock-type derived from partial melting of crustal rocks under upper mantle conditions. Contrib Mineral Petrol 103:510–522

Vrána S, Blümel P, Petrakakis K (1995) Moldanubian Zone: metamorphic evolution. In: Dallmeyer D, Franke W and Weber K (eds), Pre-Permian Geology of the Central and Western Europe. Springer, Berlin, pp 453–466

Vrána S, Šrámek J (1999): Geological interpretation of detailed gravity survey of the granulite complex in southern Bohemia and its structure. Bull Geol Surv Prague 74:261–277

Vrána S, Bártek J (2005): Retrograde metamorphism in a regional shear zone and related chemical changes: the Kaplice Unit of muscovite-biotite gneisses in the Moldanubian Zone of southern Bohemia, Czech Republic. J Czech Geol Soc 50:43–57

Wendt I, Kröner A, Fiala J, Todt W (1994) U–Pb zircon and Sm–Nd dating of Moldanubian HP/HT granulites from South Bohemia, Czech Republic. J Geol Soc London 151:83–90

Wenzel Th, Mertz DF, Oberhänsli R, Becker T, Renne PR (1997) Age, geodynamic setting, and mantle enrichment processes of a K-rich intrusion from the Meissen massif (northern Bohemian massif) and implications for related occurrences from the mid-European Hercynian. Geol Rundsch 86:556–570

White RW, Powell R, Holland TJB (2001) Calculation of partial melting equilibria in the system Na_2O-CaO-K_2O-FeO-MgO-$Al2O_3$-SiO_2-H_2O (NCKFMASH). J Metamorph Geol 19:139–153

Williams PF (1985) Multiply deformed terrains—problems of correlation. J Struct Geol 7:269–280

Willner AP, Sebazungu E, Gerya TV, Maresch WV, Krohe A (2002) Numerical modelling of PT-paths related to rapid exhumation of high-pressure rocks from the crustal root in the Variscan Erzgebirge Dome (Saxony/Germany). J Geodyn 33:281–314

Winchester JA (2002) Palaeozoic amalgamation of Central Europe: new results from recent geological and geophysical investigations. Tectonophysics 360:5–21

Žák J, Holub FV, Verner K (2005) Tectonic evolution of a continental magmatic arc from transpression in the upper crust to exhumation of mid-crustal orogenic root recorded by episodically emplaced plutons: the Central Bohemian Plutonic Complex (Bohemian Massif). Int J Earth Sci 94:385–400

Žák J, Paterson SR, Memeti V (2007) Four magmatic fabrics in the Tuolumne batholith, central Sierra Nevada, California (USA): implications for interpreting fabric patterns in plutons and evolution of magma chambers in the upper crust. Geol Soc Am Bull 119:184–201

GENERAL CONCLUSIONS

The presented studies wanted to clear up the conditions and mechanism of melt formation in the high-grade felsic rocks and its possible relation to the subduction of continental crust material. Our results should be instrumental to understand whole metamorphic history of the subducted rocks.

- The presence of leucocratic bands is the common feature of many felsic granulites in Moldanubian Zone. In addition, the felsic granulites in the Kutná Hora complex contain mesocratic garnets with relatively Ca-rich cores (Grs_{41}) and leucocratic garnets have a similar composition as a mesocratic garnet rims. The occurrence of two ternary feldspars, perthitic K-feldspar and anthiperthitic plagioclase, preserved as inclusions in garnet together with kyanite is also characteristic for these rocks.

- The constructed *P-T* pseudosections show wide stability fields of quartz + K-feldspar + phengitic muscovite + kyanite + garnet + omphacite + rutile that are located above *P* = 1.3 GPa at *T* = 550 °C and *P* = 2.3 GPa at *T* = 1000 °C. The location of the low-pressure boundary of this assemblage depends on H_2O activity and it slightly shifts to higher pressures at lower H_2O activities. At medium pressures, the mineral assemblages are quartz + K-feldspar + plagioclase + garnet ± biotite + phengitic muscovite + rutile; the latter two phases would become replaced by sillimanite and ilmenite, respectively, at very low pressures. In the high-pressure granulite facies, both samples are predicted to become partially molten but they remain multiply saturated by quartz, two feldspars, kyanite, garnet and rutile, owing to the predicted small amount of the granitic melt formed.

- Our thermodynamic modeling of phase equilibria indicates that phengite dehydration melting commenced along a prograde path from eclogite to granulite facies at *T* ~ 940 ^{o}C and *P* = 2.6 GPa. Our samples contain rare garnet-plagioclase symplectites, retrogressed to biotite-plagioclase intergrowths, which are interpreted to result from phengite breakdown. Importantly, the felsic granulites from the Kutná Hora complex contain phengite inclusions in garnet grains that were enclosed at this stage as evidenced by preserved prograde chemical zoning. Ca-rich garnets, which formed along the HP prograde path during the phengite dehydration melting, were found in

the mesocratic layers or as rare unstable relics with atoll shapes in the leucocratic layers. By contrast, small garnet grains that formed newly in the leucocratic portions lack the Ca enrichment but have elevated Mg and Fe concentrations, consistent with *P-T* conditions of the subsequent decompressional heating with progressive dehydration melting at 1020 ^{o}C and 2.1 GPa. Our experiments performed along the dehydration melting (T = 900 ^{o}C and P = 1.7-2.1 GPa, runs #2-4) show formation of granitic partial melt and new kyanite. Small garnet grains formed in the quartz + ternary feldspar + melt pools in our experimental runs #3 and 4 also show composition similar to that found in the leucocratic layers.

- For the reconstructed *P-T* path, the granulite precursor contains 0.75-1.10 wt. % H_2O, as maximum values, stored in phengite prior to the high-pressure dehydration melting. We have used these results to constrain the maximum melt productivity in the granulite facies. The amount of partial melt formed along the reconstructed P-T path increases to 18-26 vol. % as the peak temperature (1020 ^{o}C) was approached.

- In order to constrain the extent and conditions of the melt migration, we have calculated a composition section along our reconstructed metamorphic path. The melt composition was in equilibrium with the mineral assemblage at peak temperature. The preserved granulite assemblage with abundant garnet and minor biotite corresponds to ~1-3 vol. % melt existing at the solidus at 740-770 ^{o}C and 1.0-1.2 GPa. If the granulite precursor had contained a maximum of 1.05 wt. % H_2O in the eclogite facies prior to the phengite dehydration melting, about 15-25 vol. % melt must have been lost during decompression path. The melt loss occurred early in the granulite facies, from 1000 ^{o}C and 2.2 GPa to 1020 ^{o}C and 2.0 GPa, simultaneously with progressive heating and melt formation. The melt migration during partial melting and the deformation can be responsible for the formation of foliation-parallel leucosome-mesosome texture, the presence of the partial melt in the both types of layers probably facilitates the attainment of equilibrium during granulite facies overprint. This explains the absence of relics of eclogite-facies mineral assemblages (e.g., phengite, omphacite) in the felsic granulites and their presence (e.g., diopside replacing omphacite) in the adjacent mafic varieties and eclogites that have not undergone partial melting. The modal layering of felsic granulites in the Kutná Hora complex was a result of partial melting that has occurred contemporaneously with deformation during heating and

decompression from the eclogite to the granulite facies, during orogenic exhumation. The presence of partial melt in felsic granulites may have exerted primary rheological control on mechanics of enclosing the lenses and boudins of mafic and ultramafic metamorphics and it may be responsible for their common spatial association in the orogenic exhumation regions.

- The garnet inclusions (muscovite, omphacite) from prograde part of *P-T* path in felsic granulites may transformed during high-temperature granulite facies metamorphism, partial melting and decompression to other phases, and so the original mineral can only be deduced from the inclusion morphology and reaction products. These inclusions may have columnar shapes and may consist of K-feldspar + kaolinite, albite + Fe-oxide, plagioclase + Fe-oxide, or albite + K-feldspar, respectively. The pseudomorphs with albite/plagioclase occuring in a Ca-rich garnet which have a prograde zoning. Pressure-temperature (*PT*) evolution, derived from mineral assemblages in granulite and based on the inclusions, suggests a prograde metamorphism from amphibolite through eclogite to granulite facies conditions with subsequent amphibolite facies overprint during exhumation. The estimated *P-T* trajectory for the studied granulites, which also host lenses or boudins of eclogites and garnet peridotites, allow reconstruction of the complete clockwise metamorphic path that is consistent with subduction geotherm prior to the tectonic amalgamation within the continental collisional root.